Biomarkers for Metabolic Drug Activation: Towards an Integrated Risk Assessment for Drug-Induced Liver Injury (DILI)

Inauguraldissertation

zur

Erlangung der Würde eines Doktors der Philosophie

vorgelegt der

Philosophisch-Naturwissenschaftlichen Fakultät

der Universität Basel

von

Marieke Teppner

aus Kiel, Deutschland

Basel, 2016

Genehmigt von der Philiosophisch-Naturwissenschaftlichen Fakultät
auf Antrag von

Fakultätsverantwortlicher: Prof. Dr. Beat Ernst
Dissertationsleiter: Dr. Axel Pähler
Ko-Referent: Dr. Amit Kalgutkar

Basel, 22.04.2014

Prof. Dr. Jörg Schibler
Dekan

TABLE OF CONTENTS

This thesis is presented in the form of four scientific papers that are published or in preparation for publication. Reference lists can be found at the end of each result chapter.

ACKNOWLEDGEMENT

I would like to express my gratitude towards all people at the Pharmaceutical Sciences department at Roche Basel who supported me and my work with a lot of helpfulness and kindness.

Especially, I would like to thank Dr. Axel Pähler for giving me the opportunity to perform this exciting project under his supervision and for his continuous support, advice and discussions during the last three years.

Many thanks go to Prof. Beat Ernst for accepting to be my academic supervisor and reviewing my work.

I am very grateful to Dr. Amit Kalgutkar for being the co-referee of this thesis.

Special thanks go to the people who contributed to my work with their scientific knowledge: Dr. Fränzi Böss, Dr. Tobias Heckel and Isabelle Walter were always ready for help and discussions around experimental and analytical questions. Dr. Holger Fischer, Dr. Neil Parrott and Dr. Antonello Caruso supported me with respect to mathematical, statistical and modeling questions.

Also, I would like to acknowledge Sandrine Simon, Aynur Ekiciler, Nathalie Schaub and Evelyne Durr for their help with hepatocyte isolation and handling as well as Andreas Goetschi for sharing his broad instrumental and analytical knowledge.

Everybody from the drug metabolism group was especially helpful to give advice and solve scientific, technical and personal trouble. Andreas, Bernd, Christophe, Kirsten, Manfred, Michaela, Russell, Ruth and Thomas: thanks for being great colleagues.

Special thanks go to Dr. Kajsa Kanebratt for introducing and inspiring me for scientific work.

I would like to acknowledge all members of the Molecular Pharmacy and Molecular Modeling at the University of Basel for welcoming and accepting me as a member of their group.

Finally, I would like to thank my family and Michel for their constant support, patience and encouragement.

ABBREVIATIONS

15*R*-PD_2	15*R* prostaglandin D_2
8,12-iso-$iPF_{2\alpha}$-VI	8,12-iso-isoprostane $F_{2\alpha}$-VI
ADH	Aldehyde dehydrogenase
AKR	Aldo-keto reductase
ALT	Alanine aminotransferase
APC	antigen presenting cell
ARE	Antioxidant response element
AST	Aspartate aminotransferase
BSEP	Bile salt export pump
CCl_4	Carbon tetrachloride
CE	Collision energy
CES1	Carboxylesterase 1
CID	Collision-induced dissociation
CL	Clearance
CL_{int}	Intrinsic clearance
CVB	Covalent protein binding
CXP	Cell exit potential
CYP	Cytochrome P450
DHN-MA	1,4-dihydroxy-2(*E*)-nonene mercapturic acid
Dihydro-keto PD_2	13,14-dihydro-15-keto prostaglandin D_2
Dihydro-keto PE_2	13,14-dihydro-15-keto prostaglandin E_2
DILI	Drug-induced liver injury
DILIN	Drug-induced liver injury network
DNA	Deoxyribonucleic acid
DP	Declustering potential
ECH	erythroid cell-derived protein with CNC homology
EIA	Enzyme immunoassay
EPI	Enhanced product ion
ER	Enhanced resolution
ESI	Electrospray ionization
F	Bioavailability
F_a	Fraction absorbed
FDA	Food and drug administration
F_{Dp}	Fraction of dose reaching the portal vein
Fe(III)NTA	Ferric nitrilotriacetic acid
f_m	Fraction metabolized
FMO	Flavin-containing monooxygenase
F_{oral}	Oral bioavailability
GC	Gas chromatography
GCLC	Glutamate-cysteine ligase
GLDH	Glutamate dehydrogenase
GSH	Glutathione
GST	Glutathione-*S*-transferase
HIV	Human immunodeficiency virus
HLA	Human leukocyte antigen
HLM	Human liver microsomes
HMG-CoA	3-Hydroxy-3-methylglutaryl-coenzyme A
HMOX	Heme oxygenase
HNE	4-Hydroxy-2(*E*)-nonenal
HNE-MA	HNE mercapturic acid
HPLC	high performance liquid chromatography
HRP	Horseradish peroxidase
HSP	Heat shock protein
I_{av}	Systemic concentration
IDILI	Idiosyncratic drug-induced liver injury
I_{in}	Liver inlet concentration
INR	International normalized ratio
IgE	Immunoglobulin E
$iPF_{2\alpha}$-III	8-isoprostane $F_{2\alpha}$
$iPF_{2\alpha}$-VI	5-iso prostaglandin $F_{2\alpha}$-VI
IVIVC	*In vitro-in vivo* correlation
k_a	Absorption constant
Keap1	Kelch-like ECH-associated protein 1

LC	Liquid chromatography
LC-MS/MS	Liquid chromatography / tandem mass spectrometry
LDH	Lactate dehydrogenase
LLE	Liquid liquid extraction
LM	Liver microsomes
LogD	Distribution coefficient
logP	Partition coefficient
LOQ	Limit of quantification
LPS	Lipopolysaccharide
MA	Mercapturic acid
MDA	Malondialdehyde
mEH	Microsomal epoxide hydrolase
MHC	Major histocompatibility complex
MIP-DILI	Mechanism based integrated systems for the prediction of drug-induced liver injury
MPO	Myeloperoxidase
mRNA	Messenger RNA
MRP2	Multi-drug resistance protein 2
MS	Mass spectrometry
MS/MS	Tandem mass spectrometry
NaNTA	Nitrilotricacetic acid sodium
NAT	N-Acetyl transferase
NICI	Negative ion chemical ionization
NPV	Negative predictive value
NQO	NAD(P)H:quinone oxidoreductase
Nrf2	Nuclear factor erythroid 2-related factor 1
NSAID	Non-steroidal anti-inflammatory drug
PGZ	Pioglitazone
PD_2	Prostaglandin D_2
PD_2-d4	deuterated Prostaglandin D_2
PE_2	Prostaglandin E_2
$PF_{2\alpha}$	Prostaglandin $F_{2\alpha}$
P-I	Pharmacological interaction
PI	Precursor ion
PLA-DA	Partial least squares discriminant analysis
PPARγ	Peroxisome proliferator-activated receptor gamma
PSA	Polar surface area
QC	Quality control
Q_h	Hepatic bloodflow
UDP	Uridine diphosphate
UGT	UDP-glucuronosyl transferase
ULN	Upper limit of normal
R^2	Coefficient of determination
RGZ	Rosiglitazone
RM	Reactive metabolite
ROS	Reactive oxygen species
SD	Standard deviation
SDH	Sorbitol dehydrogenase
SOD	Superoxide dismutase
SPE	Solid phase extraction
SRM	Selected reaction monitoring
SULT	Sulfotransferase
TGZ	Troglitazone
XO	Xanthine oxidase

1 INTRODUCTION

1.1 Background

Drug-induced liver injury (DILI) is one of the major reasons for severe adverse reactions upon therapeutic drug intake today. It has led to many cases of drug attrition, withdrawal or restricted usage and is the leading cause of acute liver failure [8-10]. Promising innovative medications like the antidiabetic troglitazone and the anticoagulant ximelagatran had to be removed from the market shortly after approval. Other drugs like the antituberculotic isoniazid and the anticonvulsant valproate were labeled with a black box warning which controls and limits their prescription. Case estimates of DILI are around 19 per 100'000 treated individuals [11]; however, it is supposed that these numbers suffer from large underreporting [12]. Heterogeneous symptoms, delayed onset, lack of dose dependence and incomplete awareness of contributing risk factors hinder control and diagnosis of liver toxicity. A large impact on patients' health and on pharmaceutical industry and a challenge for authorities and scientific community is the result. Many efforts to understand mechanisms and develop mitigation strategies have been undertaken by researching companies and academia. Even holistic collaborative networks have been founded to better monitor DILI and explore approaches for improved safety [13, 14].

To improve risk assessment and promote causality elucidation, it is important to understand underlying physiological processes and their interaction with an administered drug. Therefore, the current understanding of DILI will be explored in the following sections and put into context with relevant body functions, available test systems and analytical markers.

1.2 The liver in context of drug metabolism

The liver is the most important organ for metabolic activity and the biggest exocrine gland in the human body. It is located centrally in the torso and well connected to the blood flow by two afferent vessels, the *Arteria hepatica* and the *Vena portae*, which transport arterial (*A. hepatica*) and venous blood (*V. portae*) from the unpaired abdominal viscera. Following the passage of the hepatic capillary system, the blood is released through the *Vena hepatica* and the *Vena cava inferior* to systemic circulation (Figure 1.1A). With its gate-keeping function the liver has various responsibilities. Important ones are synthesis and breakdown of endogenous substrates in carbohydrate, protein and lipid metabolism as well as regulation of coagulation and hormone homeostasis. Besides, it is essentially involved in the process of detoxification and excretion of xenobiotics.

The liver tissue is composed by different cell types, non-parenchymal cells (sinusoidal endothelial cells, Kupffer cells, and stellate cells) and parenchymal cells, the hepatocytes. With 80% of total volume, the latter represent the largest cell population of the liver and are its most important functional subunit. The enzymatic equipment for biotransformation of most xenobiotic compounds is located here; catalysis of drug modifications to more hydrophilic species enables their excretion via bile or urine.

Biotransformation is generally divided into two phases, an activating (phase I) and a conjugating step (phase II). Activation of chemical entities can be achieved by hydrolytic, reductive, or oxidative processes. The most frequent pathway is the oxidation of alkylated heteroatoms or aromatic / hydroxylated functions, predominantly catalyzed by monooxygenases of the cytochrome P450 (CYP) enzyme superfamily. Other phase I drug-metabolizing enzymes are flavin-containing monooxygenases (FMO), alcohol / aldehyde oxidases (oxidation), esterases, epoxide hydrolases (hydrolysis) and NADPH-cytochrome P450 reductases (reduction). To enable elimination activated species are then mostly coupled to hydrophilic endogenous substances such as glucuronic acid, sulfonic acid or glutathione (GSH) by transferases [15].

Metabolism of xenobiotics during the first liver passage can prevent or reduce their systemic circulation and is therefore called “first pass effect”. It can result into decreased plasma levels or bioavailability, but also support the activation of a pro-drug.

Functionality of the hepatocytes are closely related to the histo-anatomic architecture of the liver lobes: An oxygen gradient between portal triad (hepatic artery, hepatic portal vein, bile duct) and the central hepatic vein defines different metabolic zone within the hepatocytes along the sinusoid with decreasing oxidative activity (Figure 1.1B).

In summary, the liver is a particular target for xenobiotic respectively drug action and effects, but even more importantly for interactions and side effects. All blood from the gastrointestinal tract, containing orally absorbed drug, passes the liver with the potential of first metabolic interaction. Clearance of an active compound from the systemic circulation is prepared via biotransformation in the liver. Direct effects of a xenobiotic or those of a metabolite bear the potential of harming the liver, e.g. by altering functions or triggering immune response.

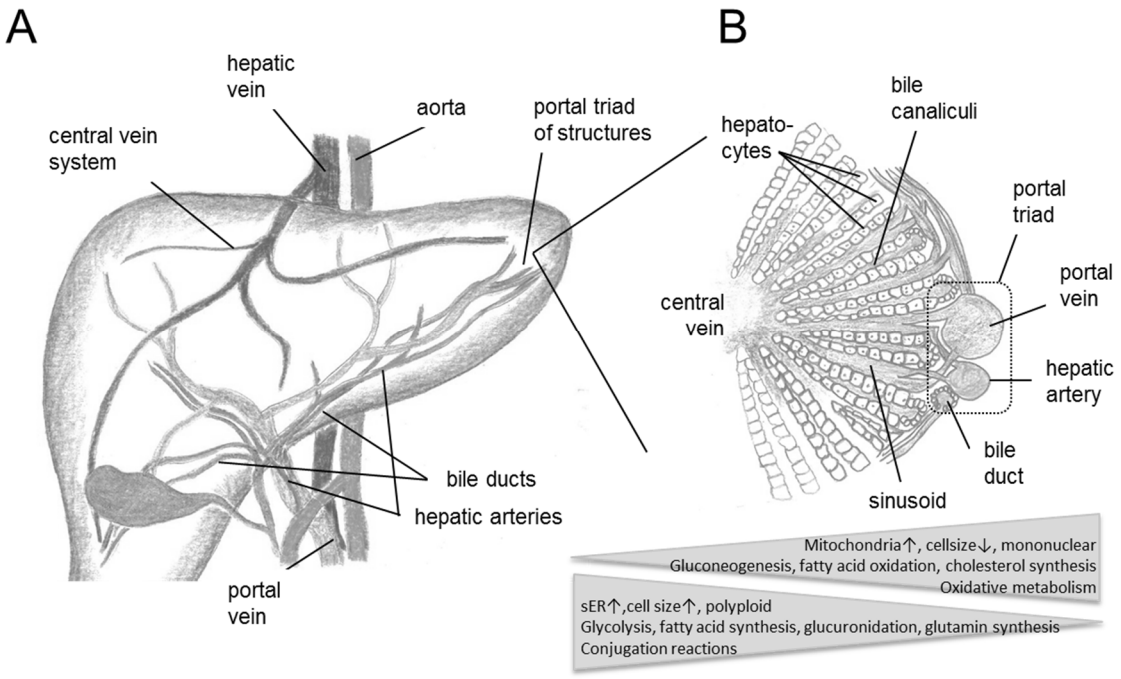

Figure 1.1: Functional macro- and microanatomy of the liver

1.3 Drug-induced liver injury (DILI)

1.3.1 Definition of DILI

Drug-induced liver injury (DILI) is defined as an adverse effect upon drug intake at therapeutic doses. It may cause pathophysiological or pathological alterations of liver parameters or liver function with diverse severity. Many contributing factors to DILI remain unclear today. Thus, the term 'DILI' and its diagnosis are mainly characterized by exclusion of other possible etiologies except for the side effect of an administered xenobiotic agent. It is characterized by time to onset, clinical features, course of recovery, specific risk factors, previous reports on hepatotoxicity of the implicated agent and can be supported by knowledge on effects after rechallenge and liver biopsy [16]. It is widely accepted that environmental factors such as comedications and host factors such as genetic predisposition and underlying disease impact the manifestation of DILI to at least the same extent as the liability of the drug itself do.
Significant clinical DILI determinants are either changes in the hepatic biomarker status or functional loss. The former comprise of 5-fold elevation of aspartate transaminase (AST) or alanine transaminase (ALT) as compared to the upper limit of normal (ULN) or 2-fold elevations in either alkine phosphatase or bilirubin plus any rise in ALT or AST levels [17]. The latter arise from degenerative processes with steatotic, cholestatic, cirrhotic, or necrotic characteristics [18]. Hyman Zimmerman observed a correlation between the occurrence of jaundice and fatality of DILI. On this basis, the FDA defined "Hy's law" as predictor for fatal hepatotoxicity with bilirubin levels higher than 2 mg/mL and AST / ALT higher than 3-times ULN [19]. An overview on different DILI phenotypes is given in Table 1.1, illustrating that it can mimic various types of liver injury, and even one drug may cause different clinical pattern. E.g. Isoniazid is known to cause three types of acute liver impairment as well as chronic hepatitis [20]. The term DILI is often accompanied by the attribute 'idiosyncratic' (also IDILI), literally meaning 'mixture of characteristics'. This expression points towards the unpredictable character of these adverse effects. They lack dose dependence, occur in low incidence, cannot be addressed in animal models and are therefore not detected in drug discovery. Fatalities in patients, high therapeutic costs for the health care system and economic damage for the pharmaceutical industry are the consequences. Consequently drug developing companies but also health care authorities and the

scientific community are highly interested in improving mechanistic understanding and safety assessment of new drugs. Dedicated projects in industry are promoted, research groups in academia investigate underlying mechanisms and even holistic collaborations have been launched: a drug-induced liver injury network (DILIN) was initiated by the US National Institute of Diabetes and Digestive and Kidney Diseases aiming for a better documentation and critical review of hepatotoxicity cases [13] and project called MIP-DILI (mechanism-based integrated systems for the prediction of drug-induced liver injury) was launched as a collaboration between academia and industry, supported by the European [14]. Both aim for a better documentation, understanding and improved analytical tools for liver toxicity.

Table 1.1: Clinical phenotypes of DILI adopted from [18]

Phenotype	Characteristics	Example drug
Immunoallergic hepatitis	skin rash, eosinophilia, fever	phenytoin
autoimmune hepatitis-like	autoantibodies detectable	nitrofurantoin
acute hepatic necrosis	parenchymatic necrosis	isoniazid
acute viral hepatitis-like	fatigue	isoniazid
Acute liver failure	parenchymatic necrosis, INR > 1.5, encephalopathy	bromfenac
cholestatic hepatitis	alkaline phosphatase and bilirubin elevations	amoxicillin clavulanate
bland cholestasis	pruritis	anabolic steroids
acute fatty liver with lactic acidosis	steatosis, mitochondrial dysfunction	valproate
nonalcoholic fatty liver	steatosis (steatohepatitis)	Amiodarone
sinusoidal obstruction syndrome	obliteration of central veins	cyclophosphamide
chronic hepatitis	fatigue, bilirubin elevation necrosis	isoniazid
nodular regeneration	formation of nodules	azathioprine
vanishing bile duct syndrome	loss of interlobular bile ducts, cholestasis	β-lactam antibiotics
cirrhosis	collagenization	methotrexate

1.3.2 Mechanistic hypotheses

Different hypotheses have been established which try to explain the heterogeneous pattern of DILI. None of them is currently able to describe all cases of drug induced hepatotoxicity; however, for individual examples they may apply.

Bioactivation

Bioactivation is widely accepted as important contributing factor to the pathogenesis of hepatotoxicity. In situations where reactivity of phase I metabolites is too high or phase II substrates are depleted, they are prone to bind to any partner of matching nucleophilicity in immediate vicinity. Less frequently, also phase II metabolism can lead to bioactivation. E.g., the glucuronic acid in acyl glucuronides displays a good leaving group which can be substituted by an amino acid residue. For instance, this mechanism was observed in non-steroidal anti-inflammatory drugs (NSAIDs). They contain free carboxylic acid moieties that can be conjugated via UDP glucuronosyl transferases (UGTs) [21].

Drugs that directly impair function of macromolecules upon binding are alkylating cytostatic agents. They contain structural elements that can be activated to carbokations and are prone to react with nucleic acids which disables their reduplication by crosslinking or disruption of DNA strands. This is pharmacologically intended to stop tumor growth; however, unspecific reactivity can be responsible for various adverse effects on proliferating tissues [22]. A prominent example is cyclophosphamide, an anticancer drug used for treatment of many types of tumors. Its alkylating principle is phosphoramide mustard, which is generated from the pro-drug after CYP2B6-mediated activation and subsequent non-enzymatic cleavage [23]. As shown in Figure 1.2, also other alkylating by-products emerge from this pathway, exhibiting non-target effects. One of them is acrolein, which is renally cleared and prone to react with bladder epithelia, resulting in cystitis or even cancer [24]. Adverse effects in liver and heart may also be mediated via formation of covalent DNA or enzyme adducts and GSH depletion by acrolein [25, 26].

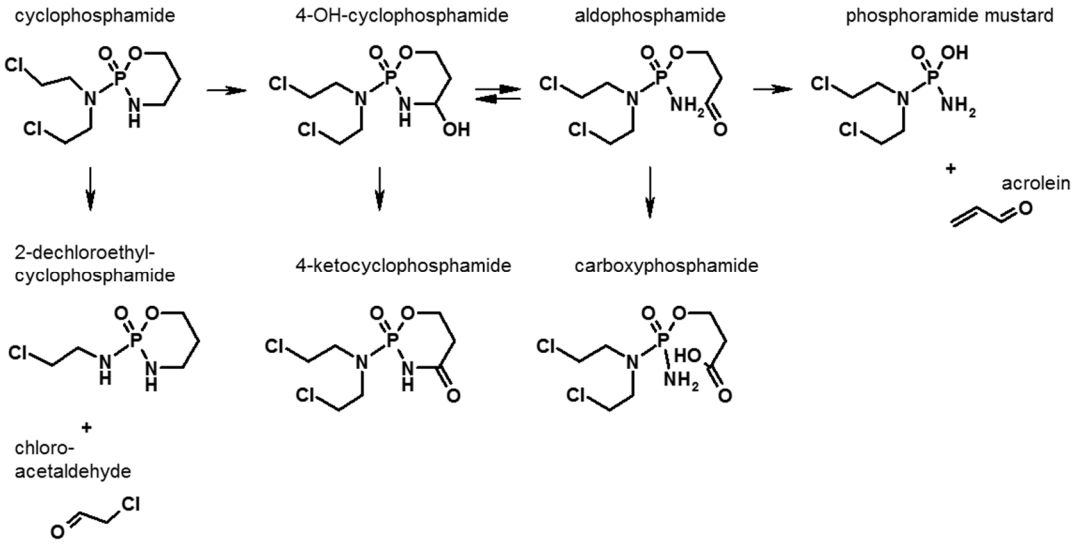

Figure 1.2: Metabolic pathways and bioactivation of cyclophosphamide

Hapten hypothesis

Covalent modifications on proteins can result in direct functional impairment or loss but also in neoantigen formation. The novel adduct, unknown to the body, is able to trigger immunogenicity which involves uptake of the modified protein by antigen presenting cells (APC), hydrolytic processing and surface presentation in the major histocompatibility complex to T cells. This process activates the immune cascade including autoantibody formation and was observed for the first time by Landsteiner. He detected that small molecules could only act as immunogens when bound to proteins and are thus referred to as ‘haptens’ [27, 28].

Relevance of this hypothesis was demonstrated for antibiotics of the penicillin family. Their β lactam ring is a target for nucleophilic attack by free amino groups of proteins resulting in ring opening and covalent adducts formation mainly with the generated penicilloyl group. These adducts are known to trigger formation of specific IgE antibodies and thus to mediate allergic reactions [29, 30].

Danger hypothesis

Drugs such as raloxifen, simvastatin and olanzapine form covalent protein adducts [3, 31], however, they do not cause idiosyncratic reactions. Hence, another hypothesis, called “danger hypothesis”, was formulated by P. Matzinger. She postulated the necessity of a danger signal in addition to the modified protein to trigger immunogenicity. She refers to the fact that also during physiological defense a

secondary stimulation of T-cells is needed to activate APCs and initiate immune response instead of tolerance [32]. This danger signal might be triggered by e.g. cellular stress from reactive drug metabolites, heat shock proteins (HSP) or bacterial endotoxins such as lipopolysaccharide (LPS) from underlying infections [33, 34].

Pharmacological interaction (P-I) hypothesis

A third important theory is based on Pichler's observation that drug-exposed cloned T cells proliferated in absence of metabolic activity [35]. He presumed that some drugs can bind directly to the MHC T cell receptor complex and provoke an immune response without any preceding metabolic activation, binding to free proteins or digestion by APCs. An example for this hypothesis is sulfamethoxazole which was shown to be presented in an unstable, but MHC-restricted fashion independent of processing [36]. The name P-I hypothesis derives from the suggestion that a drug can interact directly as pharmacological agent with the immune receptor [37].

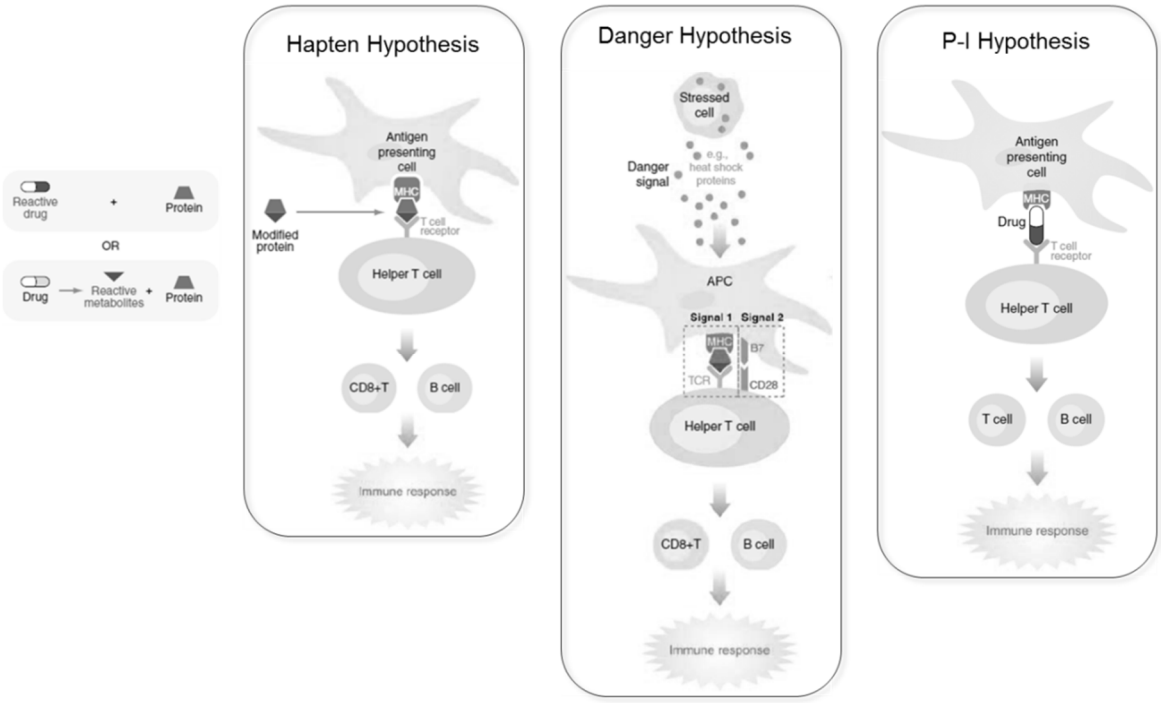

Figure 1.3: Key mechanistic hypotheses for idiosyncratic drug reactions: Bioactivation or intrinsic activity of a drug leads to binding to residues of free proteins or the T-cell receptor and triggers an immune response. Adopted from Uetrecht, 'Idosyncratic Drug reactions: Current Understanding' [38].

Non immune hypotheses

Besides the discussed theories there are other mechanistic concepts describing examples where characteristics for hypersensitivity reactions are not present. For these cases, mitochondrial impairment or presence of an inflammagen such as lipopolysaccharides (LPS) is discussed as risk factors [39, 40].

Despite these theories, important mechanistic knowledge to explain unexpected drug reactions is missing and only individual examples fit to the given explanations, even though, as stated by Uetrecht, hypotheses are not mutually exclusive. Reactive intermediates might act as danger signal on top of being a hapten [38]. An overview of the three most important hypotheses is shown in Figure 1.3.

1.3.3 Risk factors for DILI

Various factors are discussed to contribute to the pathogenesis of DILI in susceptible individuals in contrast to tolerant ones. These comprise of characteristics of the drug itself (pharmacokinetics and -dynamics), environmental factors (e.g. diet or comedication) and, probably of major importance, host dependent risk factors, both genetic and non-genetic ones. An overview is given in Table 1.2.

The influence of gender or age as susceptibility factor for DILI has been assessed in several studies with no clear evidence for increased risk in one demographic subpopulation. Even though some investigations found women at higher risk than men [41, 42] and children as compared to adults [43, 44], these did not correct for differences in patient prevalence and disease incidence / medication profile for the different patient groups [45, 46]. Also dietary liabilities, like alcohol or tobacco consume as source of liver stress or inflammation factors have not been clearly matched with increased susceptibility [47].

Drug related risk factors, in contrast, are characterized in a more substantial manner. Compounds given at less than 50 mg per day in contrast to higher dosing regimens lack the risk of liver impairment [48]. This observation by Lammert et al. implicates that idiosyncrasy, in contrast to general belief, is dose dependent, but saturated at concentrations where a dose-response for effects are seen.

Lammert also reported a correlation between increased incidence for adverse effects and a high degree (>50%) of hepatic metabolism [49]; specifically, metabolism via

CYP2C9 and CYP2C19 was found to be associated with increased risk as compared to transformation via other CYPs [50]. This may be due to their polymorphic character, i.e. in differences in catalytic activity. Toxicity of tienilic acid for example is mediated by metabolic activation via CYP2C9: Its oxidized metabolite readily inactivates the enzyme by formation of covalent adducts [51]. Circulating antibodies against CYP2C9 drug conjugates were found to be responsible for the autoimmune response of affected patients [52]. Moreover, polypharmacy represents a risk for pharmacokinetic interactions, such as potentiated effects of two drugs that are eliminated over the same pathway [18]. E.g., co-administration of cerivastatin and fibrates enhanced the risk of rhabdomyolysis and resulted in the withdrawal of the HMG-CoA inhibitor cerivastatin. It is meanwhile known that adverse effects were caused by increased plasma levels due to inhibition of CYP3A4.

Also, patients exposed to comedications often suffer from underlying diseases which can modulate the risk for toxicity, especially when the liver is affected e.g. by hepatitis or HIV. However, data quality on this aspect is poor and does not allow definite conclusions [47].

Table 1.2: Overview of contributing factors for idiosyncratic drug reactions

Risk factor	Example	Involved drug
Drug class /structural alert	Primary aromatic amine moiety	sulfamethoxazole
Exposure	Dose Metabolic pathways	troglitazone, pioglitazone
Co-medication	drug-drug interactions at DM enzymes	ketoconazole, terfenadin
genetic difference of enzyme equipment	CYP2C polymorphism	tienilic acid
Genetic differences of the immune system	HLA genotype	lumiracoxib

In the last decades improved analytical tools and method allowed for a more in-depth analysis of genetic differences in patients. Mainly polymorphic proteins resp. enzymes involved in drug metabolism have been identified as risk factors. Differences in expression of the phase II detoxifying enzymes N acetyl transferase (NAT) and S transferase (GST) as well as polymorphic CYP enzymes (e.g. CYP2D6, CYP2C9, as

mentioned above) can influence the metabolic pattern and thus a drug's safety. Moreover, interindividual differences in the immune response via specific human lymphocyte antigen (HLA) variations co-determine tolerance or occurrence of idiosyncratic reactions. One of the best studied example in this context is abacavir-induced hypersensitivity, which is correlated to the HLA B*5801 genotype [53]. Other drugs bearing increased risk in patients with specific HLA types are lumiracoxib, ximelagatran and amoxicillin-clavulanate [54-56]. However, the lumiracoxib example also shows limitations of isolated consideration of the HLA liabilities: Selection of patients based on this criterion results in a massive over-exclusion, as 94.4% of patients with the respective HLA type do not develop liver toxicity [54].

1.3.4 Oxidative stress as risk factor for DILI

During oxidative stress the balance between oxidant and antioxidant forces in the body is disturbed. The liver is especially sensitive to this disturbance as some of its major functions include handling reactive oxygen species (ROS): Activation of molecular oxygen to superoxide during mitochondrial ATP production can form hydrogen peroxide (H_2O_2) or hydroxyl radicals ($OH^{\bullet}$), biotransformation of xenobiotics by monooxygenase enzymes produces H_2O_2 and superoxide as byproducts, physiological immune defense involves peroxisomal H_2O_2 formation in hepatocytes and superoxide generation in Kupffer cells and neutrophils [57, 58]. These reactive species can readily react with nucleophilic structures in proximity, i.e. proteins, DNA and lipids which may then be altered in function [59]. Modification of sulfhydryl and aromatic moieties in proteins may induce harmful conformational changes, oxidation of mitochondrial DNA can cause interference for transcription, and lipid peroxidation may result in reduced membrane integrity. E.g., $OH^{\bullet}$-catalyzed lipid peroxidation generates peroxy intermediates which can recruit further fatty acids for oxidation and thus initiate a chain reaction. This process has been demonstrated for carbon tetrachloride toxicity [60] and can result in serious membrane damage and even inflammatory effects via activation of stellate cells [61].

In physiological conditions pro-oxidant processes are balanced by the antioxidant response pathway, a cellular, gene regulated protection mechanism against radical-induced damage [62], as depicted in Figure 1.4: The cytosolic Kelch-like ECH-associated protein 1 (Keap1) suppresses the nuclear factor erythroid 2-related

factor 2 (Nrf2), a transcription factor, in the normal state. However, under oxidative stress conditions Nrf2 is released, translocates to the nucleus and binds to a DNA promotor sequence, the antioxidant response element (ARE). This triggers transcription of the affected genes, encoding for cytoprotective proteins such as detoxifying phase II enzymes and antioxidants to support inactivation of endogenous and xenobiotic reactive species. Examples are aldo-keto reductases (AKR), heme oxygenases (HMOX), microsomal epoxide hydrolases (mEH), NADPH:quinone oxidoreductases (NQO), UGTs, superoxide dismutases (SOD) and various enzymes involved in GSH metabolism. GSH (γ-L-glutamyl-L-cysteinylglycine) is the most important free radical scavenger in the human body; with its intracellular concentration of up to 10 mM it supports spontaneous and enzymatic detoxification and regeneration via its reactive thiol group [63].

However, when the oxidative stress is too excessive, cellular defense mechanisms may be insufficient: Examples are the intake of > 4 g acetaminophen which depletes the GSH pool by adduct formation with the iminoquinone metabolite or menadione-induced redox cycling which is mediated by P450 reductase-catalyzed formation of radicals, followed by regeneration of parent [64, 65]. In these cases free radicals cannot be managed anymore and pathophysiological changes occur.

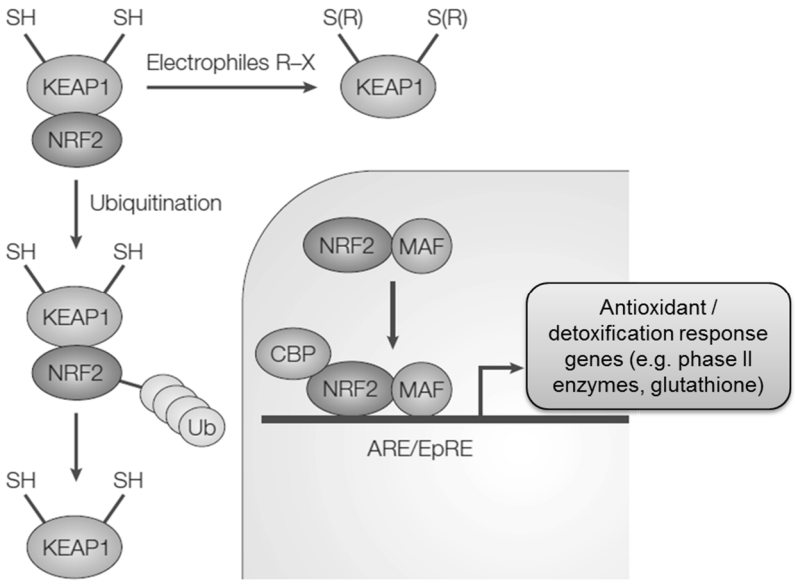

Figure 1.4. Activation of Nrf2 as redox sensitive signaling factor. Ubiquitination of Nrf2 results in cleavage of the Nrf2-Keap1 complex and translocation to the nucleus. As a heterodimer with Maf, Nrf2 binds to ARE and activates transcription. Adapted by permission from Macmillan Publishers Ltd: Nat Rev Drug Discov (Ref [66]) copyright (2005).

1.3.5 Drug examples

Many DILI drugs that were investigated with respect to their toxicity mechanism possess several liabilities that may contribute to their safety profile. This complicates identification of susceptible discovery drugs and discrimination from safe analogues. Diclofenac and troglitazone are examples where toxicity most likely results from the interplay of some of the discussed risk factors.

Diclofenac

Diclofenac is an NSAID widely prescribed against rheumatoid disorders. However, it is associated with liver injury and liver failure [67, 68] which was not predicted in animal models nor correlated to the dose. Mechanistic investigations identified several drug-related liabilities for toxicity which are summarized in Figure 1.5.

Diclofenac undergoes CYP2C9- and CYP3A4-catalyzed hydroxylation of its aromatic rings in para-position to the imino group. Further P450- and MPO-mediated oxidations result in the formation of imino-quinone species which readily react with nucleophilic protein residues. In addition, UGT-mediated conjugation of diclofenac forms unstable acyl glucuronides. The ester bridge carbon exhibits electrophilic properties and attracts nucleophilic partners. Isomerization from the 1-O-β- to a 3-O-β-form can also give rise to electrophilic aldehydes that form covalent adducts with nucleophiles [51]. Accordingly, changes in genes encoding for the involved enzymes can decrease susceptibility towards DILI [69, 70]. Disposition of the major acyl glucuronide metabolite is mainly in the canalicular plasma membrane, mediated via active MDR2-transport. Thus, decreased transporter activity also reduces the risk for DILI [70]. In addition, diclofenac metabolites were shown to decrease the cellular ATP content [71, 72] and to impair mitochondrial function via respiration uncoupling after disruption of the proton gradient [73]. Furthermore, oxidative stress has been described as risk factor, originating from the activation of the antioxidant response pathway by diclofenac metabolites [74, 75]. Imino-quinone-like intermediates are also prone to undergo redox cycling and potentiate the pro-oxidant state [76]. Besides, in some patients hypersensitivity symptoms were observed and IgM antibodies were identified, reactive against erythrocytes only in presence of 4’-hydroxydiclofenac acyl glucuronide [77]. This provides evidence for involvement of the immune system and may offer an explanation for the diverging safety pattern in patients. However, no

genetic polymorphisms or underlying disease could be clearly correlated with increased risk for diclofenac-induced hepatotoxicity [73].

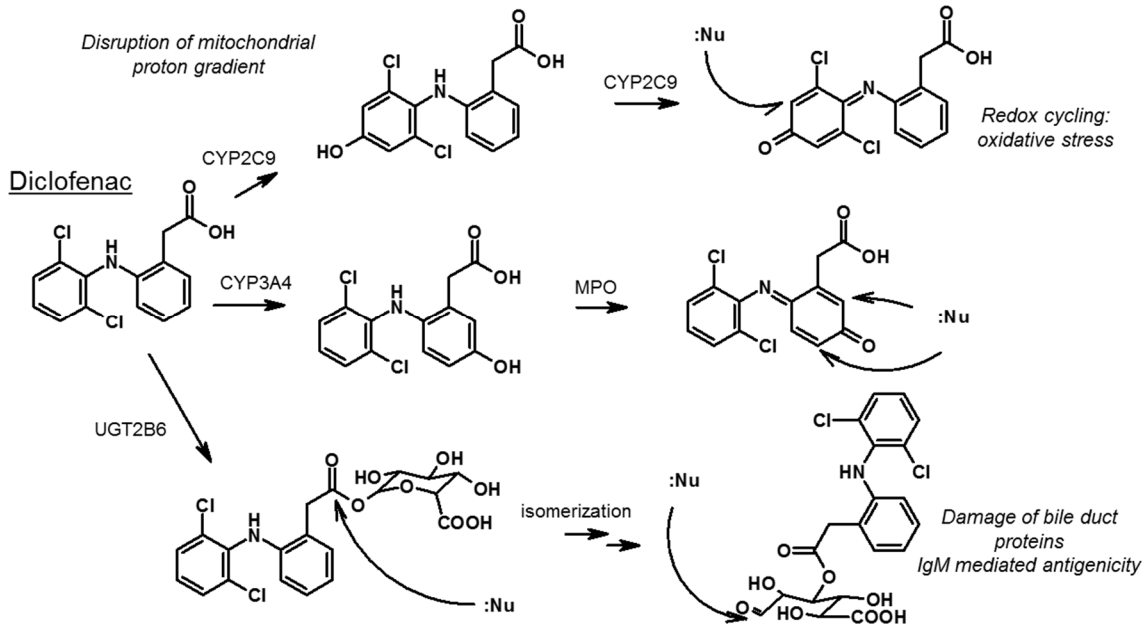

Figure 1.5: Metabolic pathways of diclofenac and their functional consequence

Troglitazone

Troglitazone (TGZ) was the first peroxisome proliferator-activated receptor gamma (PPARγ) agonist from the thiazolidinedione group in use for treatment of type II diabetes [78]. However, the FDA decided to withdraw TGZ from the market in 2000 due to high incidence of reports hepatotoxicity [79, 80].

After numerous studies, several factors contributing to hepatotoxicity have been found (see Figure 1.6). Two structural moieties of TGZ undergo CYP-mediated bioactivation: The chromane moiety can be oxidized to an electrophilic quinone-methide intermediate prone to react with nucleophilic acceptors [81]. Besides, the thiazolidinedione residue can undergo S-oxidation resulting in ring scission with increased electrophilicity. This feature is common within the group of structural analogue glitazone drugs. Rosiglitazone (RGZ) and pioglitazone (PGZ) were also found to form GSH conjugates, but are generally considered as safe [82]. One reason

may be the cytotoxicity caused by TGZ but not RGZ and PGZ in humans [83]. In addition, the parent TGZ and its major sulfate metabolite are related to cholestasis. Both species were found to inhibit the bile salt export pump (BSEP) in rat and human [84, 85]. The resulting intracellular accumulation of bile salts causes mitochondrial toxicity and a loss of membrane potential [86, 87]. Remarkably, RGZ and PGZ possess a similar potential to inhibit BSEP [88].

Summarizing these effects, it can be concluded that hepatotoxicity is related to the TGZ-unique chromane moiety which may, as additional risk factor, induce oxidative stress via redox cycling of the quinone metabolite. Furthermore, the higher dosage as compared to RGZ and PGZ may provoke the manifestation of effects like BSEP inhibition into cholestasis.

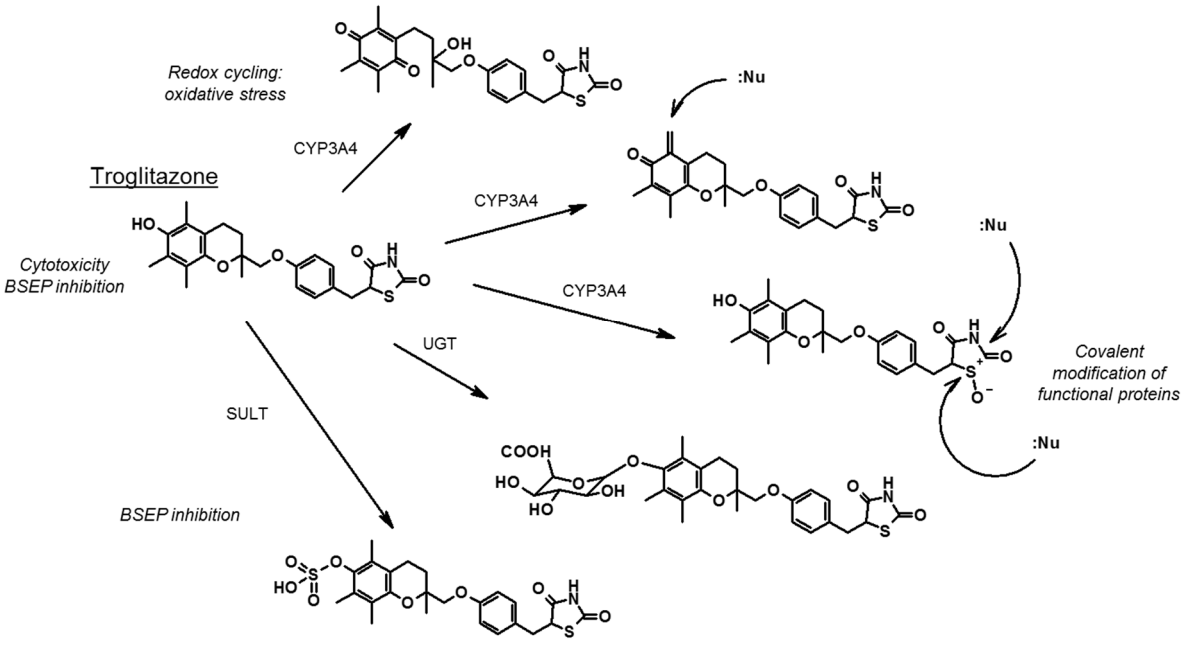

Figure 1.6: Selected metabolic pathways of troglitazone and functional consequence

1.4 Tools for investigation of metabolism and drug safety

1.4.1 Hepatic *in vitro* systems for drug metabolism

To study pharmacokinetic and related safety questions, it is important to use test systems that can mimic the liver with respect to the needed functions, as it would be unethical to conduct early screening and safety studies in humans. Likewise animal experimentation should be applied only when reasonable to assure compliance to the 3R principle of replacement, reduction and refinement in animal testing. Interspecies differences are another reason for waiving them. Thus, several *in vitro* model systems are employed to provide information on selected pathways with different abilities to reflect hepatic function.

Cellular systems

The gold standard for metabolism studies are primary hepatocytes. They provide a realistic image of hepatic biotransformation because all relevant drug-metabolizing enzymes are present and also influence of active and passive transport on cellular drug uptake can be studied. Additionally, changes in gene expression e.g. via enzyme induction can be detected with RNA profiling, protein quantification or functional assays. Metabolism-induced and direct cytotoxicity can be assessed and enables DILI studies. However, cells from different donors may show large interindividual differences such as in activity of polymorphic enzymes. Moreover, access to human tissue is limited and handling and storage with retained viability is laborious. To cope with these problems, techniques like stem cell-derived hepatocytes or tumor derived cell lines have been emerging in the last years. They can be used for specific questions but are not valid to replace functional, mature hepatocytes yet.

Subcellular fractions

Liver microsomes (LM) are the most popular system to investigate hepatic metabolism. These artificial vesicles from the endoplasmatic reticulum comprise mainly CYP enzymes, FMOs and UGTs. They can be prepared easily and pooling of many donors can provide a representative enzyme pattern. Long-time storage without activity loss is possible which facilitates handling and enables high throughput-based applications. However, limitations are the lack of cofactors, which must be added separately to start the enzymatic reaction. Also the enzyme abundance does not represent the *in vivo*

situation and may result in overestimation of oxidative pathways. Another subcellular model for metabolism studies is the S9 fraction. This is the supernatant after centrifugation of cell homogenate at 9000*g* and is comprised by the microsomal and cytosolic fraction. Hence, as compared to LM, it additionally contains sulfotransferases, GSTs, xanthine oxidases (XO), aldehyde dehydrogenases (ADH) and NATs.
Both systems are employed for kinetic and metabolic profiling of a drug, but mainly for inhibition studies in the context of drug-drug interactions.

Recombinant enzymes
The simplest method to study selected metabolic pathways is by using single drug metabolizing enzymes, e.g. CYPs. They can be generated recombinantly in host organisms like yeast, *E. coli* or other bacterial cell lines. Often co-expressed with P450 oxidoreductase they are employed for reaction phenotyping, drug-drug interaction studies (enzyme inhibition) and specialized mechanistic questions. Due to the high concentration of CYPs as compared to other metabolic systems, recombinant enzymes are valuable to study metabolism of stable compounds. However, a full metabolic pattern cannot be deducted and only some specific enzymes are available. To compare results with microsomal activities, correction factors must to be integrated.

1.4.2 Reactive metabolite assessment

Reactive metabolite formation has been generally accepted as one major contributing factor to DILI. Thus, minimization of human exposure to reactive metabolites is desirable and should be controlled by identification of metabolic soft spots early in drug discovery [6].
As electrophilic metabolites have a short lifespan, it is more appropriate to monitor stable reaction products with nucleophilic acceptors. The most reliable way to detect and quantity reactive metabolites is via determination of covalent binding of ^{14}C-radiolabeled compound to cellular proteins in *in vitro* metabolism systems such as hepatocytes or microsomes. After removal of free compound, the protein bound radioactivity can be easily quantified by e.g. scintillation counting. However, synthesis of radiolabeled compound is laborious and thus expensive. Therefore, assays using cold substrate have emerged as well. Most reactive intermediates can be trapped as sulfur-adducts with the soft nucleophilic scavenger GSH. Detection of GSH conjugates

is routinely done with mass spectrometry which allows for untargeted analysis [89, 90]. However, hard electrophiles such as iminium-containing intermediates do not form stable adducts with GSH. They can be trapped using ^{14}C-labeled cyanide as trapping agent and are quantified over radioactivity counting [91]. Also, other preclinical screening assays such as enzyme inhibition assays can give information on binding of reactive species to functional proteins. Time-dependent inhibition of CYP enzymes indicates irreversible conjugation of parent or metabolite to the active or an allosteric site of the enzyme.

1.4.3 Investigation of cellular oxidative stress and related toxicity

Consequences of oxidative stress can be examined on different levels within the cell. These are adaptation of cell homeostasis as a response to oxidative stress, specific damage of cell organelles, or cytotoxicity, all providing different types of information.
To monitor cellular adaptation towards pro-oxidant states, it is beneficial to observe effects related to the antioxidant response pathway. For example, the increased transcription of genes encoding for cytoprotective proteins manifests in elevated mRNA levels. Activity determination of dependent antioxidant enzymes (e.g. SOD, GSH peroxidase, and catalase) or agents (e.g. ascorbate, tocopherol) may serve as complementary markers. Most frequently GSH depletion or dimerization is used as analytical marker [92]. These adaptive processes indicate alterations in the cellular health state, also transient or prolonged ones, early before overt damage occurs. However, it may be difficult to decide whether changes are physiological or will result in pathological effects.
Another strategy is the detection of modified end-products that do not occur physiologically, such as carbonylation of amino acid residues due to protein oxidation or 8-hydroxy-2'-deoxyguanosine formation due to DNA oxidation. Lipid peroxidation can be determined via conjugates of specifically formed aldehydes, malondialdehyde and 4-hydroxynonenal, both cleavage products of peroxidized polyunsaturated fatty acids. Peroxidation of arachidonic acid gives rise to isoprostanes, the *cis*-isomers to the prostaglandins. They are chemically stable and can be measured from different biological fluids noninvasively. These markers clearly indicate a pathophysiological excess of pro-oxidant species that the cell cannot balance anymore. Still, in some

cases this damage may be repaired whereas in others it may be persistent and result in cell toxicity.

Finally, it is possible to monitor effects based on major functional impairment or even cell death, such as deficient ATP production or cell membrane leakage via extracellular occurrence of lactate dehydrogenase (LDH), or alanine aminotransferase (ALT) and aspartate aminotransferase (AST) *in vivo*. However, these markers can only reveal evident toxic effects and do not give insight on preceding mechanistic pathways. In summary all groups of markers are complementary and contribute to a comprehensive picture of mechanisms and outcomes of disturbance of cell homeostasis.

1.4.4 DILI in drug development: Screening approaches

The illustrated examples show that many aspects of idiosyncratic DILI remain unclear and that working hypotheses cannot be translated to all cases. Therefore, the perception of valuable safety assessment moved away from isolated evaluation of bioactivation towards the generation of differentiated mechanistic information on a drug's toxicity risk as illustrated in Figure 1.7. Experience from drug discovery showed that the simplification 'structural alert = bioactivation = toxicity' does not apply, mainly because *in vivo* metabolism often differs from the detected *in vitro* pathways [93]. However, as reactive metabolite formation is the only accepted evidence in the development of DILI, use of this information as a starting point for risk assessment is reasonable. Recent approaches improved the safety prediction of absolute covalent binding data by normalizing to the dose [5, 31, 48, 94] or by estimation of a covalent binding body burden [3, 95]. Still, false positive and false negative results are remaining and consequently it was suggested to consider mechanistic effects on cell health state to characterize compounds reliably [7]. Thompson and coworkers applied this strategy by defining a panel of *in vitro* assays addressing cellular endpoints. Together with covalent binding data, these were then combined to an integrated in vitro hazard matrix which allowed for distinction of a safe and different hazard zones [96]. However, most development drug candidates possess at least some *in vitro* alerts that would translate into a hazard. Thus, an evaluation of *in vivo* risk would remain problematic for them.

In summary, recognition of the complexity of idiosyncratic toxicity in the last years resulted in the creation of integrated mitigation strategies which may compensate for incomplete mechanistic understanding of DILI. However, all attempts show that a comprehensive risk assessment is not possible from the existing *in vitro* tools yet.

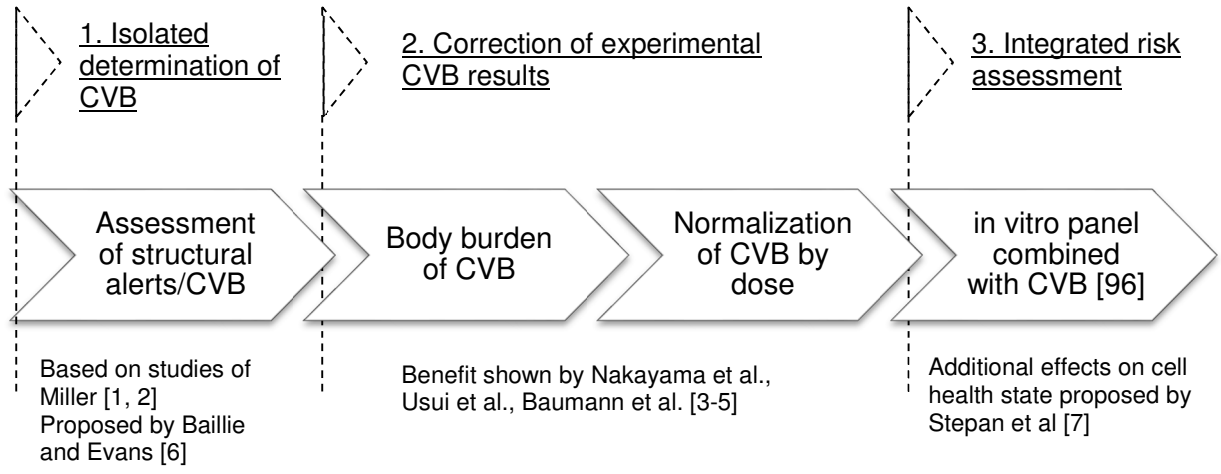

Figure 1.7. Changing understanding of reasonable safety assessment for DILI from covalent binding determination to an integrated mitigation strategy.

1.5 References

1. Miller, J.A., Carcinogenesis by chemicals: an overview--G. H. A. Clowes memorial lecture. Cancer Res, 1970. 30(3): p. 559-76.
2. Miller, J.A., Brief history of chemical carcinogenesis. Cancer Lett, 1994. 83(1-2): p. 9-14.
3. Bauman, J.N., et al., Can in vitro metabolism-dependent covalent binding data distinguish hepatotoxic from nonhepatotoxic drugs? An analysis using human hepatocytes and liver S-9 fraction. Chem Res Toxicol, 2009. 22(2): p. 332-40.
4. Nakayama, S., et al., Combination of GSH trapping and time-dependent inhibition assays as a predictive method of drugs generating highly reactive metabolites. Drug Metab Dispos, 2011. 39(7): p. 1247-54.
5. Usui, T., et al., Evaluation of the potential for drug-induced liver injury based on in vitro covalent binding to human liver proteins. Drug Metab Dispos, 2009. 37(12): p. 2383-92.
6. Evans, D.C. and T.A. Baillie, Minimizing the potential for metabolic activation as an integral part of drug design. Current Opinion in Drug Discovery and Development, 2005. 8(1): p. 44-50.
7. Stepan, A.F., et al., Structural alert/reactive metabolite concept as applied in medicinal chemistry to mitigate the risk of idiosyncratic drug toxicity: a perspective based on the critical examination of trends in the top 200 drugs marketed in the United States. Chem Res Toxicol, 2011. 24(9): p. 1345-410.
8. Watkins, P.B. and L.B. Seeff, Drug-induced liver injury: summary of a single topic clinical research conference. Hepatology, 2006. 43(3): p. 618-31.
9. Ostapowicz, G., et al., Results of a prospective study of acute liver failure at 17 tertiary care centers in the United States. Ann Intern Med, 2002. 137(12): p. 947-54.
10. Temple, R., Drug-Induced Liver Injury Impacts on the Food and Drug Administration (FDA), in Drug-Induced Liver Injury: A National and Global Problem 2001: Westfields Conference Center, Chantilly VA.
11. Hussaini, S.H. and E.A. Farrington, Idiosyncratic drug-induced liver injury: an update on the 2007 overview. Expert Opin Drug Saf, 2014. 13(1): p. 67-81.
12. Meier, Y., et al., Incidence of drug-induced liver injury in medical inpatients. Eur J Clin Pharmacol, 2005. 61(2): p. 135-43.
13. Hoofnagle, J.H., Drug-induced liver injury network (DILIN). Hepatology, 2004. 40(4): p. 773.
14. Drugs that are kinder to the liver - new collaborative project "MIP-DILI". 2012.
15. Evans, W.E. and M.V. Relling, Pharmacogenomics: translating functional genomics into rational therapeutics. Science, 1999. 286(5439): p. 487-91.
16. Fontana, R.J., et al., Standardization of nomenclature and causality assessment in drug-induced liver injury: summary of a clinical research workshop. Hepatology, 2010. 52(2): p. 730-42.
17. Devarbhavi, H., An Update on Drug-induced Liver Injury. J Clin Exp Hepatol, 2012. 2(3): p. 247-259.
18. Tujios, S. and R.J. Fontana, Mechanisms of drug-induced liver injury: from bedside to bench. Nat Rev Gastroenterol Hepatol, 2011. 8(4): p. 202-11.
19. Temple, R., Hy's law: predicting serious hepatotoxicity. Pharmacoepidemiol Drug Saf, 2006. 15(4): p. 241-3.
20. Stine, J.G. and J.H. Lewis, Hepatotoxicity of antibiotics. A review and update for the clinician. Clinics in liver disease, 2013. 17(4): p. 609-642.
21. Horng, H., H. Spahn-Langguth, and L.Z. Benet, Mechanistic role of acyl glucuronides, in Drug-Induced Liver Disease. 2013. p. 35-70.
22. Mutschler, E., et al., Chemotherapie maligner Tumoren, in Mutschler Arzneimittelwirkungen. 2001, Wissneschaftliche Verlagsgesellschaft mbH Stuttgart. p. 873-907.
23. de Jonge, M.E., et al., Clinical pharmacokinetics of cyclophosphamide. Clin Pharmacokinet, 2005. 44(11): p. 1135-64.
24. Cox, P.J., Cyclophosphamide cystitis--identification of acrolein as the causative agent. Biochem Pharmacol, 1979. 28(13): p. 2045-9.
25. Levine, E.S., et al., Cardiac cell toxicity induced by 4-hydroperoxycyclophosphamide is modulated by glutathione. Cardiovasc Res, 1993. 27(7): p. 1248-53.
26. DeLeve, L.D., Cellular target of cyclophosphamide toxicity in the murine liver: role of glutathione and site of metabolic activation. Hepatology, 1996. 24(4): p. 830-7.
27. Uetrecht, J., Idiosyncratic drug reactions: past, present, and future. Chem Res Toxicol, 2008. 21(1): p. 84-92.

28. Landsteiner, K. and J. Jacobs, Studies on the sensitization of animals with simple chemical compounds. J Exp Med, 1935. 61: p. 643-656.
29. Weltzien, H.U. and E. Padovan, Molecular features of penicillin allergy. J Invest Dermatol, 1998. 110(3): p. 203-6.
30. Parker, C.W., et al., The preparation and some properties of penicillenic acid derivatives relevant to penicillin hypersensitivity. The Journal of experimental medicine, 1962. 115: p. 803-819.
31. Nakayama, S., et al., A zone classification system for risk assessment of idiosyncratic drug toxicity using daily dose and covalent binding. Drug Metab Dispos, 2009. 37(9): p. 1970-7.
32. Matzinger, P., An innate sense of danger. Semin Immunol, 1998. 10(5): p. 399-415.
33. Harris, H.E. and A. Raucci, Alarmin(g) news about danger: workshop on innate danger signals and HMGB1. EMBO Rep, 2006. 7(8): p. 774-8.
34. Roth, R.A., et al., Inflammation and drug idiosyncrasy - Is there a connection? Journal of Pharmacology and Experimental Therapeutics, 2003. 307(1): p. 1-8.
35. Zanni, M.P., et al., HLA-restricted, processing- and metabolism-independent pathway of drug recognition by human alpha beta T lymphocytes. J Clin Invest, 1998. 102(8): p. 1591-8.
36. Schnyder, B., et al., Direct, MHC-dependent presentation of the drug sulfamethoxazole to human alphabeta T cell clones. J Clin Invest, 1997. 100(1): p. 136-41.
37. Pichler, W.J., Pharmacological interaction of drugs with antigen-specific immune receptors: the p-i concept. Curr Opin Allergy Clin Immunol, 2002. 2(4): p. 301-5.
38. Uetrecht, J., Idiosyncratic drug reactions: current understanding. Annu Rev Pharmacol Toxicol, 2007. 47: p. 513-39.
39. Pessayre, D., et al., Hepatotoxicity due to mitochondrial dysfunction. Cell Biol Toxicol, 1999. 15(6): p. 367-73.
40. Roth, R.A., et al., Inflammation and drug idiosyncrasy--is there a connection? J Pharmacol Exp Ther, 2003. 307(1): p. 1-8.
41. Bjornsson, E. and R. Olsson, Outcome and prognostic markers in severe drug-induced liver disease. Hepatology, 2005. 42(2): p. 481-9.
42. Takikawa, H., et al., Drug-induced liver injury in Japan: An analysis of 1676 cases between 1997 and 2006. Hepatology research : the official journal of the Japan Society of Hepatology, 2009. 39(5): p. 427-31.
43. Dreifuss, F.E., et al., Valproic acid hepatic fatalities: a retrospective review. Neurology, 1987. 37(3): p. 379-85.
44. Zimmerman, H.J., Effects of aspirin and acetaminophen on the liver. Arch Intern Med, 1981. 141(3 Spec No): p. 333-42.
45. Bell, L.N. and N. Chalasani, Epidemiology of idiosyncratic drug-induced liver injury. Seminars in liver disease, 2009. 29(4): p. 337-47.
46. Larrey, D., Epidemiology and individual susceptibility to adverse drug reactions affecting the liver. Seminars in liver disease, 2002. 22(2): p. 145-55.
47. Vuppalanchi, R. and N. Chalasani, Risk factors for drug-induced liver disease, in Drug-Induced Liver Disease. 2013. p. 265-274.
48. Lammert, C., et al., Relationship between daily dose of oral medications and idiosyncratic drug-induced liver injury: search for signals. Hepatology, 2008. 47(6): p. 2003-9.
49. Lammert, C., et al., Oral medications with significant hepatic metabolism at higher risk for hepatic adverse events. Hepatology, 2010. 51(2): p. 615-20.
50. Chalasani, N. and E. Bjornsson, Risk factors for idiosyncratic drug-induced liver injury. Gastroenterology, 2010. 138(7): p. 2246-59.
51. Kalgutkar, A.S., et al., A comprehensive listing of bioactivation pathways of organic functional groups. Curr Drug Metab, 2005. 6(3): p. 161-225.
52. Dansette, P.M., et al., Hydroxylation and formation of electrophilic metabolites of tienilic acid and its isomer by human liver microsomes. Catalysis by a cytochrome P450 IIC different from that responsible for mephenytoin hydroxylation. Biochem Pharmacol, 1991. 41(4): p. 553-60.
53. Mallal, S., et al., HLA-B*5701 screening for hypersensitivity to abacavir. N Engl J Med, 2008. 358(6): p. 568-79.
54. Singer, J.B., et al., A genome-wide study identifies HLA alleles associated with lumiracoxib-related liver injury. Nat Genet, 2010. 42(8): p. 711-4.
55. Lucena, M.I., et al., Susceptibility to amoxicillin-clavulanate-induced liver injury is influenced by multiple HLA class I and II alleles. Gastroenterology, 2011. 141(1): p. 338-47.

56. Kindmark, A., et al., Genome-wide pharmacogenetic investigation of a hepatic adverse event without clinical signs of immunopathology suggests an underlying immune pathogenesis. Pharmacogenomics J, 2008. 8(3): p. 186-95.
57. Kuthan, H. and V. Ullrich, Oxidase and oxygenase function of the microsomal cytochrome P450 monooxygenase system. Eur J Biochem, 1982. 126(3): p. 583-8.
58. McGill, M.R. and H. Jaeschke, Oxidant stress, antioxidant defense, and liver injury, in Drug-Induced Liver Disease. 2013. p. 71-84.
59. Avery, S.V., Molecular targets of oxidative stress. Biochem J, 2011. 434(2): p. 201-10.
60. Recknagel, R.O. and A.K. Ghoshal, Lipoperoxidation as a vector in carbon tetrachloride hepatotoxicity. Lab Invest, 1966. 15(1 Pt 1): p. 132-48.
61. Comporti, M., et al., F2-isoprostanes stimulate collagen synthesis in activated hepatic stellate cells: a link with liver fibrosis? Lab Invest, 2005. 85(11): p. 1381-91.
62. Copple, I.M., et al., The keap1-nrf2 cellular defense pathway: mechanisms of regulation and role in protection against drug-induced toxicity. Handb Exp Pharmacol, 2010(196): p. 233-66.
63. Reed, D.J., Glutathione: toxicological implications. Annu Rev Pharmacol Toxicol, 1990. 30: p. 603-31.
64. Di Monte, D., et al., Alterations in intracellular thiol homeostasis during the metabolism of menadione by isolated rat hepatocytes. Arch Biochem Biophys, 1984. 235(2): p. 334-42.
65. Brigelius, R. and M.S. Anwer, Increased biliary GSSG-secretion and loss of hepatic glutathione in isolated perfused rat liver after paraquat treatment. Res Commun Chem Pathol Pharmacol, 1981. 31(3): p. 493-502.
66. Liebler, D.C. and F.P. Guengerich, Elucidating mechanisms of drug-induced toxicity. Nat Rev Drug Discov, 2005. 4(5): p. 410-20.
67. O'Connor, N., P.I. Dargan, and A.L. Jones, Hepatocellular damage from non-steroidal anti-inflammatory drugs. Qjm, 2003. 96(11): p. 787-91.
68. Mindikoglu, A.L., L.S. Magder, and A. Regev, Outcome of liver transplantation for drug-induced acute liver failure in the United States: analysis of the United Network for Organ Sharing database. Liver transplantation : official publication of the American Association for the Study of Liver Diseases and the International Liver Transplantation Society, 2009. 15(7): p. 719-29.
69. Aithal, G.P., et al., Relationship of polymorphism in CYP2C9 to genetic susceptibility to diclofenac-induced hepatitis. Pharmacogenetics, 2000. 10(6): p. 511-8.
70. Daly, A.K., et al., Genetic susceptibility to diclofenac-induced hepatotoxicity: contribution of UGT2B7, CYP2C8, and ABCC2 genotypes. Gastroenterology, 2007. 132(1): p. 272-81.
71. Masubuchi, Y., S. Yamada, and T. Horie, Possible mechanism of hepatocyte injury induced by diphenylamine and its structurally related nonsteroidal anti-inflammatory drugs. J Pharmacol Exp Ther, 2000. 292(3): p. 982-7.
72. Bort, R., et al., Diclofenac toxicity to hepatocytes: a role for drug metabolism in cell toxicity. J Pharmacol Exp Ther, 1999. 288(1): p. 65-72.
73. Boelsterli, U.A., Diclofenac-induced liver injury: a paradigm of idiosyncratic drug toxicity. Toxicol Appl Pharmacol, 2003. 192(3): p. 307-22.
74. Cantoni, L., et al., Induction of hepatic heme oxygenase-1 by diclofenac in rodents: role of oxidative stress and cytochrome P-450 activity. Journal of hepatology, 2003. 38(6): p. 776-83.
75. Takakusa, H., et al., Markers of electrophilic stress caused by chemically reactive metabolites in human hepatocytes. Drug Metab Dispos, 2008. 36(5): p. 816-23.
76. Galati, G., et al., Idiosyncratic NSAID drug induced oxidative stress. Chem Biol Interact, 2002. 142(1-2): p. 25-41.
77. Bougie, D., et al., Sensitivity to a metabolite of diclofenac as a cause of acute immune hemolytic anemia. Blood, 1997. 90(1): p. 407-13.
78. Reginato, M.J. and M.A. Lazar, Mechanisms by which Thiazolidinediones Enhance Insulin Action. Trends Endocrinol Metab, 1999. 10(1): p. 9-13.
79. Henney, J., From the Food and Drug Administration: Withdrawal of Troglitazone and Cisapride. JAMA, 2000. 283(10): p. 2228.
80. Vella, A., P.C. de Groen, and S.F. Dinneen, Fatal hepatotoxicity associated with troglitazone. Ann Intern Med, 1998. 129(12): p. 1080.
81. Tettey, J.N., et al., Enzyme-induction dependent bioactivation of troglitazone and troglitazone quinone in vivo. Chem Res Toxicol, 2001. 14(8): p. 965-74.
82. Alvarez-Sanchez, R., et al., Thiazolidinedione bioactivation: a comparison of the bioactivation potentials of troglitazone, rosiglitazone, and pioglitazone using stable isotope-labeled analogues and liquid chromatography tandem mass spectrometry. Chem Res Toxicol, 2006. 19(8): p. 1106-16.

83. Honma, W., et al., Phenol sulfotransferase, ST1A3, as the main enzyme catalyzing sulfation of troglitazone in human liver. Drug Metab Dispos, 2002. 30(8): p. 944-9.
84. Yabuuchi, H., et al., Cloning of the dog bile salt export pump (BSEP; ABCB11) and functional comparison with the human and rat proteins. Biopharm Drug Dispos, 2008. 29(8): p. 441-8.
85. Funk, C., et al., Troglitazone-induced intrahepatic cholestasis by an interference with the hepatobiliary export of bile acids in male and female rats. Correlation with the gender difference in troglitazone sulfate formation and the inhibition of the canalicular bile salt export pump (Bsep) by troglitazone and troglitazone sulfate. Toxicology, 2001. 167(1): p. 83-98.
86. Krahenbuhl, S., et al., Toxicity of bile acids on the electron transport chain of isolated rat liver mitochondria. Hepatology, 1994. 19(2): p. 471-9.
87. Tirmenstein, M.A., et al., Effects of troglitazone on HepG2 viability and mitochondrial function. Toxicol Sci, 2002. 69(1): p. 131-8.
88. Paehler, A. and C. Funk, Drug-induced hepatotoxicity: Learning from recent cases of drug attrition, in Advances in Molecular Toxicology. 2008. p. 25-56.
89. Dieckhaus, C.M., et al., Negative ion tandem mass spectrometry for the detection of glutathione conjugates. Chem Res Toxicol, 2005. 18(4): p. 630-8.
90. Wen, B., et al., High-throughput screening and characterization of reactive metabolites using polarity switching of hybrid triple quadrupole linear ion trap mass spectrometry. Anal Chem, 2008. 80(5): p. 1788-99.
91. Argoti, D., et al., Cyanide trapping of iminium ion reactive intermediates followed by detection and structure identification using liquid chromatography-tandem mass spectrometry (LC-MS/MS). Chem Res Toxicol, 2005. 18(10): p. 1537-44.
92. Therond, P., et al., Biomarkers of oxidative stress: an analytical approach. Curr Opin Clin Nutr Metab Care, 2000. 3(5): p. 373-84.
93. Kalgutkar, A.S. and M.T. Didiuk, Structural alerts, reactive metabolites, and protein covalent binding: how reliable are these attributes as predictors of drug toxicity? Chem Biodivers, 2009. 6(11): p. 2115-37.
94. Sakatis, M.Z., et al., Preclinical strategy to reduce clinical hepatotoxicity using in vitro bioactivation data for >200 compounds. Chem Res Toxicol, 2012. 25(10): p. 2067-82.
95. Obach, R.S., et al., Can in vitro metabolism-dependent covalent binding data in liver microsomes distinguish hepatotoxic from nonhepatotoxic drugs? An analysis of 18 drugs with consideration of intrinsic clearance and daily dose. Chem Res Toxicol, 2008. 21(9): p. 1814-22.
96. Thompson, R.A., et al., Risk assessment and mitigation strategies for reactive metabolites in drug discovery and development. Chem Biol Interact, 2011. 192(1-2): p. 65-71.

2 OBJECTIVE OF THE WORK

This work was conducted to establish improved *in vitro* testing strategies to address risk factors for DILI in context with metabolic drug activation. Thus, the goal was a better differentiation between safe and DILI drugs.

Bioactivation potential should be evaluated in combination with pharmacokinetic properties as surrogate for DILI risk. As complementary tool to current risk assessment, robust safety biomarkers from non-invasive sources should be identified and validated with DILI model compounds. The main focus was on investigation of oxidative stress. This compound-related risk factor for hepatotoxicity gives insight into cellular mechanisms and may also serve as markers for monitoring of patients. Overall, an extrapolation across species from rodent to human as well as from *in vitro* model systems to the *in vivo* situation should be established.

3 RESULTS AND DISCUSSION

3.1 The value of bioactivation assessment for the prediction of DILI

Can Drug-Induced Liver Injury Correctly Be Classified by Quantitative Covalent Binding Assessment?

Marieke Teppner[1 2], Isabelle Walter[1], Charles Tournillac[1], Sandrine Simon[1], Bernd Steinhuber[1], Andreas Brink[1], Antonello Caruso[1], Neil Parrott[1], Beat Ernst[2] and Axel Pähler[1]

[1] DMPK, Pharmaceutical Sciences; Pharma Research and Early Development (pRED); F. Hoffmann-La Roche Ltd., Grenzacherstrasse 124; CH-4070 Basel, Switzerland

[2] Institute of Molecular Pharmacy; University of Basel, Klingenbergstrasse 50; CH-4040 Basel, Switzerland

Draft version.

Personal contribution: Data collection, correlation and interpretation; manuscript preparation

Abstract

Idiosyncratic drug-induced liver injury (DILI) is a major concern for pharmaceutical industry. Chemical reactive drug metabolites (RM) and subsequent covalent protein binding (CVB) are believed to contribute to mechanisms leading to DILI. Various efforts have been made in the past to proof or disproof the correlation between CVB properties, daily dose and other pharmacokinetic properties and a drug's susceptibility to cause DILI. Most of the concepts including the 'zone classification system' previously established by Nakayama suffer from a high number of false positive correlations or equivocal classifications. Here, we examined a large set of 91 drugs with different history of DILI. An improved classification of DILI properties from 85 to 94% correctly classified compounds was achieved by correcting CVB by intrinsic clearance. A further improvement to 97% correct classifications was achieved by substituting daily dose by the hepatic inlet concentration, determined by systematic concentration and absorption. As the intrinsic property of covalent binding alone does not correlate quantitatively with DILI risk, we propose to use microsomal glutathione (GSH) trapping as binary output and surrogate for CVB. A good correlation to high risk DILI drugs was evident, especially when integrating daily dose. Here, a sensitivity of 78% and a specificity of 94% for correct classification were achieved. Even though GSH trapping may miss certain electrophiles and phase II bioactivation is not captured in microsomes, fewer false negative classifications were observed than by hepatocyte CVB. In contrast, the integration of drugs with intermediate risk for DILI (based on case reports) decreased the correlation significantly. This may be due to misleading classification but also to the fact that mechanisms independent from bioactivation are involved in development of DILI.

Introduction

Idiosyncratic drug-induced liver injury (DILI) is a major concern for pharmaceutical industry as it occurs only rarely, but is often related to serious outcomes such as liver failure and death. Due to the low frequency and poor predictability in preclinical studies, DILI has led to late stage attrition or withdrawal of promising new medical treatments [1, 2]. Investigation of case examples of affected drugs led to the generation of different hypothesis for the development of DILI which suggest an involvement of chemical reactive metabolites. These may be able to exert covalent binding (CVB) to cellular macromolecules and damage their function, a process which is generally accepted as initializing or at least contributing mechanism to DILI. Therefore assessment of CVB properties of a drug is nowadays frequently conducted in drug discovery with the aim to reduce bioactivation to a minimum [3].

However, a growing body of evidence exists on the fact that CVB does not determine toxicity alone, including qualitative and quantitative aspects. Some drugs that exhibit CVB do not cause problems in clinics and some drugs that bind to proteins to a high extent exhibit less toxicity than others with a low degree of CVB. These findings suggest that additional risk factors must be involved in modulation of DILI response [4, 5].

The original approach of quantitative determination of CVB from microsomal matrix was able to detect hepatotoxins [6], however resulting in many false positive results due to the exaggerated ratio of bioactivation relative to detoxification pathways. Therefore, hepatocytes were then selected as more appropriate system which accounted for phase II conjugation reactions as alternative or detoxification pathways besides oxidative bioactivation. The gained quantitative improvement could still did not result in the avoidance of false correlations. It was therefore attempted to incorporate relevant pharmacokinetic parameters that could normalize the amount of *in vitro* CVB to its relevant equivalent *in vivo*. Bauman et al. used a ‘total body burden of CVB’ (calculated from total and CVB related intrinsic clearance together with the daily dose) as correction factor for absolute data to improve separation of hepatotoxins and non hepatotoxins [7]. The finding, that a relationship exists between daily dose and DILI [8] was also applied by Nakayama et al.. The authors established a ‘zone classification system’ for toxic versus safe drugs by multiplication of hepatocyte CVB data and daily dose as decision criteria [9]. Here, it was possible for the first time to cluster

compounds based on bioactivation properties. Based on this knowledge Satakis and coworkers designed a decision tree for continuation or termination of suspicious drug candidates using clinical dose and an '*in vitro* reactive metabolite assay signal' [10]. As none of these approaches could avoid an overlap of toxic and non-toxic compounds with false positive and false negative outcomes, Thompson at al. defined an '*in vitro* hazard matrix' comprised by a CVB burden together with cellular toxicity endpoints as additional risk factors for DILI [11]. With this approach the authors managed to eliminate false negative, but not false positive results. Although this approach eliminates the risk of moving potential DILI drugs into clinical development, this approach likewise is overly sensitive and may unduly eliminate potentially safe and efficacious new drugs. This shortcoming of most approaches applied to reactive metabolite characterization during drug discovery and early development has recently been summarized by a consortium of scientists from pharmaceutical industry and academia [12]. The considerations in this article that for the first time attempted to reflect a consensus on common strategy regarding reactive metabolite characterization proposes daily dose as critical input parameter to DILI risk.

The rationale of the described strategies to incorporate dose or clearance was to more precisely and realistically estimate the drug's exposure to the body, in particular the liver. Exposure is influenced by various factors from all pharmacokinetic phases which need to be considered for evaluation. Namely, the fraction absorbed, first-pass intestinal metabolism, systematic distribution, fraction of hepatic (first pass) metabolism and elimination modulate the total *in vivo* exposure. In this study, we evaluated the contribution of different input variables to the correct classification of DILI outcomes for a dataset of 91 drugs by statistical approaches. The aim was to numerically describe risk factors for DILI by incorporation of normalized daily dose (body burden) and other pharmacokinetic parameters in order to provide a numerical classification of critical parameters such as "high" and "low" dose. *In vitro* microsomal intrinsic clearance or the theoretical liver inlet concentration as correction factors were incorporated into CVB data to better classify DILI drugs. We used a comprehensive data set of 91 drugs with and without DILI history, having CVB data for 51 of them. For these compounds the relationship between CVB properties and daily dose as originally shown by Nakayama was applied and compared to the proposed new correlation models. To account for the supposed small impact of absolute CVB, the potential to replace quantitative CVB data by qualitative bioactivation data was investigated as

well. The ability of drugs to form stable glutathione (GSH)-drug conjugates was evaluated as binary output.

In vitro data was generated in house and completed with data from literature. Clinical pharmacokinetic data was extracted from literature. It has to be noted that most of the chosen toxic compounds cause hepatotoxicity as adverse endpoint. However, also some drugs whose idiosyncrasy manifests in immune- or hemotoxicity were included. It is believed that underlying mechanisms are comparable or mediated via similar pathways. All results were investigated by ordinal logistic regression and confusion matrix evaluation as statistical tools.

Material and Methods

Chemicals

Williams' medium E, dimethyl sulfoxide p.a., formic acid p.a., insulin, streptomycin, penicillin, hydrocortisone, glucose-6-phosphate disodium salt hydrate, β-nicotinamide adenine dinucleotide phosphate hydrate (NADP), were obtained from Sigma Aldrich (St. Louis, MO, USA). Glutamine, gentamycin were purchased from Life Technologies Invitrogen (Lucerne, Switzerland) and acetonitrile LC-MS grade from Fisher Scientific (Wohlen, Switzerland). Water of chromatography grade and magnesium dichloride ($MgCl_2$) was obtained from Merck (Darmstadt, Germany). Radiolabeled and unlabeled compounds were synthesized in house. Human liver microsomes were purchased from BD Biosciences, Woburn, MA.

CVB to human hepatocytes

For 51 marketed compounds CVB data was received from different sources which were either from in house studies or published results (in house, n=11; Nakayama et al., n=33 [9]; Thompson et al., n=4 [11]; Bauman et al., n=2 [7]; Lévesque et al., n=1 [13]) using a comparable experimental setup. For the in house experiment procedure was as follows: Human cryopreserved hepatocytes were thawed in accordance to the supplier's protocol and diluted to a final concentration of 10^6 cells / ml in incubation medium. After 15 minutes of pre-incubation 10 µM ^{14}C-radiolabeled compound was added and cells were kept at 37°C in a humidified atmosphere (5% CO_2/95% air) for 3 h. Incubation was stopped by precipitation with one volume of acetonitrile on a filter plate (Multiscreen deep well solvinert, Millipore). After 15 min of mixing, the plate was centrifuged at 20°C for 20 min at 1800*g*, collecting the filtrate into a deep well plate. The remaining precipitate was washed 8 times with MeOH/0.1%H_2SO_4, collecting the eluting wash solution in four portions by centrifugation for 3 min at 1500*g*. An aliquot of the filtrate and each wash step was transferred to labeled microscintilation plate (LumaPlate™-96, Perkin Elmer) and radioactivity measured on a scintillation counter (Topcount NXT HTS, Perkin Elmer) to determine recovery of radiolabeled compound and progress of the wash steps.

The amount of CVB was calculated from the non-extractable radioactivity after solubilization of the denaturated protein with 0.1 M NaOH/1% SDS as determined by

β-scintillation counting (TriCarb 3100 TR, Packard) and colorimetric determination of the protein concentration, as shown in Equation 3.1.1.

$$CVB\left[\frac{pmol}{mg}\right] = \frac{meas.act.[\mu Ci]}{spec.act.[\frac{\mu Ci}{pmol}]} * \left(protein.conc\left[\frac{mg}{mL}\right]\right)^{-1} * (sample\_volume\ [mL])^{-1} \quad \textbf{Eq. 3.1.1}$$

GSH trapping assay

Human liver microsomes at a concentration of 1 mg/mL were incubated with 20 µM compound in 0.1 M sodium phosphate buffer substituted with 1 mM NADPH and 5 mM GSH. After 60 minutes incubation time reaction was stopped by adding one volume acetonitrile Organic solvent was then evaporated under a stream of nitrogen. After centrifugation at 5000*g* at 4°C for 10 min samples were injected to the LC-MS system.

LC-MS analysis of GSH trapping samples

LC-MS/MS analysis were performed on a triple quadrupole mass spectrometer (QTRAP 4000, AB Sciex, Warrington, UK) interfaced with a Shimadzu high performance liquid chromatography system. Analytes evaporated sample were enriched and separated by on-line SPE coupled chromatography within 14 min. Mass spectrometric detection was executed in negative electrospray ionization mode using a precursor ion (PI) scan with dependent enhanced resolution (ER) and enhanced product ion (EPI) scan. This method was previously reported by others [14, 15].

Human liver microsomal stability assay

Compounds were dissolved in DMSO to obtain a 4 mM stock solution which was further diluted in incubation medium for use in experiments. Microsomal incubation was prepared by supplementation of 0.1 M sodium phosphate buffer (pH 7.4) with 3 mM glucose 6 phosphate, 0.5 mg/mL HLM, 3 mM $MgCl_2$ and 10 µM of the respective compound. Incubation was started by addition of 1 mM NADPH and stopped after 1, 3, 6, 9, 15, 25, 35, and 45 min by precipitation with three volumes acetonitrile containing internal standard. Samples were analyzed using LC-MS/MS (see there). Intrinsic clearance was calculated with the slope of the degradation curve as depicted in Equation 3.1.2 and 3.1.3.

$$t_{1/2}[min] = \frac{ln2}{k[min^{-1}]} \quad \textbf{Eq. 3.1.2}$$

$$CL_{int} = \frac{ln2 * V}{t_{1/2}}$$ **Eq. 3.1.3**

LC-MS/MS analysis of in vitro stability samples

The system consisted of a Shimadzu HPLC connected to a triple quadrupole tandem mass spectrometer (5500 QTRAP, AB Sciex, UK) equipped with either a XBridge phenyl column, 3.5 µm, 1.0 x 50 mm (Waters, Ireland) or with an Supelco Ascentis express C18 column, 2.7 µm, 2.1 x 20 mm (Sigma-Aldrich, St. Louis, MO). Two microliter sample were injected to the system and separated by gradient elution with mobile phase one consisting of water containing 0.5% formic acid/methanol (eluent A1; 95/5, v/v) and methanol (eluent B1) or mobile phase two consisting of water containing 20 mM ammonium bicarbonate/methanol (eluent A2; 95/5, v/v) and methanol (eluent B2). The gradient started with a total flow of 0.500 ml/min at 100% A which was kept for 0.07 min. Eluent B was then increased in a ballistic-shaped manner from 0% to 100% within 0.7 min. The flow was increased to 0.700 ml/min and the system flushed with 100% B for 0.18 min. From 0.91 to the end of the run at 1.4 min the system was re-equilibrated with 100% eluent A. MS detection was performed by selected reaction monitoring. Tuning parameters were defined for each analyte by the help of compound standards in positive or negative electrospray ionization mode depending on structural properties.

Calculation of liver inlet concentration

For the calculation of a theoretical liver inlet concentration ($[I]_{in}$, Equation 3.1.4) the sum of the systematic average ($[I]_{av}$, Equation 3.1.5) and the uptake to the liver was calculated considering the following parameters: logD at pH 6.0, polar surface area (PSA), absorption rate constant (k_a, Equation 3.1.6), clearance after oral dose (CL/F), dose (D), dose interval (τ), fraction of dose reaching the portal vein (F_{Dp}=fraction absorbed x fraction escaping gut metabolism) and hepatic blood flow (Q_h).

$$[I]_{in} = [I]_{av} + \frac{k_a * F_{Dp} * D}{Q_h}$$ **Eq. 3.1.4**

$$[I]_{av} = \frac{D/\tau}{CL/F}$$ **Eq. 3.1.5**

$$\log k_a = 0.623 + 0.154 * \log D_{6.0} - 0.007 * PSA \quad [16] \qquad \textbf{Eq. 3.1.6}$$

Lipohilicity was calculated with the following software tools: ClogP v4.94 program (BioByte Corp., Claremont, USA) for logP, Moloc (Gerber Molecular Design, Amden, Switzerland) for PSA and MoKa 1.1.0 (Molecular Discovery Ltd, Pinner Middlesex, UK) for pK_a. The values used and the result can be found in Table A3.1.2.

Statistical analysis

Statistical determination of ordinal logistic regression for the correlation of different dependent variables was performed using the software Matlab 7.12. Equation 3.1.7 describes the variables as follows: β are the coefficients of the regression and p the probability for a drug to be in one of the risk categories. *Var1* and *Var2* are the covariates that were correlated to generate a clustering of the compounds as shown in Table 1. The separation line between two risk categories was defined for the case the odds were unity as described by Nakayama el al., by application of Equation 3.1.8 [9].

Dependent on the results of the ordinal logistic regression, sensitivity, specificity, positive (precision) and negative predictive value (NPV) were determined for the correct classification of DILI risk from a confusion matrix (Figure A3.1.1). Separation of low risk from risk and high risk drugs (condition A) was assessed and compared the separation in a reduced dataset containing low risk and high risk drugs (condition B). A similar approach was applied to validate the quality of the different correlation approaches after incorporation of pharmacokinetic parameters and substitution of CVB data by reactive metabolite formation (GSH trapping).

$$\log\left(\frac{p}{1-p}\right) = \beta_0 + \beta_1 * \log(Var1) + \beta_2 * \log(Var2) \qquad \textbf{Eq. 3.1.7}$$

$$\log(Var2) = \frac{\beta_0}{\beta_2} - \frac{\beta_1}{\beta_2} * \log(Var1) \qquad \textbf{Eq. 3.1.8}$$

Table 3.1.1: Definition of covariates used for ordinal logistic regression analysis.

	Var1	*Var2*
Model 1 (Nakayama)	Daily dose	CVB_heps
Model 2 (this work)	Daily dose	CVB_heps /CL_{int}
Model 3 (this work)	Liver inlet concentration	CVB_heps

Results

Experiment design

Ninety-one model compounds were classified based on their history of safe use or development of DILI (Table A3.1.1). Compounds were classified in three categories with respect to their safety profile as previously reported [17]. Drugs withdrawn from the market or carrying a hepatotoxicity-related label were classified as 'high risk' drugs, substances with known history of liver injury were assigned as 'risk' drugs and those without increased incidence for liver damage were marked as 'low risk'. For all drugs intrinsic clearance determination and GSH trapping assay was performed in microsomes or taken from the literature [18-20]. Oral plasma clearance data and other pharmacokinetic properties were extracted from literature (Table A3.1.2). For a subset of 51 compounds quantitative CVB data was collected (in house and literature results as described in Material and Methods, Table A3.1.1) and a theoretical portal vein concentration ('liver inlet') was calculated (Table A3.1.2). A quantitative evaluation of the different approaches for classification of DILI based on selected input variables results was conducted after ordinal logistic regression and further determination of descriptors for predictive values based on a confusion matrix approach.

Statistical evaluation of variables describing DILI classification

The present study was designed with the goal to evaluate the most sensitive variables for DILI classification based on drug bioactivation propensities and generic pharmacokinetic properties. Inspection of parameters of the present data set revealed that none of the used parameters was able to predict DILI in isolation. Means of CVB and clearance data did not show any obvious trend and possessed a wide standard deviation. This observation was also confirmed by a partial least squares discriminant analysis (PLA-DA) of the variables: The highest contributing value to separate the different classes was seen for dose and hepatic inlet concentration which are closely related (see Equation 3.1.5) with a trend towards a connection of high dose and high risk. Clearance was classified as minor determinant and covalent binding as important contribution factor, however not significant for one group (Figure 3.1.3).

In order to investigate a potential improvement of the prediction of hepatotoxicity based on drug bioactivation, we build on the established zone classification system by Nakayama and coworkers [9]. This approach utilized hepatocyte covalent binding

(CVB_{hep}) and daily dose as variables to classify drugs with different DILI properties. We used this approach as reference model that we further developed by modifying the input variables to two dependent models. An overview of the outcome is displayed in Table 1. As reference, model 1 corresponds to the original Nakayama model with an extended dataset, model 2 uses intrinsic clearance normalized covalent binding (CVB/CL_{int}) and dose as determinants and model 3 employed covalent binding in combination with the hepatic inlet concentration as covariates.

Quantitative CVB properties as prediction factor for DILI

Inspection of individual input variable of the present data set revealed that none of the used parameters was able to predict DILI when applied in isolation. Means of CVB and clearance data did not show any obvious trend and possessed a wide standard deviation. This observation was also emphasized by a partial least squares discriminant analysis (PLA-DA) of the variables: The highest contributing value on separation of different classes of DILI was evident for dose and hepatic inlet concentration which are closely related (see Equation 3.1.5). These parameters revealed a trend towards the correlation of “high dose” with “high risk”. Clearance was classified as minor determinant and covalent binding as important contribution factor, however not statistically significant for one group.

However, a combination of different parameters that previously had been argued to determine the classification of DILI resulted in distinct clusters for the different categories of DILI drugs. The results are graphically displayed in Figure 3.1.1. This classification was largely confounded when the entire dataset of compounds (n=51) was analyzed including those compounds classified as “risk” (Figure 3.1.1, left). Reducing the compound set to those compounds that were classified as “low risk” and “high risk” (n=33) a significantly better separation of both groups was achieved (Figure 3.1.2, right). Visual inspection of the data suggests an improved classification of DILI drugs when comparing to the reference model 1 to the most comprehensive approach in model 3. This included pharmacokinetic parameters and physico-chemical properties of drugs that were used to derive a liver inlet concentration. A cut-off line to separate safe from high risk drugs could be calculated by ordinal logistic regression with only one false positive classification (#42, gemfibrozil).

A quantitative summary of the descriptive values of the different models is shown in Table 3.1.2. It was retrieved using a confusion matrix with the cut-off lines calculated

from the regression analysis for the three models. The values emphasize the differences in correct prediction for low risk (safe) versus risk and high risk drugs (condition A) and the reduced data set (low risk vs. high risk, condition B). The percentage of correctly classified compounds in average is 14% better for condition B as compared to condition A. For condition B an improvement for all parameters for model 3 as compared to model 2 and for model 2 as compared to model 1 indicates that the inclusion of clearance and liver inlet data results in an overall better predictivity. For condition A that attempt to classify safe drugs relative to risk and high risk drugs, an improvement for the most complex correlation of model 3 was not observed. Here, specificity and precision increased slightly whereas sensitivity and NPV decreased.

Reactive metabolite formation as prediction factor for DILI

We further investigated the substitution of CVB data by the qualitative potential of reactive metabolite formation as indicated by trapping of reactive species with glutathione (GSH) that was available for a set of n=91 compounds. Therefore, the first step was to assess the overlap between results from CVB assessment and its potential surrogate GSH trapping.

A positive outcome in CVB assessment was defined with a threshold of greater than 10 pmol drug derived material bound per milligram of hepatocyte protein. This value is derived from historical background data. The same outcome in both assays for the chosen data was achieved for 35 of 51 compounds (positives and negatives). Only 4 of the 19 ‘true’ positives are classified as safe, all of them being low dose drugs (0.035 mg – 20 mg/d). On the other hand, 9 (of 16) of of the ‘true’ negative compounds do have DILI alerts, for them, the average dose was 1700 mg/d. One of them, zomepirac (#91), which is known to form instable acyl glucuronides, has been recently found positive in CVB assessment, however only with 19.8 pmol/mg after 4 h of incubation [11]. With respect to the deviating results, the predicitvity of GSH adducts seems to be better as compared to CVB. 90% of the compounds with GSH alert and without CVB alert are classified as DILI drugs. Here, the oxidative activation seems to be the bioactivation pathway involved in reactive metabolite formation. This may not be captured in hepatocytes due to lack of dynamic range in hepatocyte CVB studies. The amount of toxic compounds in the false negative section, in contrast, is only 50%.

The correlation between CVB and body burden was further confirmed by substitution of quantitative CVB with GSH adduct formation which was done for a largely expanded data set (n=91 vs n=51 for CVB properties).

Here, GSH adduct formation as qualitative outcome succeeded in classifying 64% of all compounds correctly for condition A (n=91 compounds). For the reduced data set (condition B eliminating the intermediate DILI risk category, n=54 compounds) even 70% true results were obtained The sensitivity of the assay for condition B was at 77% suggesting that only 4 out of 18 DILI drugs were not correctly classified (Figure 3.1.2, bottom). Three of those four drugs were high dose drugs. E.g. ritonavir does form reactive metabolites which directly bind to the active side of the involved enzyme, namely CYP3A4 and are not able to diffuse away from the binding pocket. The precision of 55% reveals that the GSH experiment is over-sensitive (Figure 3.1.2, top). 10 over 36 low risk drugs possess the potential to from RM. However, one of them was the aforementioned drug gemfibrozil (#42) whose classification may have to be reviewed. The other compounds were low dose drugs with an average dose of 28 mg per day.

In general, the majority (76%) of high risk compounds given at > 100 mg per day possess a GSH flag, however, only the minority (15%) of low risk compounds given at > 100 mg per day do so. Low risk drug with a dose of < 100 mg per day had 35% GSH trapping positive results. One example is Ethinylestradiol (#35). Its ethinyl moiety is prone to form reactive metabolites, however as the daily dose is only 0.035 mg, the exposure to the reactive metabolite is not sufficient to cause toxicity.

Based on these findings the daily dose was integrated as secondary criteria for risk assessment via GSH trapping. Applying this definition for the 54 safe and high risk drugs resulted in a vast improvement of prediction power (Figure 3.1.3). With only 4 false negative and 2 false positive results (11%) a sensitivity of 78%, a specificity of 94%, a precision of 88% and an NPV of 89% were achieved.

Integration of the intermediate DILI risk category also revealed a substantial reduction of false positive results, i.e. a relevant reduction of over-exclusion of compounds. However, in parallel, the number of false negatives is increasing. Judging GSH adduct formation or a high dose as positive outcome leads to the invert effect: Whereas false positives are increased, the number of false negative results is reduced which is equivalent with an increase in sensitivity. In addition to the dose correlation a slight trend could be seen for high risk compounds that did not have a GSH trapping alert

when incorporating plasma clearance. Low clearance drugs may be underestimated in their CVB risk from short-period *in vitro* assays if bioactivation processes are quantitatively too slow.

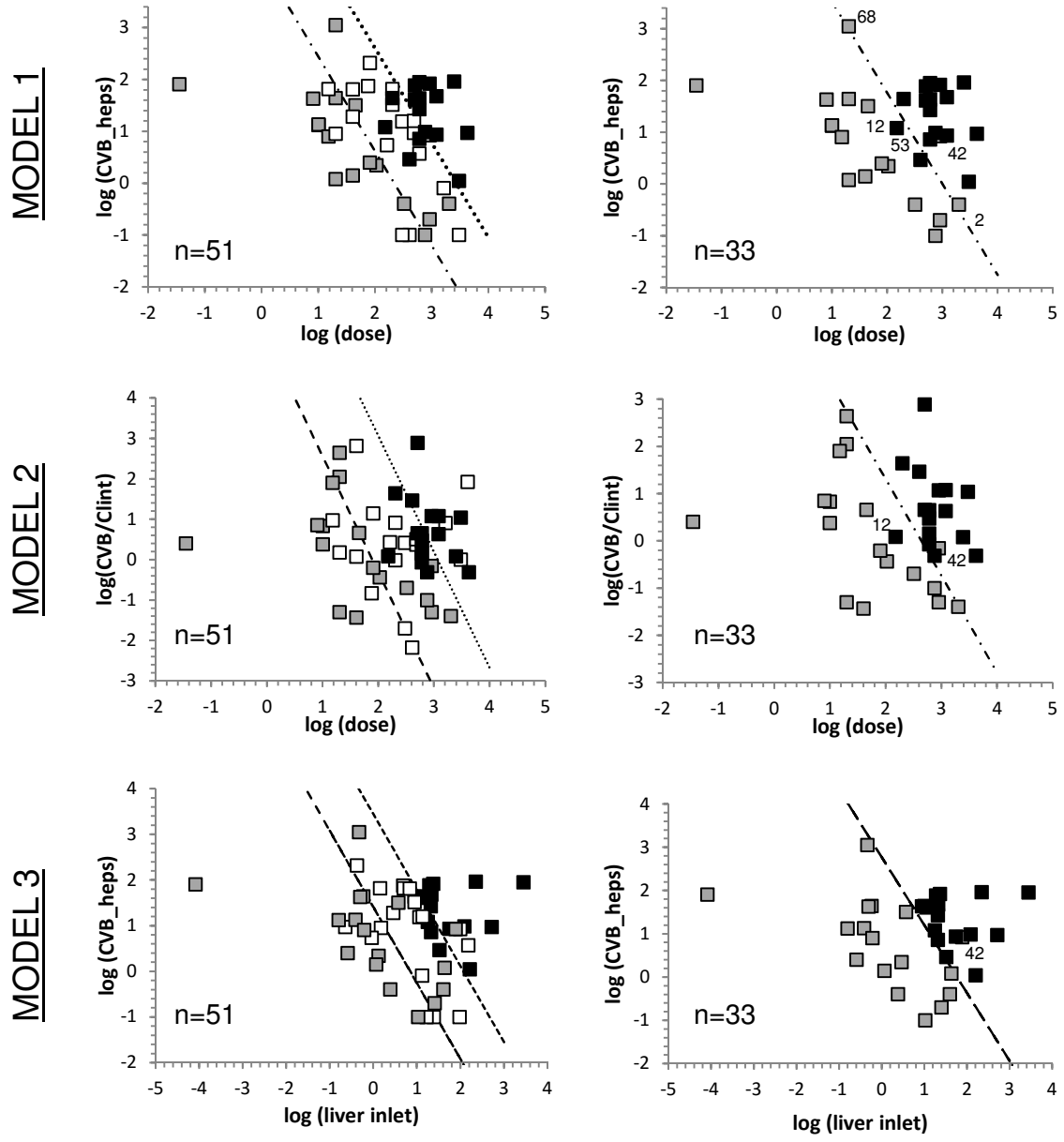

Figure 3.1.1: Correlation of different variables for a zone classification of compounds of different classes of DILI properties as separated after linear logistic regression. Drugs with a low risk (▪), risk (□) or high risk (■) were clustered using the established Nakayama model (CVB in hepatocytes and daily dose) [model 1] or intrinsic clearance normalized CVB and daily dose [model 2] or CVB and hepatic inlet concentration [model 3]. Condition A (left) used three groups to DILI outcome (high risk, risk, low risk drugs) and condition B used a reduced data set (high risk, low risk drugs).

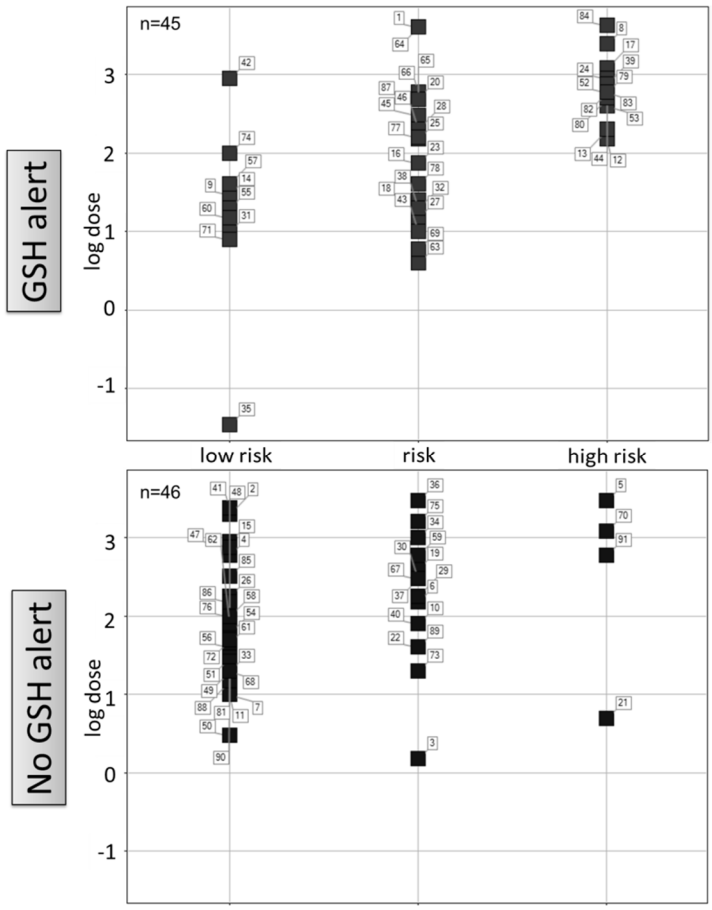

Figure 3.1.2: Reactive metabolite formation as results from GSH trapping (alert on top and absence of alert on bottom) in relation to daily dose and DILI category.

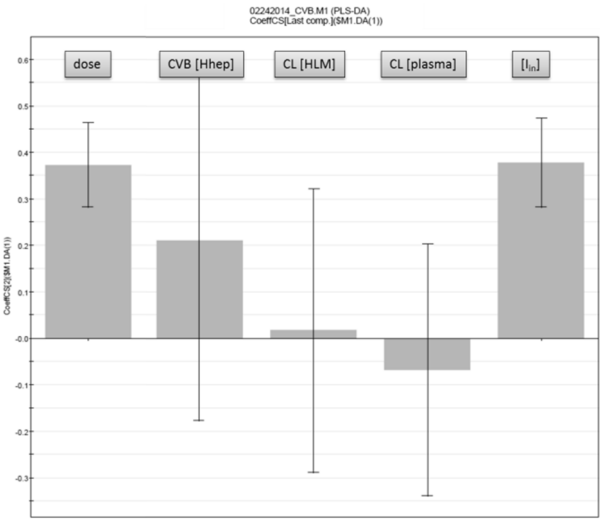

Figure 3.1.3 Correlation plot for different variables for toxicity prediction. Height of the column corresponds to the amount of contribution. Standards deviations ranging from positive to negative indicate the absence of a significant trend within one of the tested groups.

Table 3.1.2: Predictive value of the different correlation models as determined after ordinal logistic regression and confusion matrix evaluation. Condition A (top) refers to the comparison of the group of the low risk compounds against risk and high risk and the condition (B) (bottom) to the comparison of low risk drugs against high risk compounds.

		Sensitivity	Specificity	Precision	NPV	Correct
Condition A (low risk vs. risk, high risk)	Model 1	85%	71%	85%	71%	80%
	Model 2	82%	59%	80%	63%	75%
	Model 3	85%	65%	83%	69%	78%
Condition B (low risk vs. high risk)	Model 1	88%	82%	82%	88%	85%
	Model 2	94%	94%	94%	94%	94%
	Model 3	100%	94%	94%	100%	97%

Table 3.1.3: GSH adduct formation as prediction factor for DILI. A GSH alert in combination with a daily dose higher than 100 mg was judged as positive outcome to predict the classification of high dose and low risk drugs.

		Risk for DILI		
	n=54	high	low	
GSH alert at > 100 mg	yes	14	2	88%
	no	4	34	89%
		78%	94%	89%

Discussion

CVB as prediction factor for toxicity

Although it is a generally accepted hypothesis that excessive covalent binding or critical covalent binding to sensitive cellular target proteins is related to development of toxicity, the quantitative relationship between both remains vague. Several groups have demonstrated the progress and limitations of a quantitative risk assessment based on covalent binding data over the last couple of years. The major shortcoming of several models was a remaining amount of false classified compounds. A reason may be the lack of mechanistic parameters in these analyses. Complex secondary mechanisms cannot be captured *in vitro* such as binding of reactive metabolites to physiologically sensitive proteins or the formation of neo-antigens triggering immune response only in certain cases. Therefore the susceptibility of individual patients remains elusive. In contrast to previous studies we applied a global inspection of a large dataset consisting of in house and collected literature data. We applied statistical analysis to describe the obtained results and compared different scenarios, namely the whole data set and a reduced set consisting of safe and high risk drugs.

Using these prerequisites, the aim of this study was to review the relevance of covalent binding properties of compounds relative to their administered dose, systemic clearance and liver burden over time. It was presumed that a rapidly metabolized compound would not interact with a potential target in the same manner as a slowly activated compound. Therefore, bioactivation data was corrected for experimental (intrinsic) clearance. However, as integration of CLint data does only add value for drugs with an at least moderate turnover *in vitro*, oral plasma clearance data from clinical trials is needed for more meaningful information. As most comprehensive parameter for a drug's potential to (adversely) interact with the liver the portal vein concentration was deemed. The applied calculation (see Equation 3.1.4) was comprised by two main components, the systematic average concentration and the absorption. Here, physicochemical properties and clinical pharmacokinetic data were integrated.

Correlation of the present, extended data set (n=51) using the well accepted Nakayama-model (model 1) showed a comparable zone classification as described [9]. Normalization of the absolute CVB for the intrinsic clearance (model 2) and transformation of the maximum daily dose to a theoretical liver inlet concentration of

the (model 3) resulted in an improvement of predictability for low risk and high risk drugs. Here, sensitivity, selectivity, precision and NPV were increased by 9% from model 1 to 2, and by additional 3% for model 3.

An improvement was seen namely for drugs where the primary input variable biased the classification in model 1. Acetyl salicylic acid [ASS] (#2) and rimonabant (#68) are generally considered as safe but exhibit a high dose (up to 2 g for ASS) and absolute CVB (1114 pmol/mg for rimonabant). On the other side benzbromarone (#12) and nevirapine (#53) are toxic drugs that show relatively low CVB in hepatocytes (12.1 and 2.9 pmol/mg) and were therefore judged as safe. However, integration of *in vivo* clearance and bioavailability over the liver inlet concentration resulted in an adjustment to the correct area. The only false clustered compound in the latter model was gemfibrozil (#42) ranging as low risk compound in the hepatotoxic area. Although gemfibrozil is generally considered as relatively safe, reports on cholestatic events upon drug intake have been reported [21]. Besides, occurrence of myotoxicity is reported to be elevated, especially in combination with statins [22, 23]. The reason that the present study revealed benefit from incorporation of pharmacokinetic parameters which was not seen in a comparable extent in previous works as conducted by Bauman et al [7] may be due to the selection of extreme case examples (by excluding of the intermediate risk category for analysis) which however still represented a substantially larger data set (n=33 vs. n=18). This enabled the detection of general trends that may not apply for every individual drug.

Nonetheless, integration of the ‘risk’ drug class as unacceptable group did not result into an improved prediction for the complex models. A positive change in one quality parameter was accompanied by a negative change in another one, resulting in an overall similar prediction power that did not improve (see Table 3.1.3, lower part). The reason for these findings can be understood when inspecting the applied statistical model (PLS-DA). Dose and CVB were identified as most contributing variables for the separation of the different classes. Figure 3.1.3 emphasizes that CVB alone is not indicative for DILI classification. The most important factor for the calculated liver inlet concentration is the dose; the impact of both variables is comparable. For a comprehensive comparison of the models it has to be considered also, that data collection is much more complicated for *in vivo* parameters as used in model 3. For safety and monetary reasons the aim of industry and authorities is to learn about potential adverse reactions as early as possible, at a point where pharmacokinetic

data are rarely available. Substitution of clinical data by physiology-based pharmacokinetic modeling displays a source of ambiguity.

The constant prediction power may originate from the uncertainty in extracted and calculated results. As data on the fraction absorbed (F_a) is rarely accessible, mostly oral bioavailability (F_{oral}) was used as parameter. In cases where no value was available, 1.0 (equivalent to 100%) was assumed. However, the difference between F_a and F_{oral} can be crucial if the compound possesses a high first pass (gut and liver) metabolism. In these cases, the fraction absorbed would be underestimated by F_{oral}. In addition to the included parameters, knowledge on the fraction metabolized (f_m) as opposed to renal or biliary excretion of unchanged drug is crucial [24]. Only if the amount of hepatic metabolism equals 1 (i.e. 100% of the elimination of the compound is via metabolism) the *in vitro* bioactivation is comparable to the *in vivo* situation.

The case of gemfibrozil illustrates a bottleneck of the compound classification. For very toxic or extremely well-tolerated substances (here: high risk and low risk) the DILI history is very clear. However, several drugs possess case reports of hepatic alterations and for most of them an exclusion of other causalities such as co-medication or underlying disease is rarely possible. This may lead to false positive conclusions [25]. On the other hand, DILI is also believed to be underreported because of insufficient pharmacovigilance systems or awareness of the causative context [26]. Strategies for the handling of DILI cases by the authorities may also deviate depending on indication of the drug, medication alternatives or class effects. It is therefore a primary challenge to rate the 'true' safety profile of a drug.

GSH adduct formation as prediction factor for toxicity

Analyses of the present and previously reported data indicate a limited impact of quantitative covalent binding in human hepatocytes and their narrow dynamic range (a background of approx. 2 pmol/mg up to 100 pmol/mg for high-binding compounds). It was therefore hypothesized that assessing bioactivation in a binary yes/no manner by GSH adduct formation may be sufficient for reliable evaluation.

Previous studies showed that the amount of GSH adducts and the amount of covalent binding are not correlated. It was suggested recently that this is due to the differences in reactivity of glutathione and microsomal protein, as well as the deficiency of glutathione to trap hard electrophiles and the differences in life time and partition (aqueous/protein) of RMs [27]. However, conduction of GSH trapping is much simpler

and does not require radiolabeling of compounds. Therefore, GSH trapping assays are frequently incorporated into preclinical risk assessment strategies. GSH adduct formation, mainly in combination with CYP mechanism-based inhibition data can serve as indicator for the risk of hepatotoxicity and substitute CVB data [10, 17]. Likewise, we found a correlation between GSH adduct formation and toxicity which was improved after integration of dose, as it was proposed recently [28]. Only a small amount of false positive as well as negative results were retrieved when 100 mg daily dose was added as criterion (Table 3). This correction may account for detoxification mechanisms that are depleted at higher drug doses.

As GSH trapping is routinely conducted in liver microsomes and hepatocytes are considered as gold standard for covalent binding assessment, potential differences in outcome of the assays may be also due to the metabolic system. To exclude this bias the correlation of covalent binding data in microsomes and hepatocytes of the present data set were confirmed (data not shown). A comparison of GSH and CVB assay showed a congruence of 69%. Detailed inspection of the results showed a higher failure for quantitative CVB evaluation in human hepatocytes to correctly classify toxicity as compared to GSH adduct formation. The majority of compounds with positive GSH trapping result and lack of significant CVB were indeed DILI drugs. The reason may be predominant activation via CYP enzymes in the present cases. CYPs are higher expressed in microsomes, which is the test system of the GSH trapping assay. The lower sensitivity and dynamic range of CVB determination in hepatocytes may result in failed recognition of CVB properties in that assay. Remarkably 47% of the compounds that tested negative for bioactivation by quantitative CVB and GSH trapping belong to the DILI classes (risk and high risk) drugs. This can be explained by the high clinical dose (average1400 mg/day) together with a low rate of bioactivation *in vitro*: The CL_{int} values for the affected compounds range from 0 to 19.2 mL/min/mg with a mean of 5.8 mL/min/mg and median of 2-5 mL/min/mg. Alternatively it is also likely that other, non bioactivation related mechanisms contribute to the observed toxicity of these molecules.

Perspective for future risk assessment of DILI

The central question of this research was to find better ways of classifying DILI properties for drug candidates. It is appreciated that this early classification is by no

means a predictive measure of DILI outcome in the clinical setting. Still the existing correlation between bioactivation, pharmacokinetic parameters including daily dose emphasizes that bioactivation may leads to a substantially increased DILI risk. This particularly holds true for cases where a certain dose threshold is exceeded. The comprehensive analysis of the set of 91 drugs with classified DILI properties suggests 100 mg as a threshold dose for additional safety considerations. Considering the limited impact of the absolute amount of CVB, we suggest to non-quantitatively determine reactive metabolite formation by e.g. GSH trapping. In contrast, a better understanding of the drug exposure is of major importance as mitigation factor for DILI risk [29]. The integration of pharmacokinetic knowledge can support a reliable judgment of the outcome of a bioactivation assay. This may be not applicable for screening tasks, however, this tool may confirm the decision on whether to terminate or continue drug development for individual cases.

Another strategy for a better understanding of the relationship between protein covalent binding and toxicity outcomes is the detailed analysis of protein targets of reactive metabolites. It is hypothesized that the specific modification of critical protein targets and not the total unspecific covalent binding in general determines the risk for toxicity.

For a consolidated evaluation of this hypothesis a reactive metabolite target protein database has been created by Hanzlik and coworkers. Their goal was to provide a listing of known RM targets to enable the identification of general protein patterns that determine toxicity [30]. However, until now database entries are mainly available for chemicals. Additionally, association of protein bands on a gel do not necessarily reflect that these proteins were covalently modified until the protein modification has been unequivocally demonstrated on a peptide or amino acid level. The identification of peptide targets from functional enzymes was reported for a model compound known to induce high CVB to rat and human hepatic tissue by application of a targeted proteomics approach [31]. However, detection of protein targets can be challenging when the absolute covalent binding is low or the abundance of the target is minute relative to a large excess of unmodified proteins. A comprehensive correlation of protein targets and DILI impact will be revealed in the future when more proteomic data is available.

Besides the limitations of existing RM assessment tools, one must also be aware that bioactivation is almost never the only determinant for drug-induced hepatotoxicity.

Heterogeneous mechanisms are involved in its development and do not allow the prediction via one single approach. Thus, for a significant improvement of safety assessment causalities have to be understood in detail and translated into investigation models and biomarkers [12]. These may then replace or complement the need of integrating bioactivation findings in a proper context [32].

In summary, the current knowledge advises to design potent, selective and therefore low dose drugs with moderate turnover and minimal undesired bioactivation. For drug candidates that are deficient of some of the desired properties, the presented assessment tools can support the rating of these compounds and the selection of the best among a series of related compounds. It may be necessary to embark on detailed assessment of secondary toxicity endpoints as potential contributing factors in order to estimate the DILI risk for a predicted dose range in case a DILI risk cannot be excluded.

Appendix

		Condition			
		positive	negative		
Test	+	true positive (TP)	false positive (FP)	**Precision**	TP/TP+FP
	-	false negative (FN)	true negative (TN)	**NPV**	TN/TN+FN-
		Sensitivity	**specificity**		
		TP/ TP+FN	TN/ TN+FP		

Figure A3.1.1: Definition of a confusion matrix with output parameters to evaluate the qualitative outcome of an individual experimental set-up.

Table A3.1.1: Experimental data for low risk drugs

index	name	daily dose [mg]	RM alert by GSH trapping	CL_{int}_HLM* [mL/min/mg]	CVB_heps [pmol/10^6 cells]	Source CVB
2	Acetyl salicylic acid	2000	no	10.0	0.4	int.
4	Amantadine	600	no	3.0	*nd*	
7	Amlodipine	10	no	5.6	13.3	[9]
9	Aripiprazole	30	yes	5.0	*nd*	
11	Baclofen	10	no	[0.1]	*nd*	
14	Buspirone	30	yes	19.0	*nd*	
15	Caffeine	900	no	4.0	0.2	[9]
26	Dextromethorphan	180	no	16.0	*nd*	
31	Donepezil	10	yes	2.0	13.5	[9]
33	Enalapril	20	no	2.0	*nd*	
35	Ethinylestradiol	0.035	yes	32.0	80.6	[9]
41	Gabapentin	2400	no	8.5	*nd*	
42	Gemfibrozil	900	yes	12.0	8.4	int.
47	Levofloxacin	750	no	[0.1]	0.1	[9]
48	Lidocaine	105	yes	6.0	2.2	int.
49	Lisinopril	20	no	2.8	*nd*	
50	Lorazepam	3	no	2.0	*nd*	
51	Memantine	30	no	[0.1]	*nd*	
54	Nifedipine	60	yes	7.0	*nd*	
55	Olanzapine	20	yes	[0.1]	43.8	[11]
56	Olmesartan	40	no	38.0	1.4	[9]
57	Paroxetine	40	yes	6.0	*nd*	
58	Pentobarbital	100	no	6.0	*nd*	
60	Pindolol	15	yes	[0.1]	*nd*	
61	Pioglitazone	45	no	7.0	31.9	[11]
62	Pravastatin	80	yes	4.0	2.5	[9]
68	Rimonabant	20	no	10.0	1114.8	[11]
71	Rosiglitazone	8	yes	6.0	42.5	[9]
72	Sertraline	50	no	5.0	*nd*	
74	Sitagliptin	100	yes	[0.1]	*nd*	
76	Sumatriptan	100	no	11.4	*nd*	
81	Tocopherol acetate	20	no	24.0	1.2	int.
85	Valsartan	320	no	2.0	0.4	[9]
86	Venlafaxine	150	no	[0.1]	*nd*	
88	Warfarin	15	no	[0.1]	8	[9]
90	Zolpidem	20	no	6.0	*nd*	int.

Table A3.1.1 contd: risk drugs

index	name	daily dose [mg]	RM alert by GSH trapping	CL_{int}_HLM* [mL/min/mg]	CVB_heps [pmol/10^6 cells]	Source CVB
1	Acetaminophen	4000	yes	[0.1]	8.4	[9]
3	Alprazolam	1.5	no	3.0	*nd*	
6	Amitriptyline	150	no	6.0	*nd*	
10	Atorvastatin	80	no	15.0	209.2	[9]
16	Captopril	75	yes	[0.1]	*nd*	
18	Carvedilol	25	yes	8.0	*nd*	
19	Celecoxib	400	no	15.0	7.1	[9]
20	Chlorpromazine	500	yes	7.0	*nd*	
22	Citalopram	40	no	3.0	*nd*	
23	Clopidogrel	75	yes	513.0	75	[9]
25	Desipramine	150	yes	5.0	*nd*	
27	Diazepam	15	yes	7.0	0.1	[33]
28	Diclofenac	200	yes	68.0	65.8	int.
29	Diltiazem	180	no	5.0	*nd*	
30	Diphenhydramin	300	no	5.0	0.1	[7]
32	Duloxetine	20	yes	37.9	*nd*	
34	Erythromycin	1000	no	3.0	*nd*	
36	Felbamate	3000	no	[0.1]	0.1	[7]
37	Fenofibrate	300	no	515.4	*nd*	
38	Fluoxetine	20	yes	6.0	9	[9]
40	Furosemide	80	no	2.0	*nd*	
43	Haloperidol	10	yes	4.0	*nd*	
45	Imipramine	300	yes	6.0	15.5	[9]
46	Indomethacin	200	yes	4.0	32.9	int.
59	Phenytoin	600	no	2.0	3.7	[9]
63	Prazosin	4	yes	5.0	*nd*	
64	Procainamide	4000	yes	8.0	*nd*	
65	Propranolol	480	yes	4.0	9.4	[9]
66	Quetiapine	600	yes	11.0	*nd*	
67	Ranitidine	300	no	[0.1]	*nd*	
69	Risperidone	6	yes	6.0	*nd*	
73	Simvastatin	20	no	124.0	*nd*	
75	Sulfamethoxazole	1600	no	[0.1]	0.8	[9]
77	Tacrine	160	yes	2.0	5.4	[9]
78	Tamoxifen	40	yes	[0.1]	64.9	[9]
87	Verapamil	480	yes	5.0	16	[9]
89	Zafirlukast	40	no	16.0	19.1	[9]

Table A3.1.1 contd: high risk drugs

index	name	daily dose [mg]	RM alert by GSH trapping	CL_{int}_HLM* [mL/min/mg]	CVB_heps [pmol/10^6 cells]	Source CVB
5	Aminophenazone	3000	no	[0.1]	1	[9]
8	Amodiaquine	2450	yes	76	91.3	[9]
12	Benzbromarone	150	yes	10	12.1	[9]
13	Bromfenac	200	yes	1	43.8	int.
17	Carbamazepine	1200	yes	2	8.6	[11]
21	Cilazapril	5	no	67	*nd*	
24	Clozapine	900	yes	7	82.7	[9]
39	Flutamide	750	yes	20	9.7	[9]
44	Imiloxan	500	yes	9	40.8	int.
52	Nefazodone	600	yes	51	43.3	int.
53	Nevirapine	400	yes	[0.1]	2.9	[9]
70	Ritonavir	1200	no	4	47.7	[9]
79	Ticlopidine	600	yes	20	89.5	[9]
80	Tienilic acid	500	yes	[0.1]	77.2	int.
82	Tolcapone	600	yes	515.4	*nd*	
83	Troglitazone	600	yes	9	26.7	int.
84	Valproic acid	4200	yes	19.2	9.3	[9]
91	Zomepirac	600	no	5	7.2	[9]

*[0.1]: no substrate depletion observed

int: in house data

Table A3.1.2

			Calculated properties			Literature Values				
index	name	max. dose [mg]	$\log D_{6.0}$	PSA	k_a	CL oral [L/h]	Ref.	F_{oral}*	Ref.	$[I]_{in}$ [mg/L]
low risk										
2	Acetyl salicylic acid	2000	1.34	51.1	2.96	87.5	[34]	0.63	[35]	39.8
7	Amlodipine	10	1.14	83.0	1.65	22.5	[36]	0.81	[37]	0.2
15	Caffeine	900	-0.12	48.3	1.85	4.7	[38]	[1.0]		25.2
31	Donepezil	10	1.16	37.2	3.48	9.7	[39]	0.95	[40]*	0.4
35	Ethinylestradiol	0.0035	4.12	32.4	10.7	33.7	[41]	0.01	[42]*	0.0
42	Gemfibrozil	900	3.59	39.2	7.98	15.1	[43]	[1.0]		0.5
47	Levofloxacin	750	-1.61	64.6	0.84	7.6	[44]	[1.0]		10.5
48	Lidocaine	105	-0.12	25.3	2.68	248.3	[45]	0.42	[45]	1.3
55	Olanzapine	20	0.86	27.6	3.65	16.1	[46]	0.7	[47]	0.6
56	Olmesartan	40	5.59	107	5.42	4.9	[48]	0.36	[49]	1.2
61	Pioglitazone	45	4.62	60.6	8.14	3.3	[50]	0.83	[51]	3.7
62	Pravastatin	80	1.63	94.7	1.63	263	[52]	0.18	[53]	0.3
68	Rimonabant	20	2.67	42.1	5.49	4.4	[54]	0.18	[55]*	0.4
71	Rosiglitazone	8	2.67	60.4	4.09	2.1	[56]	0.99	[57]	0.5
81	Tocopherol acetate	20	12.30	29.0	206	20		[1.0]		42.8
85	Valsartan	320	0.31	96.8	0.98	8	[59]	0.23	[60]	2.4
88	Warfarin	15	2.13	49.1	4.05	26.6	[61]	0.93	[62]	0.6
risk										
1	Acetaminophen	4000	0.36	41.3	2.45	19.6	[63]	0.87	[64]	96.8
10	Atorvastatin	80	2.42	87.3	2.43	18.8	[65]	0.12	[53]	0.4
19	Celecoxib	400	3.97	68.5	5.68	28.1	[66]	[1.0]		24.1
23	Clopidogrel	75	2.16	23.6	6.18	$5.5e^4$	[67]	[1.0]		4.8
27	Diazepam	15	2.71	27.1	7.08	1.8	[68]	[1.0]		1.4
28	Diclofenac	200	1.28	40.6	3.43	26.6	[69]	0.65	[70]	4.9
30	Diphenhydramin	300	1.19	12.1	5.26	48	[71]	[1.0]		16.6
36	Felbamate	3000	0.76	90.1	1.29	2.3	[72]	[1.0]		94.3
38	Fluoxetine	20	2.35	19.7	7.03	43	[73]	[1.0]		1.5
45	Imipramine	300	2.31	6.7	8.55	240	[74]	0.42	[74]	11.2
46	Indomethacin	200	2.19	57.0	3.64	2.9	[75]	0.77	[76]	8.7
59	Phenytoin	600	2.28	51.3	4.12	0.2	[38]	0.93	[77]	149
65	Propranolol	480	0.92	35.7	3.27	325.5	[78]	0.01	[79]*	0.2
75	Sulfa-methoxazole	1600	-1.16	82.8	0.73	75.8	[80]	0.99	[81]	12.9
77	Tacrine	160	0.55	30.5	3.12	1404	[82]	0.17	[83]*	0.9
78	Tamoxifen	40	4.38	13.2	16.0	3.6	[84]	0.24	[85]	2.0
87	Verapamil	480	1.76	59.5	3.00	371.7	[86]	0.90	[87]	13.4
89	Zafirlukast	40	5.58	94.7	6.61	20	[88]	[1.0]		20.0

Table A3.1.2 contd.

			calculated properties			Literature values				
index	name	max. dose [mg]	$logD_{6.0}$	PSA	k_a	CL oral [L/h]	Ref	F_{oral}*	Ref	$[I]_{in}$ [mg/L]
high risk										
5	Amino-phenazone	3000	0.58	26.8	3.35	2.2	[89]	[1.0]		160.7
8	Amodiaquine	2450	4.00	42.2	8.77	4140	[90]	[1.0]		222.4
12	Benz-bromarone	150	4.30	39.8	10.2	3.4	[91]	[1.0]		17.6
13	Bromfenac	200	3.08	66.6	4.27	7.3	[92]	[1.0]		10.0
17	Carbama-zepine	1200	1.46	35.8	3.96	3.5	[93]	0.83	[94]	55.1
24	Clozapine	900	1.57	27.1	4.72	18	[95]	0.48	[96]	23.2
39	Flutamide	750	3.51	58.6	5.67	0.4	[97]	[1.0]		122.1
44	Imiloxan	500	1.15	31.0	3.83	655.7	[98]	[1.0]		19.9
52	Nefazodone	600	4.50	50.4	9.19	33.8	[99]	0.14	[100]*	8.7
53	Nevirapine	400	3.55	47.4	6.89	3.9	[101]	[1.0]		32.8
70	Ritonavir	1200	2.97	108	2.1	17.3	[102]	0.7	[103]	21.2
79	Ticlopidine	600	2.90	4.1	11.0	269.3	[104]	[1.0]		68.3
80	Tienilic acid	500	1.25	55.3	2.68	4.1	[105]	[1.0]		19.0
82	Tolcapone	600	1.80	86.6	1.96	7.1	[106]	0.6	[106]	10.8
83	Troglitazone	600	4.96	73.1	7.50	29.8	[107]	0.43	[107]	20.6
84	Valproic acid	4200	1.88	29.1	5.12	0.6	[108]	0.99	[108]	511.9
91	Zomepirac	600	1.31	49.7	3.00	11.3	[109]	[1.0]		20.9

[1.0]: no value found; *F in rat (propranolol, rimonabant in monkey)

Abbreviations

CL	Clearance
CL_{int}	Intrinsic clearance
CVB	Covalent protein binding
CYP	Cytochrome P450
DILI	Drug-induced liver injury
ER	Enhanced resolution
EPI	Enhanced product ion
F	Bioavailability
F_a	Fraction absorbed
F_{Dp}	Fraction of dose reaching the portal vein
f_m	Fraction metabolized
F_{oral}	Oral bioavailability
GSH	Glutathione
HLM	Human liver microsomes
I_{av}	Systemic concentration
I_{in}	Liver inlet concentration
k_a	Absorption constant
LC-MS/MS	Liquid chromatography / tandem mass spectrometry
LogD	Distribution coefficient
logP	Partition coefficient
NPV	Negative predictive value
PI	Precursor ion
PLA-DA	Partial least squares discriminant analysis
PSA	Polar surface area
Q_h	Hepatic bloodflow
RM	Reactive metabolite

References

1. Uetrecht, J., Idiosyncratic drug reactions: current understanding. Annu Rev Pharmacol Toxicol, 2007. 47: p. 513-39.
2. Kola, I. and J. Landis, Can the pharmaceutical industry reduce attrition rates? Nature Reviews Drug Discovery, 2004. 3(8): p. 711-715.
3. Evans, D.C. and T.A. Baillie, Minimizing the potential for metabolic activation as an integral part of drug design. Current Opinion in Drug Discovery and Development, 2005. 8(1): p. 44-50.
4. Obach, R.S., et al., Can in vitro metabolism-dependent covalent binding data in liver microsomes distinguish hepatotoxic from nonhepatotoxic drugs? An analysis of 18 drugs with consideration of intrinsic clearance and daily dose. Chem Res Toxicol, 2008. 21(9): p. 1814-22.
5. Kalgutkar, A.S., et al., Toxicophores, reactive metabolites and drug safety: When is it a cause for concern? Expert Review of Clinical Pharmacology, 2008. 1(4): p. 515-531.
6. Evans, D.C., et al., Drug-protein adducts: an industry perspective on minimizing the potential for drug bioactivation in drug discovery and development. Chem Res Toxicol, 2004. 17(1): p. 3-16.
7. Bauman, J.N., et al., Can in vitro metabolism-dependent covalent binding data distinguish hepatotoxic from nonhepatotoxic drugs? An analysis using human hepatocytes and liver S-9 fraction. Chem Res Toxicol, 2009. 22(2): p. 332-40.
8. Lammert, C., et al., Relationship between daily dose of oral medications and idiosyncratic drug-induced liver injury: search for signals. Hepatology, 2008. 47(6): p. 2003-9.
9. Nakayama, S., et al., A zone classification system for risk assessment of idiosyncratic drug toxicity using daily dose and covalent binding. Drug Metab Dispos, 2009. 37(9): p. 1970-7.
10. Sakatis, M.Z., et al., Preclinical strategy to reduce clinical hepatotoxicity using in vitro bioactivation data for >200 compounds. Chem Res Toxicol, 2012. 25(10): p. 2067-82.
11. Thompson, R.A., et al., In Vitro Approach to Assess the Potential for Risk of Idiosyncratic Adverse Reactions Caused by Candidate Drugs. Chem Res Toxicol, 2012.
12. Park, B.K., et al., Managing the challenge of chemically reactive metabolites in drug development. Nat Rev Drug Discov, 2011. 10(4): p. 292-306.
13. Lévesque, J.F., S.H. Day, and A.N. Jones, Protocols of in vitro protein covalent binding studies in liver. Methods in molecular biology (Clifton, N.J.), 2011. 691: p. 283-301.
14. Dieckhaus, C.M., et al., Negative ion tandem mass spectrometry for the detection of glutathione conjugates. Chem Res Toxicol, 2005. 18(4): p. 630-8.
15. Wen, B., et al., High-throughput screening and characterization of reactive metabolites using polarity switching of hybrid triple quadrupole linear ion trap mass spectrometry. Anal Chem, 2008. 80(5): p. 1788-99.
16. Linnankoski, J., et al., Computational prediction of oral drug absorption based on absorption rate constants in humans. J Med Chem, 2006. 49(12): p. 3674-81.
17. Nakayama, S., et al., Combination of GSH trapping and time-dependent inhibition assays as a predictive method of drugs generating highly reactive metabolites. Drug Metab Dispos, 2011. 39(7): p. 1247-54.
18. Kalgutkar, A.S., et al., A comprehensive listing of bioactivation pathways of organic functional groups. Curr Drug Metab, 2005. 6(3): p. 161-225.
19. Walgren, J.L., M.D. Mitchell, and D.C. Thompson, Role of metabolism in drug-induced idiosyncratic hepatotoxicity. Crit Rev Toxicol, 2005. 35(4): p. 325-61.
20. Kalgutkar, A.S., Role of Bioactivation in Idiosyncratic Drug Toxicity: Structure–Toxicity Relationship, in Advances in Bioactivation Research, A.A. Elfarra, Editor. 2008, American Association of Pharmaceutical Scientists. p. 440.
21. Einarsson, K. and B. Angelin, Hyperlipoproteinemia, hypolipidemic treatment, and gallstone disease. Atheroscler Rev, 1986. 15: p. 67-97.
22. Liu, A., et al., Myotoxicity of gemfibrozil in cynomolgus monkey model and its relationship to pharmacokinetic properties. Toxicol Appl Pharmacol, 2009. 235(3): p. 287-95.
23. Holoshitz, N., A.A. Alsheikh-Ali, and R.H. Karas, Relative safety of gemfibrozil and fenofibrate in the absence of concomitant cerivastatin use. Am J Cardiol, 2008. 101(1): p. 95-7.
24. Zhang, H., et al., Cytochrome P450 reaction-phenotyping: an industrial perspective. Expert Opin Drug Metab Toxicol, 2007. 3(5): p. 667-87.
25. Aithal, G.P., et al., Case definition and phenotype standardization in drug-induced liver injury. Clinical Pharmacology and Therapeutics, 2011. 89(6): p. 806-815.

26. Devarbhavi, H., An Update on Drug-induced Liver Injury. Journal of Clinical and Experimental Hepatology, 2012. 2(3): p. 247-259.
27. Takakusa, H., et al., Quantitative assessment of reactive metabolite formation using 35S-labeled glutathione. Drug Metabolism and Pharmacokinetics, 2009. 24(1): p. 100-107.
28. Reese, M., et al., An integrated reactive metabolite evaluation approach to assess and reduce safety risk during drug discovery and development. Chem Biol Interact, 2011. 192(1-2): p. 60-4.
29. Srivastava, A., et al., Role of reactive metabolites in drug-induced hepatotoxicity. Handb Exp Pharmacol, 2010(196): p. 165-94.
30. Hanzlik, R.P., J. Fang, and Y.M. Koen, Filling and mining the reactive metabolite target protein database. Chem Biol Interact, 2009. 179(1): p. 38-44.
31. Tzouros, M. and A. Pahler, A targeted proteomics approach to the identification of peptides modified by reactive metabolites. Chem Res Toxicol, 2009. 22(5): p. 853-62.
32. Kalgutkar, A.S., Handling reactive metabolite positives in drug discovery: What has retrospective structure-toxicity analyses taught us? Chem Biol Interact, 2011. 192(1-2): p. 46-55.
33. Usui, T., et al., Evaluation of the potential for drug-induced liver injury based on in vitro covalent binding to human liver proteins. Drug Metab Dispos, 2009. 37(12): p. 2383-92.
34. Benedek, I.H., et al., Variability in the pharmacokinetics and pharmacodynamics of low dose aspirin in healthy male volunteers. J Clin Pharmacol, 1995. 35(12): p. 1181-6.
35. Raschka, C. and H.J. Koch, [Pharmacokinetics after oral and intravenous administration of d,l-monolysine acetylsalicylate and an oral dose of acetylsalicylic acid in healthy volunteers]. Therapie, 2001. 56(6): p. 669-74.
36. Vaidyanathan, S., et al., Lack of pharmacokinetic interactions of aliskiren, a novel direct renin inhibitor for the treatment of hypertension, with the antihypertensives amlodipine, valsartan, hydrochlorothiazide (HCTZ) and ramipril in healthy volunteers. Int J Clin Pract, 2006. 60(11): p. 1343-56.
37. Vincent, J., et al., Lack of effect of grapefruit juice on the pharmacokinetics and pharmacodynamics of amlodipine. Br J Clin Pharmacol, 2000. 50(5): p. 455-63.
38. Randinitis, E.J., et al., Drug interactions with clinafloxacin. Antimicrob Agents Chemother, 2001. 45(9): p. 2543-52.
39. Tiseo, P.J., K. Foley, and L.T. Friedhoff, An evaluation of the pharmacokinetics of donepezil HCl in patients with moderately to severely impaired renal function. Br J Clin Pharmacol, 1998. 46 Suppl 1: p. 56-60.
40. Matsui, K., S. Taniguchi, and T. Yoshimura, Correlation of the intrinsic clearance of donepezil (Aricept) between in vivo and in vitro studies in rat, dog and human. Xenobiotica, 1999. 29(11): p. 1059-72.
41. Mulford, D., M. Mayer, and G. Witt, Effect of cefditoren on the pharmacokinetics of ethinyl estradiol. 40th Intersci Conf Antimicrob Agents Chemother (ICAAC) (September 17-20, Toronto), 2000: p. Abst A-314
42. Zamek-Gliszczynski, M.J., et al., Efflux transport is an important determinant of ethinylestradiol glucuronide and ethinylestradiol sulfate pharmacokinetics. Drug Metab Dispos, 2011. 39(10): p. 1794-800.
43. Evans, J.R., S.C. Forland, and R.E. Cutler, The effect of renal function on the pharmacokinetics of gemfibrozil. J Clin Pharmacol, 1987. 27(12): p. 994-1000.
44. Ernst, M.E., E.J. Ernst, and M.E. Klepser, Levofloxacin and trovafloxacin: the next generation of fluoroquinolones? Am J Health Syst Pharm, 1997. 54(22): p. 2569-84.
45. Wing, L.M., et al., Lidocaine disposition--sex differences and effects of cimetidine. Clin Pharmacol Ther, 1984. 35(5): p. 695-701.
46. Bigos, K.L., et al., Sex, race, and smoking impact olanzapine exposure. J Clin Pharmacol, 2008. 48(2): p. 157-65.
47. Caccia, S., Biotransformation of post-clozapine antipsychotics: pharmacological implications. Clin Pharmacokinet, 2000. 38(5): p. 393-414.
48. Tanigawara, Y., et al., Comparative pharmacodynamics of olmesartan and azelnidipine in patients with hypertension: a population pharmacokinetic/pharmacodynamic analysis. Drug Metab Pharmacokinet, 2009. 24(4): p. 376-88.
49. von Bergmann, K., et al., Olmesartan medoxomil: Influence of agent, renal and hepatic function on the pharmacokinetics of olmesartan medoxomil J Hypertens, 2001. 19(Suppl. 1).
50. Karim, A., et al., Coadministration of pioglitazone or glyburide and alogliptin: pharmacokinetic drug interaction assessment in healthy participants. J Clin Pharmacol, 2009. 49(10): p. 1210-9.

51. Eckland, D.A. and M. Danhof, Clinical pharmacokinetics of pioglitazone. Exp Clin Endocrinol Diabetes 2000. 108: p. 234-42.
52. Desager, J.P. and Y. Horsmans, Clinical pharmacokinetics of 3-hydroxy-3-methylglutaryl-coenzyme A reductase inhibitors. Clin Pharmacokinet, 1996. 31(5): p. 348-71.
53. Christians, U., W. Jacobsen, and L.C. Floren, Metabolism and drug interactions of 3-hydroxy-3-methylglutaryl coenzyme A reductase inhibitors in transplant patients: are the statins mechanistically similar? Pharmacol Ther, 1998. 80(1): p. 1-34.
54. Grandison, M.K., et al., Lack of effect of mild or moderate hepatic impairment on the pharmacokinetics of rimonabant. 36th Annu Meet Am Coll Clin Pharmacol (ACCP) (September 9-11, San Francisco), 2007: p. Abst 74.
55. Rimonabant, in EPAR - Scientific Discussion. 2006, Europeen Medicine Agency. p. 41.
56. Park, J.Y., et al., Effect of ketoconazole on the pharmacokinetics of rosiglitazone in healthy subjects. Br J Clin Pharmacol, 2004. 58(4): p. 397-402.
57. Cox, P.J., et al., Absorption, disposition, and metabolism of rosiglitazone, a potent thiazolidinedione insulin sensitizer, in humans. Drug Metab Dispos, 2000. 28(7): p. 772-80.
58. Winklhofer-Roob, B.M., et al., Response to a single oral dose of all-rac-alpha-tocopheryl acetate in patients with cystic fibrosis and in healthy individuals. Am J Clin Nutr, 1996. 63(5): p. 717-21.
59. Leidig, M.F., et al., Pharmacokinetics of valsartan in hypertensive patients on long-term haemodialysis. Clinical Drug Investigation, 2001. 21(1): p. 59-66.
60. Flesch, G., P. Muller, and P. Lloyd, Absolute bioavailability and pharmacokinetics of valsartan, an angiotensin II receptor antagonist, in man. Eur J Clin Pharmacol, 1997. 52(2): p. 115-20.
61. Faaij, R.A., et al., The effect of warfarin on the pharmacokinetics and pharmacodynamics of napsagatran in healthy male volunteers. Eur J Clin Pharmacol, 2001. 57(1): p. 25-9.
62. Breckenridge, A. and M. Orme, Kinetics of warfarin absorption in man. Clin Pharmacol Ther, 1973. 14(6): p. 955-61.
63. Rawlins, M.D., D.B. Henderson, and A.R. Hijab, Pharmacokinetics of paracetamol (acetaminophen) after intravenous and oral administration. Eur J Clin Pharmacol, 1977. 11(4): p. 283-6.
64. Forrest, J.A., J.A. Clements, and L.F. Prescott, Clinical pharmacokinetics of paracetamol. Clin Pharmacokinet, 1982. 7(2): p. 93-107.
65. Corsini, A., et al., New insights into the pharmacodynamic and pharmacokinetic properties of statins. Pharmacol Ther, 1999. 84(3): p. 413-28.
66. Abstracts of the 2002 Annual Meeting of the American Society for Clinical Pharmacology and Therapeutics. Atlanta, Georgia, USA. March 24-27, 2002. Clin Pharmacol Ther, 2002. 71(2): p. P1-136.
67. Hartter, S., et al., Pharmacokinetic and pharmacodynamic effects of comedication of clopidogrel and dabigatran etexilate in healthy male volunteers. Eur J Clin Pharmacol, 2013. 69(3): p. 327-39.
68. Perucca, E., et al., Inhibition of diazepam metabolism by fluvoxamine: a pharmacokinetic study in normal volunteers. Clin Pharmacol Ther, 1994. 56(5): p. 471-6.
69. Lill, J.S., et al., Pharmacokinetics of diclofenac sodium in chronic active hepatitis and alcoholic cirrhosis. J Clin Pharmacol, 2000. 40(3): p. 250-7.
70. Hinz, B., et al., Bioavailability of diclofenac potassium at low doses. Br J Clin Pharmacol, 2005. 59(1): p. 80-4.
71. Lessard, E., et al., Diphenhydramine alters the disposition of venlafaxine through inhibition of CYP2D6 activity in humans. J Clin Psychopharmacol, 2001. 21(2): p. 175-84.
72. Glue, P., et al., Single-dose pharmacokinetics of felbamate in patients with renal dysfunction. Br J Clin Pharmacol, 1997. 44(1): p. 91-3.
73. Altamura, A.C., A.R. Moro, and M. Percudani, Clinical pharmacokinetics of fluoxetine. Clin Pharmacokinet, 1994. 26(3): p. 201-14.
74. Sallee, F.R. and B.G. Pollock, Clinical pharmacokinetics of imipramine and desipramine. Clin Pharmacokinet, 1990. 18(5): p. 346-64.
75. Khosravan, R., et al., Pharmacokinetic interactions of concomitant administration of febuxostat and NSAIDs. J Clin Pharmacol, 2006. 46(8): p. 855-66.
76. Oberbauer, R., P. Krivanek, and K. Turnheim, Pharmacokinetics of indomethacin in the elderly. Clin Pharmacokinet, 1993. 24(5): p. 428-34.
77. Aliwarga, T., et al., Excretion of the principal urinary metabolites of phenytoin and absolute oral bioavailability determined by use of a stable isotope in patients with epilepsy. Ther Drug Monit, 2011. 33(1): p. 56-63.

78. Ebihara, A., et al., Clinical pharmacology of a new beta-adrenoceptor blocking drug, befunolol. Cross-over comparison with propranolol on repeated administration. Eur J Clin Pharmacol, 1982. 23(3): p. 189-95.
79. Takahashi, M., et al., Characterization of gastrointestinal drug absorption in cynomolgus monkeys. Mol Pharm, 2008. 5(2): p. 340-8.
80. Li, X.Y., et al., Comparison of the pharmacokinetics of sulfamethoxazole in male chinese volunteers at low altitude and acute exposure to high altitude versus subjects living chronically at high altitude: an open-label, controlled, prospective study. Clin Ther, 2009. 31(11): p. 2744-54.
81. Chin, T.W., A. Vandenbroucke, and I.W. Fong, Pharmacokinetics of trimethoprim-sulfamethoxazole in critically ill and non-critically ill AIDS patients. Antimicrob Agents Chemother, 1995. 39(1): p. 28-33.
82. Forgue, S.T., et al., Inhibition of tacrine oral clearance by cimetidine. Clin Pharmacol Ther, 1996. 59(4): p. 444-9.
83. Hartvig, P., et al., Clinical pharmacokinetics of intravenous and oral 9-amino-1,2,3,4-tetrahydroacridine, tacrine. Eur J Clin Pharmacol, 1990. 38(3): p. 259-63.
84. Lonning, P.E., et al., Clinical pharmacokinetics of endocrine agents used in advanced breast cancer. Clin Pharmacokinet, 1992. 22(5): p. 327-58.
85. Shin, S.C. and J.S. Choi, Effects of epigallocatechin gallate on the oral bioavailability and pharmacokinetics of tamoxifen and its main metabolite, 4-hydroxytamoxifen, in rats. Anticancer Drugs, 2009. 20(7): p. 584-8.
86. Krecic-Shepard, M.E., et al., Gender-specific effects on verapamil pharmacokinetics and pharmacodynamics in humans. J Clin Pharmacol, 2000. 40(3): p. 219-30.
87. McTavish, D. and E.M. Sorkin, Verapamil. An updated review of its pharmacodynamic and pharmacokinetic properties, and therapeutic use in hypertension. Drugs, 1989. 38(1): p. 19-76.
88. Dekhuijzen, P.N. and P.P. Koopmans, Pharmacokinetic profile of zafirlukast. Clin Pharmacokinet, 2002. 41(2): p. 105-14.
89. Pierce, C.H., et al., Clopidogrel and drug metabolism: absence of effect on hepatic enzymes in healthy volunteers. Semin Thromb Hemost, 1999. 25 Suppl 2: p. 35-9.
90. Orrell, C., et al., Pharmacokinetics and tolerability of artesunate and amodiaquine alone and in combination in healthy volunteers. Eur J Clin Pharmacol, 2008. 64(7): p. 683-90.
91. Uchida, S., et al., Influence of CYP2C9 Genotype on pharmacokinetics and pharmacodynamics of benzbromarone. Circ J, 2007. 71(Suppl. I): p. Abst PJ-566.
92. Caspi, A., Bromfenac: A new NSAID. P and T, 1997. 22(10): p. 516-518.
93. Chien, S., et al., Pharmacokinetic interaction study between the new antiepileptic and CNS drug RWJ-333369 and carbamazepine in healthy adults. Epilepsia, 2006. 47(11): p. 1830-40.
94. Magnusson, M.O., et al., Pharmacodynamics of carbamazepine-mediated induction of CYP3A4, CYP1A2, and Pgp as assessed by probe substrates midazolam, caffeine, and digoxin. Clin Pharmacol Ther, 2008. 84(1): p. 52-62.
95. Ng, W., et al., Clozapine exposure and the impact of smoking and gender: a population pharmacokinetic study. Ther Drug Monit, 2009. 31(3): p. 360-6.
96. Toepfner, N., et al., Accidental clozapine intoxication in a toddler: clinical and pharmacokinetic lessons learnt. J Clin Pharm Ther, 2013. 38(2): p. 165-8.
97. Anjum, S., et al., Pharmacokinetics of flutamide in patients with renal insufficiency. Br J Clin Pharmacol, 1999. 47(1): p. 43-7.
98. Dow, R., The Pharmacokinetics of Imiloxan After Multiple Dosing in Volunteers. 1986, Syntex Research Scotland: EDINBURGH. p. 42.
99. Barbhaiya, R.H., K.A. Dandekar, and D.S. Greene, Pharmacokinetics, absolute bioavailability, and disposition of [14C]nefazodone in humans. Drug Metab Dispos, 1996. 24(1): p. 91-5.
100. Shukla, U.A., et al., Pharmacokinetics, absolute bioavailability, and disposition of [14C]nefazodone in the dog. Drug Metab Dispos, 1993. 21(3): p. 502-7.
101. van Heeswijk, R.P., et al., The steady-state pharmacokinetics of nevirapine during once daily and twice daily dosing in HIV-1-infected individuals. Aids, 2000. 14(8): p. F77-82.
102. Cressey, T.R., et al., Reduced indinavir exposure during pregnancy. Br J Clin Pharmacol, 2013. 76(3): p. 475-83.
103. van Heeswijk, R.P., et al., Combination of protease inhibitors for the treatment of HIV-1-infected patients: a review of pharmacokinetics and clinical experience. Antivir Ther, 2001. 6(4): p. 201-29.
104. Marzo, A., et al., Bioequivalence of ticlopidine hydrochloride administered in single dose to healthy volunteers. Pharmacol Res, 2002. 46(5): p. 401-7.

105. Kerremans, A.L., et al., Pharmacokinetic and pharmacodynamic studies of tienilic acid in healthy volunteers. Eur J Clin Pharmacol, 1982. 22(6): p. 515-21.
106. Jorga, K.M., et al., Pharmacokinetics and pharmacodynamics after oral and intravenous administration of tolcapone, a novel adjunct to Parkinson's disease therapy. Eur J Clin Pharmacol, 1998. 54(5): p. 443-7.
107. Loi, C.M., et al., Steady-state pharmacokinetics and dose proportionality of troglitazone and its metabolites. J Clin Pharmacol, 1999. 39(9): p. 920-6.
108. Sriboonruang, T., et al., The impact of dosage of sustained-release formulation on valproate clearance and plasma concentration in psychiatric patients: analysis based on routine therapeutic drug monitoring data. J Clin Psychopharmacol, 2011. 31(1): p. 115-9.
109. O'Neill, P.J., et al., Disposition of zomepirac sodium in man. J Clin Pharmacol, 1982. 22(10): p. 470-6.

3.2 Characterization and validation of biomarkers for cellular oxidative stress

3.2.1 Validation of isoprostanes as *in vitro* biomarkers for oxidative stress

Quantitative Profiling of Multiple Prostaglandin Derivatives as Biomarkers of Oxidative Stress in Primary Hepatocytes by Negative Ion Online SPE-LC-MS/MS

Marieke Teppner[1] [2], Manfred Zell[1], Christophe Husser[1], Beat Ernst[2] and Axel Pähler[1]

[1] DMPK, Pharmaceutical Sciences; Pharma Research and Early Development (pRED); F. Hoffmann-La Roche Ltd., Grenzacherstrasse 124; CH-4070 Basel, Switzerland

[2] Institute of Molecular Pharmacy; University of Basel, Klingenbergstrasse 50; CH-4040 Basel, Switzerland

Published in: *Analytical Biochemistry* 498 (2016) 68 – 77.

Personal contribution: Establishment of analytical method; conduction of validation experiments; manuscript preparation

Analytical Biochemistry 498 (2016) 68–77

Contents lists available at ScienceDirect

Analytical Biochemistry

journal homepage: www.elsevier.com/locate/yabio

Quantitative profiling of prostaglandins as oxidative stress biomarkers in vitro and in vivo by negative ion online solid phase extraction – Liquid chromatography–tandem mass spectrometry

Marieke Teppner [a, 1], Manfred Zell [a], Christophe Husser [a], Beat Ernst [b], Axel Pähler [a, *]

[a] Drug Metabolism and Pharmacokinetics, Pharmaceutical Sciences, Pharmaceutical Research and Early Development, Roche Innovation Center Basel, CH-4070 Basel, Switzerland
[b] Institute of Molecular Pharmacy, University of Basel, CH-4040 Basel, Switzerland

ARTICLE INFO

Article history:
Received 12 August 2015
Received in revised form
5 January 2016
Accepted 6 January 2016
Available online 22 January 2016

Keywords:
LC–ESI–MS/MS
Biomarker
Oxidative stress
Prostaglandins
Primary hepatocytes

ABSTRACT

Free radical-mediated oxidation of arachidonic acid to prostanoids has been implicated in a variety of pathophysiological conditions such as oxidative stress. Here, we report on the development of a liquid chromatography–mass spectrometry method to measure several classes of prostaglandin derivatives based on regioisomer-specific mass transitions down to levels of 20 pg/ml applied to the measurement of prostaglandin biomarkers in primary hepatocytes. The quantitative profiling of prostaglandin derivatives in rat and human hepatocytes revealed the increase of several isomers on stress response. In addition to the well-established markers for oxidative stress such as 8-iso-prostaglandin $F_{2\alpha}$ and the prostaglandin isomers PE_2 and PD_2, this method revealed a significant increase of 15*R*-prostaglandin D_2 from 236.1 ± 138.0 pg/1E6 cells in untreated rat hepatocytes to 2001 ± 577.1 pg/1E6 cells on treatment with ferric NTA (an Fe^{3+} chelate with nitrilotriacetic acid causing oxidative stress in vitro as well as in vivo). Like 15*R*-prostaglandin D_2, an unassigned isomer that revealed a more significant increase than commonly analyzed prostaglandin derivatives was identified. Mass spectrometric detection on a high-resolution instrument enabled high-quality quantitative analysis of analytes in plasma levels from rat experiments, where increased concentrations up to 23-fold change treatment with Fe(III)NTA were observed.

Oxidative stress describes the pathological condition where the balance between prooxidant and physiological antioxidant regulatory mechanisms is disturbed [1]. It is generally associated with the presence of reactive oxygen species (ROS) such as singlet oxygen ($^1O_2$), hydroxyl radicals (•OH), superoxide anions ($O_2^{\bullet-}$), and hydrogen peroxide (H_2O_2) [2]. Because living organisms have always been exposed to oxidative stressors naturally (e.g., endogenous via mitochondrial metabolism, exogenous via ultraviolet [UV] radiation), strategies to counteract with reductive enzyme systems such as superoxide dismutase [3] or via glutathione metabolism [4] have been developed. However, in some pathophysiological conditions, the defense mechanisms are disrupted, leading to oxidative stress and cellular damage caused by ROS. On the molecular level, there are three major targets of ROS: proteins, DNA, and lipids. The oxidation of proteins may lead to altered function, DNA oxidation can cause damage on the functional or genomic level, and lipid alteration may to lead to impaired membrane integrity [5].

Several pathological conditions such as metabolic syndrome, chronic obstructive pulmonary disease (COPD), cancer, neurodegenerative diseases, and ageing [6–9] are known to involve cellular oxidative stress. Furthermore, impaired oxidative balance is

Abbreviations: ROS, reactive oxygen species; UV, ultraviolet; LC–MS/MS, liquid chromatography–tandem mass spectrometry; HPLC, high-performance liquid chromatography; SRM, selected reaction monitoring; $iPF_{2\alpha}$-VI, 5-iso prostaglandin $F_{2\alpha}$-VI; $PF_{2\alpha}$, prostaglandin $F_{2\alpha}$; PE_2, prostaglandin E_2; PD_2, prostaglandin D_2; 15*R*-PD_2, 15(*R*)prostaglandin D_2; dihydro-keto PE_2, 13,14-dihydro-15-keto prostaglandin E_2; dihydro-keto PD_2, 13,14,-dihydro-15-keto prostaglandin D_2; PD_2-d4, prostaglandin D_2-d4; Fe(III)NTA, ferric nitrilotriacetic acid; TC, trapping column; AC, analytical column; DP, declustering potential; CE, collision energy; CXP, cell exit potential; TOF, time-of-flight; SRM–HR, high-resolution SRM; EIA, enzyme immunoassay; LLE, liquid–liquid extraction; SPE, solid phase extraction; MDA, malonyldialdehyde; GSH, glutathione; RT, retention time.

* Corresponding author.
E-mail address: axel.paehler@roche.com (A. Pähler).
[1] Current address: Evotec, 22419 Hamburg, Germany.

http://dx.doi.org/10.1016/j.ab.2016.01.005
0003-2697/

considered important in a variety of adverse reactions caused by pharmacotherapy [10]. Namely, the liver has been identified as a primary vulnerable organ due to the high metabolic load with drugs and the transformation to reactive species. Free radical-mediated lipid peroxidation or redox cycling of quinone, imino-quinone, or quinone methide type of activated drug metabolites may cause an imbalance of the cellular antioxidant system in hepatocytes [11,12]. A widely accepted hypothesis claims that the associated secondary signals (also referred to as danger signals) of oxidative stress are involved in the multifactorial mechanisms leading to liver toxicity [13]. Therefore, it is important to assess cellular oxidative stress conditions as a surrogate marker for hepatic injury early in the drug discovery and development process. Foremost, hepatocytes as primary metabolically active species have served as an experimental system to study cellular damage induced by drug metabolism [14,15].

Isoprostanes, which are isomers of prostaglandins, are one group of potential cellular biomarkers for oxidative stress. They derive from a cascade of free radical-catalyzed oxidations of arachidonic acid, the physiological precursor of prostaglandins, prostacyclins, and thromboxans. Isoprostanes have been shown to be involved in diseases such as oxidant injury and atherosclerosis [16,17] as well as in degenerative syndromes and cardiovascular diseases [18,19]. Consequently, the assessment of their levels has been suggested as biomarkers of oxidative stress or inflammation. In the past, various methods for the detection and quantification of prostaglandins have been reported. One representative of the prostaglandin family is the group of the F_2 isoprostanes, which are regarded as the "gold standard" noninvasive biomarker for oxidative stress measurement in vivo, mainly in plasma and urine. In addition, liver and brain were investigated as target tissues for prostaglandin derivatives [20,21]. Mainly immunoassays for specific isomers as well as gas chromatography coupled to mass spectrometry, mostly via negative ion chemical ionization (NICI), were applied to purify and quantify F_2 isoprostanes [22–24]. Due to increasing evidence of their role in inflammatory and oxidative stress-related processes, there has been a rising interest in the analysis of other classes of prostaglandins and isoprostanes during past years. Published comprehensive reviews give an overview of the different analytical approaches that have been established [25,26].

This study reports on the development of an integrated liquid chromatography–tandem mass spectrometry (LC–MS/MS) method for the direct analysis of isoprostanes from biological samples. It is fully automated on a 96-well plate format. An online column-switching high-performance liquid chromatography (HPLC) setup allows for enrichment of analyte by large volume injection and omits laborious a priori sample workup. Besides classical MS detection via selected reaction monitoring (SRM) on a triple quadrupole instrument, this method was also shown to be translatable as high-resolution SRM to a time-of-flight mass spectrometer. This post-acquisition selection of suitable parent–daughter ion pairs allows for the unbiased detection of a broad variety of prostaglandins because those representatives described to be the most reliable renal and plasma markers might not be the most sensitive hepatic ones. The method was applied for in vitro studies with primary rat and human hepatocytes and can also be useful for the detection of plasma analytes.

Materials and methods

Chemicals

Williams' medium E, ferric nitrate, formic acid p.a., nitrilotriacetic acid disodium salt, insulin, streptomycin, penicillin, and hydrocortisone were obtained from Sigma–Aldrich (St. Louis, MO, USA). Glutamine and gentamycin were purchased from Life Technologies Invitrogen (Lucerne, Switzerland), and acetonitrile (LC–MS grade) was purchased from Fisher Scientific (Wohlen, Switzerland). Water (chromatography grade) was obtained from Merck (Darmstadt, Germany). The prostaglandin derivatives 5-iso prostaglandin $F_{2\alpha}$-VI (i$PF_{2\alpha}$-VI) (**1**), prostaglandin $F_{2\alpha}$ ($PF_{2\alpha}$) (**2**), prostaglandin E_2 (PE_2) (**3**), prostaglandin D_2 (PD_2) (**4**), 15(*R*)prostaglandin D_2 (15*R*-PD_2) (**5**), 13,14-dihydro-15-keto prostaglandin E_2 (dihydro-keto PE_2) (**6**), 13,14,-dihydro-15-keto prostaglandin D_2 (dihydro-keto PD_2) (**7**), and prostaglandin D_2-d4 (PD_2-d4) (**8**) were purchased from Cayman Chemical (Ann Arbor, MI, USA).

Preparation of reagents

Incubation medium was prepared by supplementation of Williams' medium E with 4 mg/L insulin, 50,000 U/L penicillin, 50 mg/L streptomycin, 10 mg/L gentamycin, 0.4 mg/L glutamine, and 2.4 mg/ml hydrocortisone.

Ferric nitrilotriacetic acid [Fe(III)NTA] stock solution (20 mM) was prepared by mixing 5 ml of 0.1 M $Fe(NO_3)_3$ in 0.1 M HCl and 0.2 M NaNTA, filling up to 30 ml, and adjusting the pH to 7.4 with 1 M $NaCO_3$.

Hepatocyte incubation and workup

Primary cells were prepared freshly in-house by a two-step procedure for liver perfusion [27,28] and used in suspension. Incubation was performed at 37 °C in humidified atmosphere (5% CO_2/95% air) in 96-well plates at a cell concentration of 1 million/ml and stopped after 1 or 3 h by precipitation with acetonitrile that contained the internal standard (PD_2-d4 at a concentration of 1 ng/ml to reach a final concentration of 0.42 ng/ml). As positive control for oxidative stress conditions, cell suspensions were spiked with diluted Fe(III)NTA stock solution to reach final concentrations of 50 and 150 μM.

Quenched hepatocyte incubations were centrifuged at 5000 *g* for 11 min at 4 °C, and the transferred supernatant (500 μl diluted with 100 μl of acetonitrile/water containing 0.1% formic acid) was directly injected onto the LC–MS/MS system.

Animal study and sample workup

Animal studies were carried out in accordance with Swiss animal welfare law and the guide for the care and use of laboratory animals published by the National Institutes of Health. The animal test facility is fully accredited by the Association for Assessment and Accreditation of Laboratory Animal Care International. For the experiment, 9 male Fischer 344 rats (240–269 g) were obtained from Charles River (Sulzfeld, Germany) and maintained at 23 °C on a 12-h light:12-h dark cycle with food and water available ad libitum. Two days prior to treatment, animals were adjusted to metabolic cages. For the experiment, animals were divided into three groups ($n = 3$) and administered a single dose of Fe(III)NTA (15 and 65 mg/kg body weight i.p. treated groups 2 and 3, respectively) or 0.9% sodium chloride (control group 1). Animals were sacrificed after 3 h of treatment by CO_2 asphyxiation followed by cervical dislocation. Total blood was collected on ethylenediaminetetraacetic acid (EDTA), and plasma was prepared and stored at −20 °C.

Plasma samples were precipitated with 2 volumes of ethanol containing internal standard (PD_2-d4 at a concentration of 0.63 ng/ml to reach a final concentration of 0.42 ng/ml).

HPLC system/electrospray ionization mass spectrometric analysis

A 500-µl aliquot of the cleaned-up sample was loaded onto a trapping column (TC) (YMC AQ, 20 × 2.1 mm, 5 µm, YMC Europe) of an HPLC column-switching system (see Fig. S1 in online supplementary material) using water containing 0.2% formic acid (eluent A2) at a flow rate of 0.25 ml/min for 5.1 min using an Agilent 1100 series LC pump. The sample was further diluted by the online addition of eluent A3 at a flow rate of 1.75 ml increasing to 2.25 ml within 5.1 min to TC via a T-piece. Thereafter, TC was switched in line with an analytical column (AC) (Atlantis T3, 100 × 2.1 mm, 3.5 µm, Waters), and the retained analytes were transferred to AC using gradient elution. High-pressure gradient elution was applied at a flow rate of 0.4 ml/min using a Shimadzu LC AD vp binary pump system. The elution was performed by a mixture of water containing 0.2% formic acid (eluent A1) and 0.2% formic acid/acetonitrile (1:9, v/v; eluent B1). Whereas eluent B1 was raised from 25 to 60% in a 7.5-min trapping phase, eluent A1 was decreased complementarily. Thereafter, eluent B1 was increased to 95% and maintained for 1.5 min. After 13.5 min following injection, eluent B1 was decreased to 25%. During this sequence, TC was disconnected from AC after 5.1 min following injection and flushed with 95% 0.2% formic acid/acetonitrile (1:9, v/v; eluent B2) and 5% water containing 0.2% formic acid (eluent A2) at a flow rate of 1.0 ml/min for 5 min and then reequilibrated with water containing 0.2% formic acid (eluent A2) at a flow rate of 0.25 ml/min for 3.5 min. The overall run time of the analysis cycle was 13.5 min. The analysis sequence is represented in detail in Table S1 of the supplementary material.

The detection of isoprostanes was performed by a quadrupole mass spectrometer (QTRAP) (4000 QTRAP, AB Sciex) equipped with TurbolonSpray source. Analyst software version 1.4.2 (Applied Biosystems) was used for instrument control, data acquisition, and data analysis. The instrument was operated in the negative ion electrospray mode. Source was set at 550 °C, and ionspray voltage was −4200 V. Dwell time was 15 ms for individual transitions with entrance potential kept at −10 V. Declustering potential (DP), collision energy (CE), and cell exit potential (CXP) were optimized individually for each analyte with the following results: for $iPF_{2\alpha}$-VI (**1**), the transitions m/z 353 > 193 (DP = −65, CE = −34, CXP = −13) and m/z 353 > 115 (DP = −80, CE = −30, CXP = −9) were used; for $PF_{2\alpha}$ (**2**), m/z 353 > 309 (DP = −60, CE = −36, CXP = −15) and m/z 353 > 193 (DP = −65, CE = −34, CXP = −13); for PE_2 (**3**), PD_2 (**4**) and 15*R*-PD_2 (**5**) m/z 351 > 315 (DP = −55, CE = −18, CXP = −11) and m/z 351 > 271 (DP = −50, CE = −25, CXP = −12); for dihydro-keto PE_2 (**6**) and dihydro-keto PD_2 (**7**), m/z 351 > 333 (DP = −35, CE = −16, CXP = −13) and m/z 351 > 315 (DP = −55, CE = −18, CXP = −11); and for the internal standard PD_2-d4 (**8**), m/z 355 > 337 (DP = −65, CE = −16, CXP = −17) and m/z 355 > 319 (DP = −55, CE = −18, CXP = −11). Data acquisition was performed in the SRM mode monitoring analyte-specific transitions. Quantitation was achieved by calibration with dilution series of standard compounds against a deuterated internal standard in a concentration range from 20 to 5000 pg/ml.

Mass spectrometric detection on a QTOF system

After chromatographic separation of analytes on a column-switching LC system (see above), detection of isoprostanes was performed on a QTOF mass spectrometer (TripleTOF 5600+, AB Sciex) equipped with TurbolonSpray source operating in negative ion electrospray mode. Analyst software version 1.6 was used for instrument control and data acquisition, and PeakView 1.2 and Multiquant 2.1 were used for data analysis (all AB Sciex, Warrington, UK). Instrument calibration was performed automatically using an external calibrant delivery system infusing calibration solution prior to injection of every 10th sample. The source temperature was set at 400 °C, and ionspray voltage was −4200 V. A time-of-flight (TOF) full scan was performed using a CE of −10 eV and a DP of −80 eV in a mass range from m/z 200 to 800 with an accumulation time of 50 ms. In addition, product ion spectra for all analytes and internal standards of interest were acquired in a mass range of m/z 50 to 800 using the precursor ions of m/z 353.2, 357.3, 325.2, 351.2, and 355.2, all at unit resolution of the quadrupole. Here, the collision energy was set to −20 ± 10 eV and the accumulation time was set to 30 ms, resulting in a cycle time of 400 ms. Post-acquisition processing consisted of the selection of four major product ions (using an m/z width of 0.02 Da) and their use for setting up a selective quantitation method. This technique is also referred to as high-resolution selected reaction monitoring (SRM–HR) and is schematically displayed in Fig. S2.

Quantitation was achieved by calibration with dilution series of standard compounds against a deuterated internal standard in a concentration range from 20 to 5000 pg/ml. The fragments chosen for quantification are summarized in Table S2.

Statistical analysis

Statistical significance, defined as P-value of <0.05, was confirmed by t-test analysis using the software GraphPad Prism 6.04.

Results and discussion

Analytical method setup and validation

The analytical strategy aimed for a simple sample preparation and high analytical sensitivity for nontargeted identification and quantification of a broad variety of prostaglandins. The use of a column-switching system enabled high-volume sample injection. Due to additional online dilution, high content of organic solvent was tolerated, still allowing efficient separation of isomers. Detection of analytes by mass spectrometric selected reaction monitoring provided excellent sensitivity. Optimization of the mass spectrometer was done for commercially available standards and their stable isotope-labeled analogues by direct infusion in negative ion mode. Instrument parameters for the most abundant characteristic fragment ions were determined, and MS/MS mass transitions were defined thereby.

Groups of isomeric isobaric compounds with identical chemical substructures, such as hydroxylketocyclopentanes [(**3**)–(**8**)] and their 13,14-dihydro-15-keto isomers [(**6**) and (**7**)] as well as dihydroxycyclopentanes [(**1**) and (**2**)], were differentiated by characteristic mass transitions. $PF_{2\alpha}$ (**2**) with a precursor ion of m/z 353.1 (deprotonated form) forms fragment ions of m/z 309.1 by loss of carbon dioxide and of m/z 193.0 by cleavage of the cyclopentane and the double bond between C13 and C14 (Fig. 1B). The isobaric $iPF_{2\alpha}$-VI (**1**) forms mainly a fragment ion of m/z 114.9 via collision-induced dissociation (CID) (Fig. 1C). These product ions are not found in the hydroxycyclopentanone derivatives [(**3**)–(**7**)]. In contrast, these isomers form fragment ions by the loss of water (m/z 333.0) and carbon dioxide (m/z 315.0 and 271.1). The divergence in intensity of the specific fragment ions allowed for the separation of the dihydro-keto compounds with dominant mass fragments generated by subsequent loss of two molecules of water from the m/z 351.1 precursor ion (Fig. 1D and E). Corresponding mass fragments of +2 amu as compared with the D and E ring isomers at m/z 335.0, 317.0, and 273.1 can be found in the F-ring prostaglandins (product ion spectra not shown). This is caused by the different molecular weight of the keto form relative to the hydroxyl form.

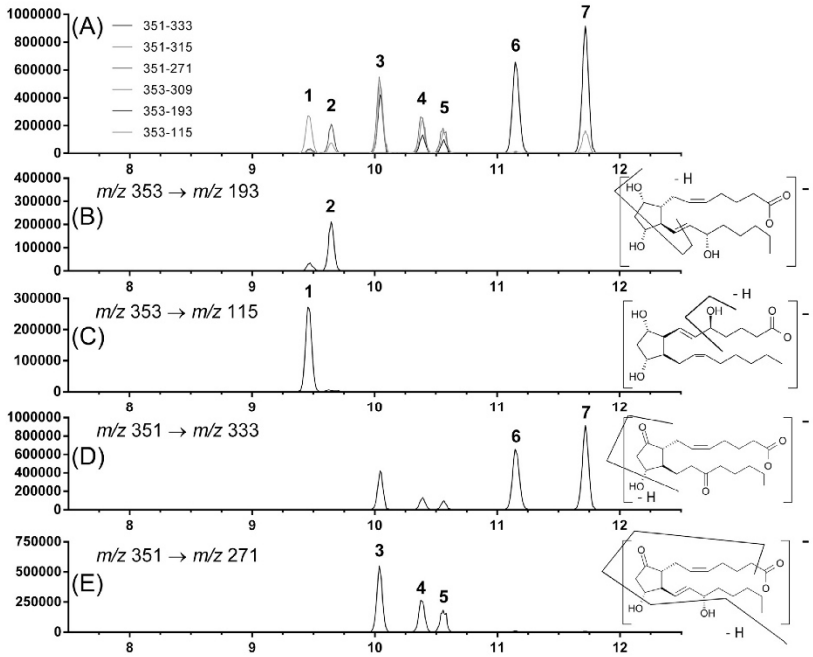

Fig.1. Chromatograms of reference standards. (A) Total ion chromatogram with characteristic selected reaction monitoring (SRM) transitions of prostaglandin standards at a concentration of 5 ng/ml: $iPF_{2\alpha}$-VI (1); $PF_{2\alpha}$ (2), PE_2 (3); PD_2 (4); 15R-PD_2 (5); dihydro-keto PE_2 (6); dihydro-keto PD_2 (7). (B–E) Specific transitions that allowed for mass spectrometric discrimination between the different groups of prostanoids and different MS/MS fragmentation using the structures of $PF_{2\alpha}$ (B), $iPF_{2\alpha}$-VI (C), dihydro-keto PE_2 (D), and PE_2 (E).

Using the specific mass spectrometric parameters, a mixture of the reference compounds resulted in a resolved mass chromatogram after a separation within 13.5 min (Fig. 1A). Analytes were successfully retained on the trapping column after large volume injection and then separated after back flush elution onto the analytical column. With the mass spectrometric resolution set to "unit" (0.7 Da), 13 data points per analyte peak could be acquired with a peak width at half height of 3.0–3.6 s. The resolution factor R (Eq. (1)) was 1.86 for the closest peaks of PD_2 (**4**) and 15R-PD_2 (**5**):

$$R = \frac{1.18(t_{R2} - t_{R1})}{w2_{0.5} + w1_{0.5}}. \quad (1)$$

The same reference compounds were diluted to final concentrations of 2000 and 200 pg/ml into precipitated hepatocytes in order to determine the matrix effect. No relevant ion suppression was observed (Table 1). Therefore, it was also decided to keep the number of internal standards as low as one (PD_2-d4).

For available authentic standards, a calibration was performed in triplicates with concentrations for anticipated levels from 20 to 5000 pg/ml. Calibration curves were obtained by using a weighting of $1/x$ for the regression analysis. The limit of quantification for all analytes was 20 pg/ml. Values for accuracy and precision (stated as percentage standard deviation) at the lowest calibration point were 107% (4.5%) for $iPF_{2\alpha}$-VI (**1**), 117% (0.4%) for $PF_{2\alpha}$ (**2**), 112% (8.6%) for PE_2 (**3**), 112% (9.6%) for PD_2 (**4**), 110% (6.2%) for 15R-PD_2 (**5**), 108% (0.1%) for dihydro-keto PE_2 (**6**), and 108% (4.8%) for dihydro-keto PD (**7**), The average accuracy of all measurements was 119% with a precision of 5.3%. In the measured range of 3 orders of magnitude, no saturation of the detector could be observed. The linearity of the calibration curves was between $R^2 = 0.993$ and 0.996 (Table 2).

Table 1
Matrix effect for online SPE–LC–MS/MS on 4000 QTRAP for two concentrations spiked into solvent (water/acetonitrile, 50:50, v/v).

	Isomer	2000 pg/ml	200 pg/ml
Relative response with matrix	$iPF_{2\alpha}$-VI (**1**)	96.0%	99.3%
	$PF_{2\alpha}$ (**2**)	103.6%	111.3%
	PD_2 (**4**)	100.3%	100.4%
	Dihydro-keto PE_2 (**6**)	106.7%	89.0%
	Dihydro-keto PD_2 (**7**)	99.7%	96.6%
Peak area	PD_2-d4 (**8**)	$9.839*10^5$	$5.196*10^4$
	PD_2-d4 in matrix	$11.780*10^5$	$6.516*10^4$

Table 2
Analytical parameters for quantitative determination of prostaglandin isomers from 20 to 5000 pg/ml.

Standard concentration (pg/ml):		20	50	100	200	500	1000	2000	5000	QC 50	QC 200	QC 1000
iPF$_{2\alpha}$-VI (**1**)	Calc'd conc.	21	45	90	177	438	1314	2383	4315	49	190	1234
	SD (%)	4.5	2.7	0.9	0.0	11.0	9.4	3.9	7.6			
	Accuracy (%)	107	91	90	88	88	131	119	86	99	95	123
PF$_{2\alpha}$ (**2**)	Calc'd conc.	23	39	74	136	328	1476	2786	5509	48	155	1334
	SD (%)	0.4	0.4	4.6	4.4	7.1	12.0	2.9	11.6			
	Accuracy (%)	117	79	74	68	66	148	139	110	95	78	133
PE$_2$ (**3**)	Calc'd conc.	22	41	86	158	355	1413	2726	5547	47	180	1328
	SD (%)	8.6	3.4	0.3	3.5	3.4	1.7	1.7	1.1			
	Accuracy (%)	112	83	86	79	71	141	136	111	94	90	133
PD$_2$ (**4**)	Calc'd conc.	22	43	81	148	335	1338	2607	5777	47	169	1222
	SD (%)	9.6	8.0	0.8	0.8	5.7	8.2	4.0	9.1			
	Accuracy (%)	112	86	81	74	67	134	130	116	95	84	122
15*R*- PD$_2$ (**5**)	Calc'd conc.	22	45	86	156	375	1235	2524	5628	48	176	1125
	SD (%)	6.0	4.2	0.9	0.7	4.1	9.6	4.2	7.6			
	Accuracy (%)	110	89	86	78	75	124	126	113	97	88	112
Dihydro-keto PE$_2$ (**6**)	Calc'd conc.	22	45	85	167	428	1215	2471	5095	47	180	1173
	SD (%)	0.1	8.7	4.4	6.1	12.2	11.4	4.9	10.3			
	Accuracy (%)	108	90	85	84	86	121	124	102	93	90	117
Dihydro-keto PD$_2$ (**7**)	Calc'd conc.	22	45	89	166	397	1325	2462	4778	47	189	1298
	SD (%)	4.8	8.9	2.0	3.0	10.2	8.3	5.4	4.8			
	Accuracy (%)	108	89	89	83	79	133	123	96	94	94	130

Note. QCs are quality controls measured at three concentrations: 50, 200, and 1000 pg/ml. Calc'd conc., calculated concentration; SD, standard deviation.

Because background levels of different prostaglandins were present in hepatocyte matrix and no matrix effect with respect to signal intensity was observed, calibration standards were diluted in cell culture medium and diluted with quench solution analogue to the experimental samples.

With respect to sample stability, repetitive injections of analyte spiked hepatocyte or plasma matrix samples were done over a maximum time of 24 h in room temperature conditions. Because no degradation was observed, this allowed for submission of a set of at least 96 samples without intervention of the analyst (data not shown). To avoid any long-term degradation, all not analyzed samples were stored at −80 °C.

Our study compares as similar or superior to studies recently performed in this field. Chromatographic (either gas or liquid) coupled mass spectrometric techniques as well as enzyme immunoassays (EIAs) have been used. Specific affinity approaches are commercially available (e.g., for the detection and quantification of 8 iso-PGF$_{2\alpha}$). EIA has been applied to analysis of rat plasma samples for determination of the effect of carbon tetrachloride treatment on iso-PGF$_{2\alpha}$ [29]. Nevertheless, immunoaffinity approaches have certain drawbacks despite being advantageous with respect to costs and handling. They can detect only known, and therefore predefined, analytes according to the availability of antibodies and radiolabelled antigens. In addition, they turned out to be less reliable due to insufficient selectivity. Deviations between immune-linked and chromatographic-coupled MS were explained by cross-reactivity with structurally similar molecules [30,31]. On the other hand, gas chromatographic separation requires beforehand purification and derivatization to generate volatile and detectable species [32]. In general, most assays described in the literature are relatively time-consuming because they involve additional preparation steps such as liquid–liquid extraction (LLE), multiple chromatographic phases, and solid phase extraction (SPE) [33] but are theoretically able to generically detect prostanoid-like analytes. Thus, mass spectrometric analysis is regarded as method of choice for the detection of prostanoids [34].

Comparable to this study, rapid sample workup followed by direct HPLC injection and online enrichment had already been used by Haschke and coworkers. The authors accomplished the detection and quantitation of a single isomer, namely 15-F$_{2t}$ IsoP (= 8-iso-PF$_{2\alpha}$), from human urine samples in 13 min and chromatographically separated this analyte from other F-ring isoprostanes [35]. Casetta and coworkers succeeded in detecting different F$_2$ isoprostanes from blood samples with the help of on-line cleanup with a chromatographic run time of 10 min [36]. Numerous research groups had analyzed F$_2$ isoprostanes by the column-switching system preceded by SPE steps that allow for the detection of up to five isomeric forms [37,38], including their separation from other metabolites of polyunsaturated fatty acid and eicosanoid metabolites [39].

Analytical investigations of PD$_2$ and PE$_2$ have also been addressed because of their (patho)physiological relevance: PE$_2$ is known to be involved in inflammation processes (e.g., caused by UV radiation in the skin) [40], whereas PD$_2$ plays a major role in immune responses such as allergic conditions and asthma [41].

A very simple method for analysis of PD$_2$ together with histamine, another marker for allergic reactions, was recently presented by Koyama and coworkers. They detected the analyte without using any workup or derivatization step on an LC–ESI–MS/MS system [42].

In terms of quantification parameters, Schmidt and coworkers presented a study where microdialysis samples were investigated for both isomers of isoprostanes with limits of quantification of 50 and 25 pg/ml [43]. Cao and coworkers described a similar study that performed the LC–MS/MS analysis of PD$_2$ and PE$_2$ within 10 min with limits of quantification of 100 and 20 pg/ml, respectively [44]. Brose and coworkers established a method that enabled chromatographic separation of several prostaglandin D and E isobaric isomers [20].

Besides various reports on the analysis of selected groups of prostaglandins and isoprostanes, analytical approaches to detect several groups have been published as well. Rinne and coworkers managed to separate seven prostaglandin isomers from the A D, E, F, and J ring group by online SPE LC–MS/MS using two trapping dimensions within the LC system, although the process needed a total run time of 35 min per injection [45].

Yu and coworkers reported an ultra-fast chromatographic separation in 0.5 min for six prostanoid-like compounds, providing the option of quantification [46].

All studies used LLE for analyte purification from matrix compounds but could not avoid impurities leading to non-analyte-related peaks. Although this step was omitted in the current

approach, a detection limit smaller than 20 pg/ml for all tested isomers could be achieved. This value results from large injected volumes containing high amounts of organic solvent.

Determination of prostaglandins/isoprostanes from hepatocyte samples in response to oxidative stress

To demonstrate applicability of isoprostane determination to biological samples, we determined prostaglandin levels from hepatocyte incubations by simulating oxidative stress with the model chelate ferric nitrilotriacetic acid [Fe(III)NTA]. This compound is known to cause oxidative stress in vitro and in vivo. The activation of lipid peroxidation is provoked by the redox activity of the reduced Fe^{2+} [47]. Different groups have shown in vitro effects such as DNA strand breaks, chromatide exchange, and nucleoside oxidation as well as malonyldialdehyde (MDA) formation [48–50]. In vivo experiments confirmed the effect on lipid peroxidation in rodents where the depletion of glutathione (GSH) and the decrease of antioxidant and GSH metabolizing enzyme were observed [51–53].

Several groups have employed primary hepatocytes or hepatoma-derived cell lines for the study of drug-induced hepatic injury [54]. As biochemical readout of these studies, general cytotoxicity was measured and gene expression profiles or the unspecific cellular antioxidant capacity were determined. However, more specific investigations on individual cellular biomarkers might represent a more direct, and thus more sensitive, readout of cellular oxidative injury. In this context, isoprostanes are considered to be superior as compared with other peroxidation products (e.g., MDA) or liver enzyme activities (transaminases) [55,56] that have been subject to investigation.

Indeed, we found that the prostaglandin pattern was altered under various conditions, that is, negative control versus the addition of Fe(III)NTA. Fig. 2 shows the extracted ion chromatogram for one transition most abundantly found in the samples (m/z 351 to 271). Referring to the optimization, the three major peaks represent PD_2 (**4**), PE_2 (**3**), and 15*R*-PD_2 (**5**). An additional non-assigned isoprostane isomer was detected at the retention time of 10.8 min.

The hepatocellular concentrations of the most responsive isomers on treatment are presented in Fig. 3. Significantly increased analyte concentrations could be observed depending on exposure time (3 vs. 1 h) and treatment concentration [50 vs. 150 μM Fe(III)NTA]. In control rat hepatocytes, the 15*R*-PD_2 (**5**) level after 3 h of incubation was at 236.1 ± 138.0 pg/ml, whereas the concentrations in hepatocytes treated with 50 and 150 μM Fe(III)NTA were significantly higher with levels of 1364 ± 262 pg/ml (5.8-fold increase) and 2001 ± 577 pg/ml (8.5-fold increase), respectively. Amounts in human hepatocytes were generally lower with

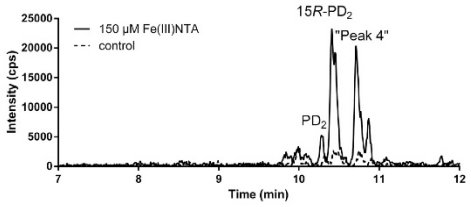

Fig.2. Extracted ion chromatogram (SRM m/z 351 to 271) of rat hepatocytes after 3 h of incubation. Peaks for PD_2 (4), 15R-PD_2 (5), and the novel analyte "peak 4" increased significantly from control (dashed line) in the sample treated with 150 μM Fe(III)NTA (solid line).

111 ± 44 pg/ml after 3 h in control cells and augmented levels of 839 ± 132 and 833 ± 323 pg/ml after treatment (7.5-fold increase). A significant increase could already be observed after only 1 h of treatment. See Table 3.

In general, a time- and concentration-dependent 2- to 8-fold increase was clearly observed: The concentration of PD_2 (**4**) after 3 h of incubation changed 8.5-fold when treated with 50 μM Fe(III)NTA and changed 9.5-fold when treated with 150 μM Fe(III)NTA (3.3- and 3.1-fold after 1 h). In human cells, the time-dependent effect was also evident for 50 μM Fe(III)NTA, whereas for the higher concentration no additional effect was detected. This might be due to saturation processes.

Because the unassigned isomer of the retention time (RT) 10.8 min has not been identified yet, peak area ratios are given for this isomer. Although the concentration is not known, the increase as compared with control was remarkable. After 1 h, the peak area in treated hepatocytes was 4.0-fold higher as compared with the control. After 3 h, augmentations to 6.7- and 8.5-fold increases were observed for 50 and 150 μM Fe(III)NTA, respectively. The same trend was detected in human cells with increasing peak areas of 7.0- and 5.0-fold after 1 h and 9.0- and 7.4-fold after 3 h for the lower and higher doses, respectively.

To our knowledge, the PD_2 isomer 15*R*-PD_2 (**5**) has not been described in the context of oxidative stress monitoring yet and was identified as a new marker for oxidative stress here. This isomer was found recently to be an equally potent agonist of the prostanoid receptor DP_2 (located on Th2 cells involved in the response to eosinophils) [57]. It was also recently investigated from mice brain tissues by Brose and coworkers, who observed a 2.5-fold alteration in levels of free and esterified 15*R*-PD_2 induced by ischemia [20].

An overview on changes in prostanoid concentration compared with results from previous studies in rat hepatocytes as a test system is shown in Fig. 4. The slope displaying the sensitivity of response is steeper for D-ring isomers than for the F-ring isomers, suggesting that they are most suitable for analysis of hepatic tissue.

The influence of oxidative stress on prostaglandin levels was studied previously with rat hepatocytes as a model system. Sicilia and coworkers found a 4.0- and 4.7-fold increase of $iPF_{2\alpha}$-III and 8,12-iso-$iPF_{2\alpha}$-VI, respectively, on treatment with CCl_4 using LLE [21]. Due to waiving the extraction step in our setup, these two isomers were below the detection limit. Levels of the F_2 isomer $iPF_{2\alpha}$-VI showed a similar response as compared with those isomers of the previous study (4-fold). However, besides the F-ring prostaglandins, we were able to detect other isoforms (D- and E-ring isomers) that seem to have higher relevance with respect to abundance and response to oxidative stress. Johnston and Kroening detected an increase in prostaglandin production in hepatocytes triggered by CCl_4 gas with levels of 144 pg/mg protein PE_2 and 6000 pg/mg protein PD_2 in hepatocyte culture determined with EIA [58].

The formation of prostaglandin E_2 and D_2 as a result of nonenzymatic processes has been observed in other matrices as well. Gao and coworkers investigated the effect of CCl_4 in rat urine, where levels of prostaglandin E_2 increased by a factor of 7 and PD_2 increased by a factor of 10 [33].

Finally, this study revealed another sensitive isomer at RT 10.8 min. However, its structure could not be identified yet. This isomer is isobaric to PD_2 (**4**), and the transition m/z 351 to 271 was used for its detection. Because of its retention time at 10.8 min (PD_2: 10.4 min) and the results of the saponification test with potassium hydroxide (leads to the degradation of all cyclopentanone isomers as well as "peak 4"), we speculate that this isomer contains a cyclopentanone ring as well. This hypothesis needs to be confirmed further.

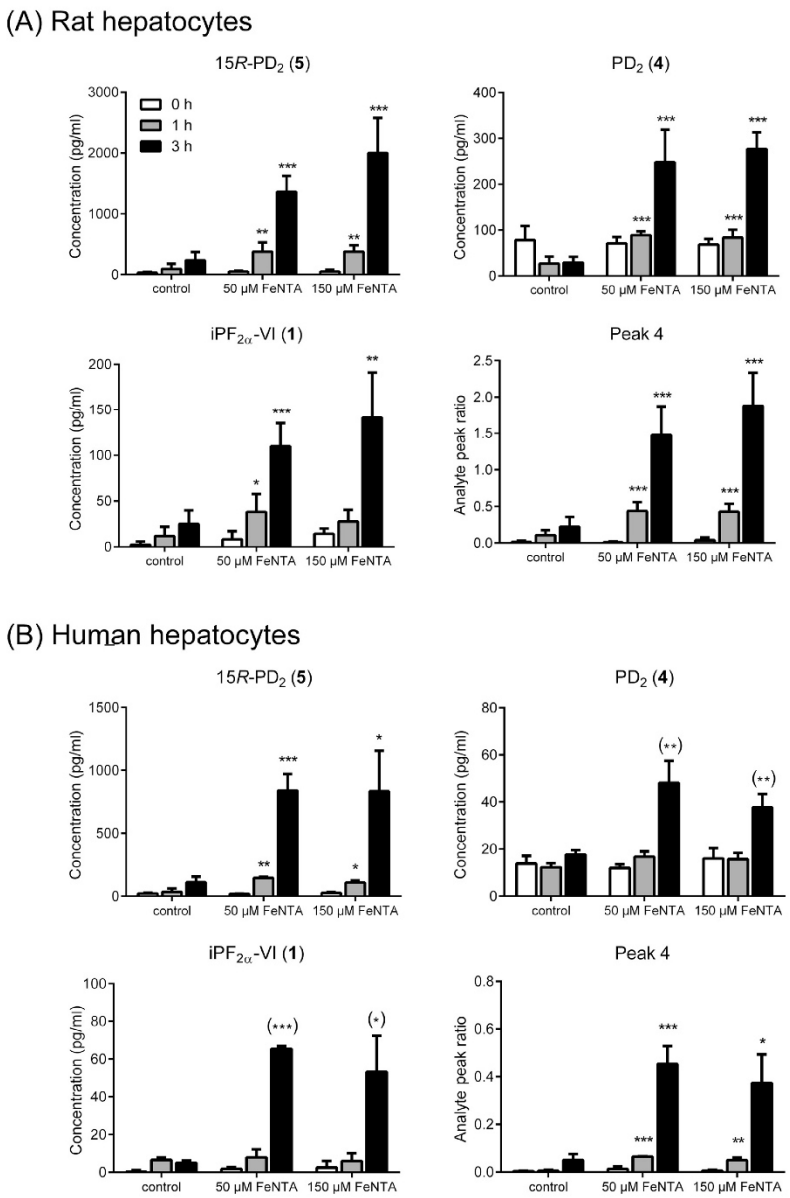

Fig.3. Increase of cellular concentration of selected prostaglandin and isoprostane isomers as a response to oxidative stress in rat (A) and human (B) hepatocytes. Samples were obtained from t = 0 as well as after 1 and 3 h of incubation with FeNTA. Values are means ± standard deviations. The identity of "peak 4" has not been elucidated yet and, therefore, is displayed as the ratio of analyte to internal standard peak area. Analyte concentrations are significantly different from the corresponding untreated samples with $^{*}P < 0.05$, $^{**}P < 0.01$, or $^{***}P < 0.001$. Asterisks are in parentheses when the concentration of controls was below the level of quantification.

Table 3
Overview of obtained results for prostaglandin/isoprostane concentrations in rat and human hepatocyte samples treated with 50 or 150 μM Fe(III)NTA for 1 or 3 h as compared with control samples.

		Rat				Human			
		1 h		3 h		1 h		3 h	
		Concentration (pg/10^6 cells)	SD	Concentration (pg/10^6 cells)	SD	Concentration (pg/10^6 cells)	SD	Concentration (pg/10^6 cells)	SD
$iPF_{2\alpha}$-VI (**1**)	Control	<20		25.1	14.7	<20		<20	
	50 μM	38.1	19.5	109.8	25.1	<20		65.4	
	150 μM	27.6	12.8	140.9	50.2	<20		53.2	19.2
PE_2 (**3**)	Control	<20		<20		<20		<20	
	50 μM	34.0	11.7	102.9	67.3	<20		<20	
	150 μM	40.9	5.2	157.3	38.0	<20		<20	
PD_2 (**4**)	Control	26.9	14.8	29.1	12.5	<20		<20	
	50 μM	88.8	8.4	247.7	71.5	<20		48.1	9.4
	150 μM	83.4	17.5	276.8	36.5	<20		37.6	5.7
15*R*-PD_2 (**5**)	Control	92.8	82.2	236.1	138.0	34.2	27.1	111.2	44.1
	50 μM	378.2	151.3	1363.5	262.3	145.8	6.9	838.9	131.6
	150 μM	378.5	101.9	2000.5	577.1	107.8	19.0	833.0	323.0
Dihydro-keto PE_2 (**6**)	Control	<20		<20		<20		<20	
	50 μM	29.8	16.2	136.0	76.0	<20		68.1	9.8
	150 μM	30.8	18.0	158.9	116.0	<20		62.9	24.8
"Peak 4"	Control	0.11	0.07	0.22	0.14	0.01	0.00	0.05	0.03
	50 μM	0.44	0.12	1.48	0.40	0.07	0.00	0.45	0.07
	150 μM	0.43	0.11	1.88	0.45	0.05	0.01	0.37	0.12

Note. Values are means ± standard deviations (SD). Basal levels of the analytes were above the limit of detection but not always above the limit of quantification (as indicated).

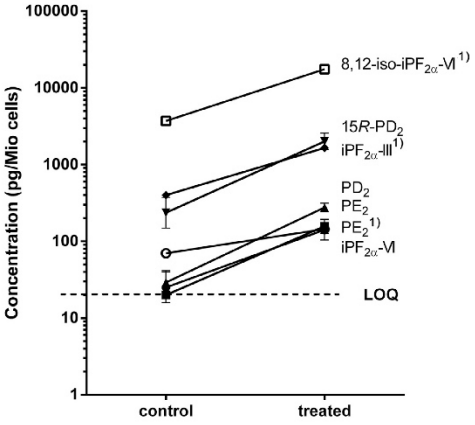

Fig.4. Overview on changes of prostaglandin/isoprostane concentration in response to treatment with 150 μM Fe(III)NTA after 3 h of incubation in rat hepatocytes. 1) indicates values reported in [21] and [58]. Literature values were expressed as pg/mg protein (1 mg protein equates approx. 1 Mio cells). Values are means ± standard deviation. Dashed line represents the limit of quantification.

Comparison of triple quadrupole mass spectrometric detection to QTOF detection

Because mass spectrometric instrumentation in drug metabolism and preclinical safety assessment is shifting more and more toward high-resolution mass spectrometers, we investigated the possibility of quantitative biomarker analysis on a QTOF instrument. Analogous to the established SRM detection on triple quadrupole instruments, we applied a novel high-resolution SRM technique consisting of a high-resolution survey scan to generate accurate mass precursor ions and different product ion scans to generate accurate mass fragment ions chosen precursor ions (quadrupole selection at "unit" resolution), as depicted in Fig. S2 of the supplementary material. Method setup was possible using generic source parameters; that is, no tuning activity was needed for the different analytes. In addition, the experimental design enabled the post-acquisition selection of multiple fragment ions for quantification (see Table S2). Due to the availability of accurate mass fragmentation, selectivity as compared with conventional SRM is increased. With an overall cycle time of 400 ms (QTRAP method: 520 ms), even more data points per peak could be recorded. Quality parameters for both instruments were inspected closely at the lowset concentration used (20 pg/ml) for two representative analytes: $iPF_{2\alpha}$-VI (**1**) and dihydro-keto PE_2 (**6**). On the QTOF instrument, the signal-to-noise ratio was increased from 4.9 to 3.9 to 18 and 9, respectively. In addition, the precision of standards was higher with 5.1% for $iPF_{2\alpha}$-VI (**1**) and 8.3% for dihydro-keto PE_2 (**6**) (QTRAP values were 14 and 18%, respectively). However, the degree of linearity showed a slight drop for the QTOF calibration with regression coefficients of 0.980 (QTRAP: 0.993) and 0.987 (QTRAP: 0.996) for both analyte calibrations in the range from 20 to 5000 pg/ml. The reason for this effect can be explained by the fact that the QTOF calibration used a weighting factor of $1/x^2$, whereas the QTRAP calibration used a weighting of $1/x$. The increased peak width from 5.2 to 6.7 s and from 5.7 to 9.5 s, together with increased signal-to-noise ratios and a higher number of points per peak (16 and 23 vs. 10 and 11, respectively), points toward increased sensitivity of the SRM–HR method. Ion suppression in plasma against solvent (67% EtOH/33% H_2O, 0.1% formic acid) lay at an average of 19%. However, while analytes and internal standard suffered from the same effect, peak area ratios stayed constant and reliable detection was possible down to the lowest concentration used for calibration.

A quantitative analytical setup for the detection of D_2 and E_2 prostanoids using QTOF MS has been reported recently by others, for example, by using an MS^{all}-type experiment and selection of the precursor and a fragment ion from the low-energy and high-energy scans, respectively [59]. However, selectivity for this experiment type is lower as compared with a precursor-dependent experiment for generation of MS2 data. Such an approach was applied for another quantitative biomarker investigation using high-resolution mass spectrometry. However, due to instrument limitations, the

addition of a low-energy full scan to the product ion mode was not possible [60]. Combination of the strengths of both approaches could be applied in the current setup.

The analytical setup enabled detection of background levels of isoprostane isomer rat plasma with 23.7 ± 0.7 pg/ml for iPF$_{2\alpha}$-VI (**1**), 769.3 ± 183.7 pg/ml for PE$_2$ (**3**), 388.2 ± 65.1 pg/ml for PD$_2$ (**4**), 35.4 ± 9.3 pg/ml for 15*R*-PD$_2$ (**5**), 134.2 ± 23.8 pg/ml for dihydro-keto PE$_2$ (**6**), and 28.1 ± 0.9 pg/ml for dihydro-keto PD$_2$ (**7**). To monitor the in vivo effect of oxidative stress on isoprostane expression, background levels of detected prostaglandin levels were compared with the concentration in rat plasma 3 h after administration of a low dose (15 mg/kg) or a high dose (65 mg/kg) of Fe(III)NTA. Significant changes were observed for the isomers 15*R*-PD$_2$ (**5**) (13.7-fold increase), iPF$_{2\alpha}$-VI (**1**) (3.4-fold increase), and dihydro-keto PE$_2$ (**6**) (23.2-fold increase) after high-dose treatment with a starting adaptation already for the lower dose. Here, significance was already observed for 15*R*-PD$_2$ (**5**) with a change from 35.4 ± 9.3 to 110 ± 10.6 pg/ml (3.1-fold change) (Fig. 5).

Different groups have already reported analytical applications to determine eicosanoids from blood matrices. A significant increase in prostaglandin concentration in human whole blood samples after calcium ionophore stimulation was reported recently for different analytes such as PD$_2$, dihydro-keto PD$_2$, and PE$_2$ [61]. Basal levels were found to be in the two- to three-digit pg/ml range, similar to those found in the current experiments in rats. Another study investigating the effect of the same activation in mice blood samples found an unchanged level of 13 ng/ml PE$_2$ [62] These results indicate that the current method is able to also detect prostaglandin levels in human in vivo matrices and may be applied to monitor oxidative stress conditions and detect changes in disease state in humans.

Conclusion

The presented method allows the chromatographic resolution and sensitive detection of various prostaglandins from in vitro toxicity screening with hepatocytes in a 96-well plate format. The assay is applicable to higher throughput applications in a drug discovery setting, allowing for the detection and quantification of prostanoids independent of a priori application of enrichment tools for specific analytes. The relevance of the assay for the detection of oxidative stress in in vitro pathophysiological conditions was proven with Fe(III)NTA. Here, the detection of prostaglandins as biomarkers for hepatic oxidative stress in rodent hepatocytes could be demonstrated and translated to human liver cells.

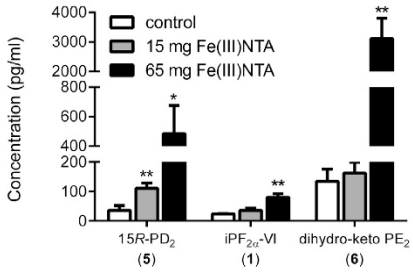

Fig.5. Increase of isoprostane plasma concentration as a response to oxidative stress in Fischer 344 rats 3 h post-administration of 15 or 65 mg/kg Fe(III)NTA as compared with control animals (0.9% sodium chloride solution). Concentrations are means ± standard deviations (n = 3). Significance is indicated by *P < 0.05 or **P < 0.01.

The potential of this method to be applied for the analysis of isoprostanes from in vivo samples was shown for rat plasma samples by demonstrating the method's applicability to a state-of-the-art QTOF mass spectrometer with an additional gain in sensitivity and selectivity. The value of isoprostanes for oxidative stress conditions as noninvasive biomarkers from, for example, urine samples is currently under investigation.

Appendix A. Supplementary data

Supplementary data related to this article can be found at http://dx.doi.org/10.1016/j.ab.2016.01.005.

References

[1] H. Sies, Biochemistry of oxidative stress, Angew. Chem. Int. Ed. Engl. 25 (1986) 1058–1071.
[2] A. Reis, C.M. Spickett, Chemistry of phospholipid oxidation, Biochim. Biophys. Acta 1818 (2012) 2374–2387.
[3] J.M. McCord, I. Fridovich, Superoxide dismutase: an enzymic function for erythrocuprein (hemocuprein), J. Biol. Chem. 244 (1969) 6049–6055.
[4] K.D. Tew, D.M. Townsend, Glutathione-S-transferases as determinants of cell survival and death, Antioxid. Redox Signal. 17 (2012) 1728–1737.
[5] S.V. Avery, Molecular targets of oxidative stress, Biochem. J. 434 (2011) 201–210.
[6] A.C. Maritim, R.A. Sanders, J.B. Watkins 3rd, Diabetes, oxidative stress, and antioxidants: A review, J. Biochem. Mol. Toxicol. 17 (2003) 24–38.
[7] E. Neofytou, E.G. Tzortzaki, A. Chatziantoniou, N.M. Siafakas, DNA damage due to oxidative stress in chronic obstructive pulmonary disease (COPD), Int. J. Mol. Sci. 13 (2012) 16853–16864.
[8] S. Basu, R. Nachat-Kappes, F. Caldefie-Chezet, M.P. Vasson, Eicosanoids and adipokines in breast cancer: From molecular mechanisms to clinical considerations, Antioxid. Redox Signal. 18 (2013) 323–360.
[9] M. Di Carlo, D. Giacomazza, P. Picone, D. Nuzzo, P.L. San Biagio, Are oxidative stress and mitochondrial dysfunction the key players in the neurodegenerative diseases? Free Radic. Res. 46 (2012) 1327–1338.
[10] D.G. Deavall, E.A. Martin, J.M. Horner, R. Roberts, Drug-induced oxidative stress and toxicity, J. Toxicol. 2012 (2012) 645460.
[11] C.V. Pereira, S. Nadanaciva, P.J. Oliveira, Y. Will, The contribution of oxidative stress to drug-induced organ toxicity and its detection in vitro and in vivo, Expert Opin. Drug Metab. Toxicol. 8 (2012) 219–237.
[12] D.C. McMillan, C.L. Powell, Z.S. Bowman, J.D. Morrow, D.J. Jollow, Lipids versus proteins as major targets of pro-oxidant, direct-acting hemolytic agents, Toxicol. Sci. 88 (2005) 274–283.
[13] J. Uetrecht, Idiosyncratic drug reactions: past, present, and future, Chem. Res. Toxicol. 21 (2008) 84–92.
[14] G. Tuschl, B. Lauer, S.O. Mueller, Primary hepatocytes as a model to analyze species-specific toxicity and drug metabolism, Expert Opin. Drug Metab. Toxicol. 4 (2008) 855–870.
[15] A.P. Li, Human hepatocytes: Isolation, cryopreservation, and applications in drug development, Chem. Biol. Interact. 168 (2007) 16–29.
[16] J. Rokach, S. Kim, S. Bellone, J.A. Lawson, D. Pratico, W.S. Powell, G.A. FitzGerald, Total synthesis of isoprostanes: Discovery and quantitation in biological systems, Chem. Phys. Lipids 128 (2004) 35–56.
[17] S.S. Fam, J.D. Morrow, The isoprostanes: Unique products of arachidonic acid oxidation: A review, Curr. Med. Chem. 10 (2003) 1723–1740.
[18] K. Yuhki, F. Kojima, H. Kashiwagi, J. Kawabe, T. Fujino, S. Narumiya, F. Ushikubi, Roles of prostanoids in the pathogenesis of cardiovascular diseases: novel insights from knockout mouse studies, Pharmacol. Ther. 129 (2011) 195–205.
[19] I.M. Koharudin, H. Liu, R. Di Maio, R.B. Kodali, S.H. Graham, A.M. Gronenborn, Cyclopentenone prostaglandin-induced unfolding and aggregation of the Parkinson disease-associated UCH-L1, Proc. Natl. Acad. Sci. U. S. A. 107 (2010) 6835–6840.
[20] S.A. Brose, B.T. Thuen, M.Y. Golovko, LC/MS/MS method for analysis of E series prostaglandins and isoprostanes, J. Lipid Res. 52 (2011) 850–859.
[21] T. Sicilia, A. Mally, U. Schauer, A. Pahler, W. Volkel, LC–MS/MS methods for the detection of isoprostanes (iPF$_{2\alpha}$-III and 8,12-iso-iPF$_{2\alpha}$-VI) as biomarkers of CCl_4-induced oxidative damage to hepatic tissue, J. Chromatogr. B. 861 (2008) 48–55.
[22] D. Sircar, P.V. Subbaiah, Isoprostane measurement in plasma and urine by liquid chromatography–mass spectrometry with one-step sample preparation, Clin. Chem. 53 (2007) 251–258.
[23] G.L. Milne, S.C. Sanchez, E.S. Musiek, J.D. Morrow, Quantification of F$_2$-isoprostanes as a biomarker of oxidative stress, Nat. Protoc. 2 (2007) 221–226.
[24] J. Nourooz-Zadeh, Key issues in F$_2$-isoprostane analysis, Biochem. Soc. Trans. 36 (2008) 1060–1065.
[25] M. Puppolo, D. Varma, S.A. Jansen, A review of analytical methods for eicosanoids in brain tissue, J. Chromatogr. B. 964 (2014) 50–64.

[26] L. Kortz, J. Dorow, U. Ceglarek, Liquid chromatography–tandem mass spectrometry for the analysis of eicosanoids and related lipids in human biological matrices: A review, J. Chromatogr. B. 964 (2014) 1–11.

[27] G. Fabre, R. Rahmani, M. Placidi, J. Combalbert, J. Covo, J.P. Cano, C. Coulange, M. Ducros, M. Rampal, Characterization of midazolam metabolism using human hepatic microsomal fractions and hepatocytes in suspension obtained by perfusing whole human livers, Biochem. Pharmacol. 37 (1988) 4389–4397.

[28] T. Seddon, I. Michelle, R.J. Chenery, Comparative drug metabolism of diazepam in hepatocytes isolated from man, rat, monkey, and dog, Biochem. Pharmacol. 38 (1989) 1657–1665.

[29] L.K. MacDonald-Wicks, M.L. Garg, Vitamin E supplementation in the mitigation of carbon tetrachloride induced oxidative stress in rats, J. Nutr. Biochem. 14 (2003) 211–218.

[30] J. Klawitter, M. Haschke, T. Shokati, U. Christians, Quantification of 15-F_{2t}-isoprostane in human plasma and urine: Results from enzyme-linked immunoassay and liquid chromatography/tandem mass spectrometry cannot be compared, Rapid Commun. Mass Spectrom. 25 (2011) 463–468.

[31] D. Il'yasova, J.D. Morrow, A. Ivanova, L.E. Wagenknecht, Epidemiological marker for oxidant status: Comparison of the ELISA and the gas chromatography/mass spectrometry assay for urine 2,3-dinor-5,6-dihydro-15-F_{2t}-isoprostane, Ann. Epidemiol. 14 (2004) 793–797.

[32] C.E. Parker, L.B. Graham, M.N. Nguyen, B.C. Gladen, M.B. Kadiiska, J.C. Barrett, K.B. Tomer, An improved GC/MS-based procedure for the quantitation of the isoprostane 15-F_{2t}-IsoP in rat plasma, Mol. Biotechnol. 18 (2001) 105–118.

[33] L. Gao, W.E. Zackert, J.J. Hasford, M.E. Danekis, G.L. Milne, C. Remmert, J. Reese, H. Yin, H.H. Tai, S.K. Dey, N.A. Porter, J.D. Morrow, Formation of prostaglandins E_2 and D_2 via the isoprostane pathway: A mechanism for the generation of bioactive prostaglandins independent of cyclooxygenase, J. Biol. Chem. 278 (2003) 28479–28489.

[34] E. Schwedhelm, R.A. Benndorf, R.H. Böger, D. Tsikas, Mass spectrometric analysis of F_2-isoprostanes: Markers and mediators in human disease, Curr. Pharm. Anal. 3 (2007) 39–51.

[35] M. Haschke, Y.L. Zhang, C. Kahle, J. Klawitter, M. Korecka, L.M. Shaw, U. Christians, HPLC–atmospheric pressure chemical ionization MS/MS for quantification of 15-F_{2t}-isoprostane in human urine and plasma, Clin. Chem. 53 (2007) 489–497.

[36] B. Casetta, M. Longini, F. Proietti, S. Perrone, G. Buonocore, Development of a fast and simple LC–MS/MS method for measuring the F_2-isoprostanes in newborns, J. Matern. Fetal Neonatal Med. 25 (Suppl. 1) (2012) 114–118.

[37] Y. Liang, P. Wei, R.W. Duke, P.D. Reaven, S.M. Harman, R.G. Cutler, C.B. Heward, Quantification of 8-iso-prostaglandin-$F_{2\gamma}$ and 2,3-dinor-8-iso-prostaglandin-$F_{2\alpha}$ in human urine using liquid chromatography–tandem mass spectrometry, Free Radic. Biol. Med. 34 (2003) 409–418.

[38] W. Yan, G.D. Byrd, M.W. Ogden, Quantitation of isoprostane isomers in human urine from smokers and nonsmokers by LC–MS/MS, J. Lipid Res. 48 (2007) 1607–1617.

[39] L. Kortz, J. Dorow, S. Becker, J. Thiery, U. Ceglarek, Fast liquid chromatography–quadrupole linear ion trap–mass spectrometry analysis of polyunsaturated fatty acids and eicosanoids in human plasma, J. Chromatogr. B. 927 (2013) 209–213.

[40] A. Nicolaou, M. Masoodi, K. Gledhill, A.K. Haylett, A.J. Thody, D.J. Tobin, L.E. Rhodes, The eicosanoid response to high dose UVR exposure of individuals prone and resistant to sunburn, Photochem. Photobiol. Sci. 11 (2012) 371–380.

[41] Y. Yang, L.Q. Tang, W. Wei, Prostanoids receptors signaling in different diseases/cancers progression, J. Recept. Signal Transduct. Res. 33 (2013) 14–27.

[42] J. Koyama, S. Taga, K. Shimizu, M. Shimizu, I. Morita, A. Takeuchi, Simultaneous determination of histamine and prostaglandin D_2 using an LC–ESI–MS/MS method with positive/negative ion-switching ionization modes: Application to the study of anti-allergic flavonoids on the degranulation of KU812 cells, Anal. Bioanal. Chem. 401 (2011) 1385–1392.

[43] R. Schmidt, O. Coste, G. Geisslinger, LC–MS/MS analysis of prostaglandin E_2 and D_2 in microdialysis samples of rats, J. Chromatogr. B. 826 (2005) 188–197.

[44] H. Cao, L. Xiao, G. Park, X. Wang, A.C. Azim, J.W. Christman, R.B. van Breemen, An improved LC–MS/MS method for the quantification of prostaglandins E_2 and D_2 production in biological fluids, Anal. Biochem. 372 (2008) 41–51.

[45] S. Rinne, C. Ramstad Kleiveland, M. Kassem, T. Lea, E. Lundanes, T. Greibrokk, Fast and simple online sample preparation coupled with capillary LC–MS/MS for determination of prostaglandins in cell culture supernatants, J. Sep. Sci. 30 (2007) 1860–1869.

[46] R. Yu, G. Zhao, J.W. Christman, L. Xiao, R.B. Van Breemen, Method development and validation for ultra-high pressure liquid chromatography/tandem mass spectrometry determination of multiple prostanoids in biological samples, J. AOAC Int. 96 (2013) 67–76.

[47] K. Jomova, M. Valko, Importance of iron chelation in free radical-induced oxidative stress and human disease, Curr. Pharm. Des. 17 (2011) 3460–3473.

[48] I. Morel, C. Hamon-Bouer, V. Abalea, P. Cillard, J. Cillard, Comparison of oxidative damage of DNA and lipids in normal and tumor rat hepatocyte cultures treated with ferric nitrilotriacetate, Cancer Lett. 119 (1997) 31–36.

[49] K. Sakurai, A.I. Cederbaum, Oxidative stress and cytotoxicity induced by ferric-nitrilotriacetate in HepG2 cells that express cytochrome P450 2E1, Mol. Pharmacol. 54 (1998) 1024–1035.

[50] A. Hartwig, H. Klyszcz-Nasko, R. Schlepegrell, D. Beyersmann, Cellular damage by ferric nitrilotriacetate and ferric citrate in V79 cells: interrelationship between lipid peroxidation, DNA strand breaks, and sister chromatid exchanges, Carcinogenesis 14 (1993) 107–112.

[51] J.G. Goddard, G.D. Sweeney, Ferric nitrilotriacetate: a potent stimulant of in vivo lipid peroxidation in mice, Biochem. Pharmacol. 32 (1983) 3879–3882.

[52] M. Iqbal, U. Giri, M. Athar, Ferric nitrilotriacetate (Fe-NTA) is a potent hepatic tumor promoter and acts through the generation of oxidative stress, Biochem. Biophys. Res. Commun. 212 (1995) 557–563.

[53] W. Volkel, R. Alvarez-Sanchez, I. Weick, A. Mally, W. Dekant, A. Pahler, Glutathione conjugates of 4-hydroxy-2(*E*)-nonenal as biomarkers of hepatic oxidative stress-induced lipid peroxidation in rats, Free Radic. Biol. Med. 38 (2005) 1526–1536.

[54] M.L. Greer, J. Barber, J. Eakins, J.G. Kenna, Cell based approaches for evaluation of drug-induced liver injury, Toxicology 268 (2010) 125–131.

[55] M.B. Kadiiska, B.C. Gladen, D.D. Baird, D. Germolec, L.B. Graham, C.E. Parker, A. Nyska, J.T. Wachsman, B.N. Ames, S. Basu, N. Brot, G.A. Fitzgerald, R.A. Floyd, M. George, J.W. Heinecke, G.E. Hatch, K. Hensley, J.A. Lawson, L.J. Marnett, J.D. Morrow, D.M. Murray, J. Plastaras, L.J. Roberts 2nd, J. Rokach, M.K. Shigenaga, R.S. Sohal, J. Sun, R.R. Tice, D.H. Van Thiel, D. Wellner, P.B. Walter, K.B. Tomer, R.P. Mason, J.C. Barrett, Biomarkers of oxidative stress study II: are oxidation products of lipids, proteins, and DNA markers of CCl_4 poisoning? Free Radic. Biol. Med. 38 (2005) 698–710.

[56] G.L. Milne, H. Yin, J.D. Morrow, Human biochemistry of the isoprostane pathway, J. Biol. Chem. 283 (2008) 15533–15537.

[57] C. Cossette, S.E. Walsh, S. Kim, G.J. Lee, J.A. Lawson, S. Bellone, J. Rokach, W.S. Powell, Agonist and antagonist effects of 15*R*-prostaglandin (PG) D_2 and 11-methylene-PGD_2 on human eosinophils and basophils, J. Pharmacol. Exp. Ther. 320 (2007) 173–179.

[58] D.E. Johnston, C. Kroening, Stimulation of prostaglandin synthesis in cultured liver cells by CCl_4, Hepatology 24 (1996) 677–684.

[59] S.A. Brose, A.G. Baker, M.Y. Golovko, A fast one-step extraction and UPLC–MS/MS analysis for E_2/D_2 series prostaglandins and isoprostanes, Lipids 48 (2013) 411–419.

[60] R. Ottria, A. Ravelli, F. Gigli, P. Ciuffreda, Simultaneous ultra-high performance liquid chromathography–electrospray ionization–quadrupole–time of flight mass spectrometry quantification of endogenous anandamide and related *N*-acylethanolamides in bio-matrices, J. Chromatogr. B. 958 (2014) 83–89.

[61] J. Song, X. Liu, J. Wu, M.J. Meehan, J.M. Blevitt, P.C. Dorrestein, M.E. Milla, A highly efficient, high-throughput lipidomics platform for the quantitative detection of eicosanoids in human whole blood, Anal. Biochem. 433 (2013) 181–188.

[62] B. Gomolka, E. Siegert, K. Blossey, W.H. Schunck, M. Rothe, K.H. Weylandt, Analysis of omega-3 and omega-6 fatty acid-derived lipid metabolite formation in human and mouse blood samples, Prostagl. Other Lipid Mediat. 94 (2011) 81–87.

3.2.2 Application of isoprostane determination using flutamide as a DILI model compound

Application of Lipid Peroxidation Products as Biomarkers for Flutamide-Induced Oxidative Stress *In Vitro*

Marieke Teppner[1] [2], Franziska Böss[1], Beat Ernst[2] and Axel Pähler[1]

[1] DMPK, Pharmaceutical Sciences; Pharma Research and Early Development (pRED); F. Hoffmann-La Roche Ltd., Grenzacherstrasse 124; CH-4070 Basel, Switzerland

[2] Institute of Molecular Pharmacy; University of Basel, Klingenbergstrasse 50; CH-4040 Basel, Switzerland

Published in: *Toxicology Letters* 238 (2015) 53 - 59

Personal contribution: Experimental design, conduction and evaluation; manuscript preparation

Toxicology Letters 238 (2015) 53–59

Contents lists available at ScienceDirect

Toxicology Letters

journal homepage: www.elsevier.com/locate/toxlet

Application of lipid peroxidation products as biomarkers for flutamide-induced oxidative stress *in vitro*

Marieke Teppner[a,b,1], Franziska Böss[a], Beat Ernst[b], Axel Pähler[a,*]

[a] Pharmaceutical Sciences, Pharma Research and Early Development, pRED, Roche Innovation Center Basel, 4070 Basel, Switzerland
[b] Institute of Molecular Pharmacy, University of Basel, Klingenbergstrasse 50, CH-4040 Basel, Switzerland

HIGHLIGHTS

- This paper describes the increase of isoprostanes and hydroxynonenal (HNE) derivatives as early safety biomarkers of hepatotoxicity caused by oxidative stress.
- The hepatotoxic drug flutamide provoked oxidative stress in primary hepatocytes resulting in a time and dose dependent increase of 15*R*-prostaglandin D_2, prostaglandin E_2, 13,14-dihydro-15-keto prostaglandin E_2 and 5-iso prostaglandin $F_{2\alpha}$ VI.
- HNE-mercapturic acid and its metabolite dihydroxynonene-mercapturic acid were also time and concentration dependently increased.
- Lipid peroxidation products as markers of reactive oxygen species were demonstrated to be more sensitive than conventional cytotoxicity markers for an early detection of drug-induced liver injury.

ARTICLE INFO

Article history:
Received 7 March 2014
Received in revised form 24 July 2015
Accepted 4 August 2015
Available online 6 August 2015

Keywords:
Primary hepatocytes
Oxidative stress
Hepatotoxicity
Lipid peroxidation
Hydroxynonenal
Isoprostanes

ABSTRACT

The early identification of hepatotoxicity is a fundamental goal of preclinical safety studies in drug discovery and early development. Sensitive biomarkers warrant the determination of potential underlying mechanisms that help characterizing a disruption of physiological conditions prior to cell death. This study shows the potential of different lipid peroxidation products, namely isoprostanes and hydroxynonenal (HNE) derivatives, to serve as early safety biomarkers of hepatotoxicity caused by oxidative stress as underlying mechanism. The hepatotoxic drug flutamide was used as model compound in primary hepatocytes. Incubation conditions were optimized by the addition of hydrogen peroxide generating substrates enhancing the cellular response upon oxidative stress. A time and dose dependent response of different isoprostanes and prostaglandins (15*R*-prostaglandin D_2, prostaglandin E_2, 13,14-dihydro-15-keto prostaglandin E_2 and 5-iso prostaglandin $F_{2\alpha}$-VI) became manifest after 6 and 24 h of treatment in 3.8- to 17.4-fold increased concentrations where no overt hepatocellular damage was observed. For HNE-mercapturic acid and its metabolite dihydroxynonene-mercapturic acid a similar response was evident with a 20- and 10-fold increase from control after 24 h of treatment, respectively. These data indicate that lipid peroxidation products as markers of reactive oxygen species are more sensitive than conventional cytotoxicity markers for an early detection of drug-induced liver injury.

1. Introduction

The imbalance between the generation of reactive oxygen species (ROS) and their detoxification within a cellular system can result in oxidative stress. Caused by glutathione depletion, lowered activity of reductive enzyme or overproduction of ROS, oxidative stress is associated with hepatotoxicity and modulation of pathophysiological conditions (McGrath et al., 2001; Jenner, 2003). Excessive production of electrophiles can trigger functional damage by modification of proteins, DNA or lipids (Avery, 2011). Especially the liver is a source of ROS, produced *e.g.* during cytochrome P450 mediated metabolism or mitochondrial

Abbreviations: 15R-PD_2, 15R-prostaglandin D_2; DHN-MA, 1,4-dihydroxynonene mercapturic acid; Dihydro-keto PE_2, 13,14-dihydro-15-keto prostaglandin E_2; DILI, drug-induced liver injury; HNE, 4-hydroxy-2(*E*)-nonenal; HNE-MA, HNE mercapturic acid; HRP, horseradish peroxidase; i$PF_{2\alpha}$-VI, 5-iso prostaglandin $F_{2\alpha}$-VI; LDH, lactate dehydrogenase; PE_2, prostaglandin E_2; ROS, reactive oxygen species.

* Corresponding author.
E-mail addresses: marieke.teppner@evotec.com (M. Teppner), axel.paehler@roche.com (A. Pähler).
[1] Current address: Evotec AG, Essener Bogen 7, 22419 Hamburg, Germany.

http://dx.doi.org/10.1016/j.toxlet.2015.08.005
0378-4274/

respiration. Various drugs have been reported to cause hepatic damage with an at least contributing role of oxidative stress.

Flutamide is a non-steroidal androgen receptor antagonist used for treatment of prostate cancer. Due to occurrence of severe incidences of hepatic injury, it has been labeled with a black box warning by the FDA (Kraus et al., 2001; Osculati and Castiglioni, 2006). Although many studies have been performed to elucidate the cause of flutamide toxicity, the exact mechanism remains elusive. Metabolic activation to reactive intermediates has been identified as contributing factor. Electrophilic intermediates are formed *via* reduction of the nitro-aromatic moiety yielding a di-imino-like structure or an iminoquinone by hydroxylation and further oxidation. Both metabolites are prone to react with nucleophilic residues of proteins and glutathione conjugates have been identified *in vitro* (Kang et al., 2008; Wen et al., 2008). Flutamide-induced hepatotoxicity had also been associated with oxidative stress conditions. Experiments in mouse models revealed impairment of glucose homeostasis and mitochondrial dysfunction upon flutamide treatment (Kashimshetty et al., 2009; Choucha Snouber et al., 2013). In addition, interleukin (IL)-4 and IL-5 induction was observed, suggesting the involvement of the immune system as contributing factor for flutamide adverse reactions in man (Higuchi et al., 2012).

Fig. 1 summarizes the potential involvement of reactive metabolites and oxidative stress to hepatotoxicity as based on mechanistic hypotheses. Drug-protein conjugates are likely to act as haptens which are able to activate the immune system. An additional danger signal generated by oxidative stress is resulting from redox cycling of the di-imine (as depicted) or the iminoquinone metabolite. This process results *e.g.* in peroxidation of cell membrane bound unsaturated lipids that are well established targets of ROS. As accepted biomarkers for oxidative stress conditions we employed the bioanalysis of two complement groups of lipid peroxidation products. These were namely isoprostanes, isomeric to the enzymatically generated prostaglandins and derived from radical catalyzed peroxidation of arachidonic acid (Johnston and Kroening, 1996; Sicilia et al., 2008; Milne et al., 2011). In addition, stable metabolites of 4-hydroxy-2(E)-nonenal (HNE) were analyzed. Free HNE is difficult to measure. However, as HNE is a strong electrophile, it readily reacts with nucleophiles like glutathione. HNE glutathione conjugates and their degradation products have been shown to serve as suitable biomarkers for oxidative stress (Boon et al., 1999; Alary et al., 2003; Volkel et al., 2005).

Analytical determination of excessive oxidative stress is difficult because of the delicate regulation machinery within the liver. To enhance pro-oxidant effects we employed a hydrogen peroxide generating system (HRP-system) that originally had been established by the group of O'Brien (Tafazoli et al., 2005). Glucose, glucose oxidase and horseradish peroxidase (HRP) generate hydrogen peroxide in situ. This system had been shown to induce cellular damage by various drugs acting *via* attenuation of oxidative stress conditions.

In this study, we used flutamide as a model compound to investigate the contribution of metabolism-induced oxidative stress as underlying mechanism for flutamide hepatotoxicity. Biomarkers of oxidative stress were analyzed in primary hepatocytes after bioactivation of flutamide leading to formation of pro-oxidant intermediates. We report on the optimization and validation of test conditions for induction of oxidative stress caused by reactive and pro-oxidant drug metabolites in primary hepatocytes. Results were generated in rat and human cells and compared to conventional markers for overt liver toxicity.

2. Material and methods

2.1. Chemicals

Williams' medium E, formic acid p.a., dimethyl sulfoxide p.a., insulin, streptomycin, penicillin, hydrocortisone, D(+)glucose, glucose oxidase from *Aspergillus niger* and peroxidase from

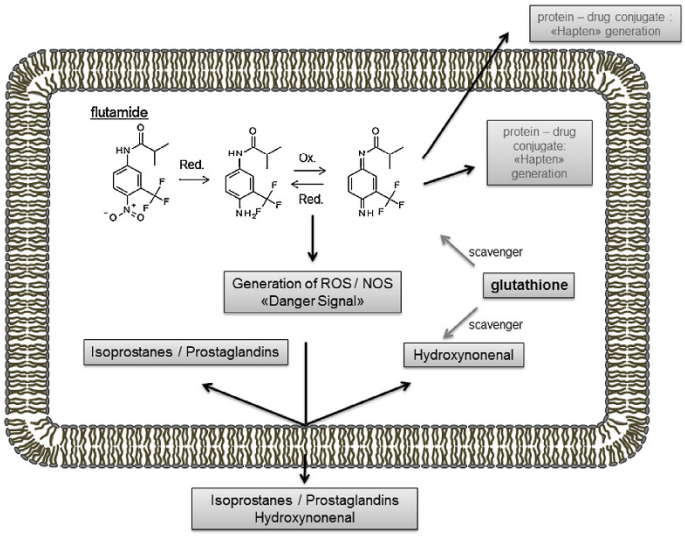

Fig. 1. Schematic overview of intracellular processes postulated to contribute to flutamide-induced hepatotoxicity.

horseradish were obtained from Sigma–Aldrich (St. Louis, MO, USA). Glutamine, gentamycin were purchased from Life Technologies Invitrogen (Lucerne, Switzerland) and acetonitrile of LC–MS grade from Fisher Scientific (Wohlen, Switzerland). Water of chromatography grade was obtained from Merck (Darmstadt, Germany). Flutamide was synthesized in house (Roche, Basel, Switzerland). The prostaglandin isomers 5-iso prostaglandin $F_{2\alpha}$-VI (i$PF_{2\alpha}$-VI), prostaglandin E_2 (PE_2), 15*R* prostaglandin D_2 (15*R*-PD_2), 13,14-dihydro-15-keto prostaglandin E_2 (dihydro-keto PE_2), prostaglandin D_2-d4, were purchased from Cayman Chemical Company (Ann Arbor, MI, USA).

2.2. Cell culture media and test compound

Incubation medium was prepared by supplementation of William's medium E with 4 mg/L insulin, 50,000 U/l penicillin, 50 mg/l streptomycin, 10 mg/l gentamycin, 2.4 mg/ml hydrocortisone. Flutamide was dissolved in DMSO to obtain a 100 mM stock solution, which was further diluted in incubation medium for use in experiments.

2.3. Cell culture and treatment

Rat primary cell were freshly prepared in house by a two-step liver perfusion procedure (Boess et al., 2007) and plated on collagen coated 24-well plates at a density of 300,000 cells per well. After 2 h attachment time the cell seeding medium (incubation medium (see above) supplemented with 10% FCS) was exchanged and non-adhesive cells were removed. Human primary hepatocytes were purchased from Hepacult Ltd., in 24-well plates at a density of 150,000 cells per cm^2. At time of arrival cells were placed into the incubator for 2 h, then medium was exchanged and non-adhesive cells removed. All experiments were carried out in the described incubation medium, a medium containing 10 mM D-glucose, 0.05 U/ml glucose oxidase and 0.5 mM horse radish peroxidase as in situ hydrogen peroxide generating system (HRP-system) was tested in parallel. Incubation was performed at 37 °C in a humidified atmosphere (5% CO_2/95% air) and stopped after 6 and 24 h by precipitation with one volume of acetonitrile containing internal standard.

2.4. LC–MS/MS analysis

The analytical setup has been previously described for the quantitative determination of hydroxynonenal derivatives from hepatic tissue (Volkel et al., 2005). For the analysis of isoprostanes *via* liquid chromatography and mass spectrometric detection it has previously been reported by others (Sicilia et al., 2008; Ecker, 2012). Briefly, quenched hepatocyte incubations were centrifuged at 5000 × *g* for 11 min at 4 °C and the transferred supernatant (500 ml diluted with 100 ml acetonitrile/water containing 0.1% formic acid) was directly injected onto the LC–MS/MS system which consisted of a YMC AQ, 20 × 2.1 mm, 5 mm column (YMC Europe) as trapping column and an Atlantis T3, 100 × 2.1 mm, 3 mm column (Waters) connected to a column 2D HPLC consisting of a Shimadzu LC ADvp binary pump system and an Agilent 1100 series LC pump connected to a triple quadrupole tandem mass spectrometer (4000 QTRAP, AB Sciex, UK) which operated in negative electrospray ionization mode using selected reaction monitoring (SRM) analysis. Transitions and tuning parameters were defined individually for each analyte by the help of authentic standards as follows: *m/z* 351.1 to *m/z* 271.1 for 15R-PD_2,*m/z* 351.1 to *m/z* 315.0 for dihydro-keto PE_2 and PE_2, *m/z* 353.1 to *m/z* 114.9 for i$PF_{2\alpha}$-VI, *m/z* 318.1 to *m/z* 189.0 for HNE-MA and *m/z* 320.1 to *m/z* 191.0 for DHN-MA. Quantitation of prostaglandins was achieved by calibration with dilution series of standard compounds against deuterated internal standard. As an authentic standard was not available for DHN-MA, HNE derivatives were quantified relatively to internal standard.

2.5. Biochemical analysis

Lactate dehydrogenase (LDH) in the supernatant was determined after 6 h and 24 h of treatment (150 ml supernatant) by a commercially available test kit (Siemens, 7.502.999) on an ADVIA 1650 autoanalyzer (Siemens Diagnostics, Erlangen, Germany). Intracellular ATP content was determined after 6 h and 24 h by means of a bioluminescence based ATP assay kit (Roche Diagnostics, Rotkreuz, Switzerland) on a Victor plate reader (PerkinElmer, Schwerzenbach, Switzerland).

2.6. Statistical analysis

Statistical significance defined as p-value of <0.05 was confirmed by t-test analysis using the software GraphPad Prism 5.03.

3. Results

3.1. Optimization of culture conditions with primary rat hepatocytes

Oxidative stress response of primary hepatocytes to flutamide treatment as measured by increase of cellular isoprostane and HNE derivative concentration was investigated under two different conditions.

Primary rat hepatocyte cultures without HRP supplementation showed a significant oxidative stress response upon high dose treatment (100 mM) with flutamide as compared to control. However, at 50 mM substrate concentration, this effect was not statistically significant (Table 1). In contrast, cells supplemented with the hydrogen peroxide generating system as amplifier of oxidative stress exhibited evident response already after treatment with 50 mM flutamide. Comparison of the detected effects clarifies that oxidative stress biomarkers were significantly increased in cells exposed to the HRP-system. Whereas a 2.2- to 3.4-fold increased concentration of lipid peroxidation derived biomarkers were measured, only minor changes (below 2-fold) were observed in the conventional cell culture.

When analyzing ATP and LDH as markers of cell viability, both systems revealed similar outcomes: ATP levels were not altered after 24 h upon high dose treatment suggesting an intact mitochondrial status. LDH levels were increased for the high treatment after one day indicating starting cytotoxic effects due to flutamide (data not shown).

From these results it was concluded that hepatocytes supplementd with the HRP-system provide a more pronounced oxidative stress response with faster onset without or only slightly affecting overall cell viability in negative controls. Hence, this setup was defined as the condition of choice for further experiments with human hepatocytes.

3.2. Effects upon flutamide treatment on primary human hepatocyte culture

3.2.1. Flutamide treatment does not affect cell viability in human hepatocytes

Cellular LDH release and ATP content over the 24 h incubation period with flutamide was examined to evaluate drug induced overt cytotoxicity as primary endpoint. This was done in order to identify experimental conditions that do not induce overt hepatocellular damage and thus possibly confounding analysis of oxidative stress biomarkers. Indeed, the applied concentrations of 50 and 100 mM flutamide did not significantly affect cellular

Table 1
Comparison of fold increase of biomarker concentration in response upon treatment with flutamide (50 mM and 100 mM) in rat and human hepatocytes treated or not treated with HRP-system.

	Analyte		Without HRP		With HRP	
			50 mM	100 mM	50 mM	100 mM
Rat hepatocytes	15*R*-PD_2	6 h	1.5	9.8***	2.6	11.0***
		24 h	1.7	4.6***	3.1*	15.3*
	Dihydro-keto PE_2	6 h	1.1	13.9***	2.2*	6.5**
		24 h	nd	nd	3.2**	13.2**
	$iPF_{2\alpha}$-VI	6 h	1.6	13.6***	2.4	9.4***
		24 h	1.7	6.2**	2.2*	6.9**
	PE_2	6 h	1.3	15.5**	1.7	7.6***
		24 h	7.5*	12.6	1.8*	9.4*
	HNE-MA	6 h	1.5	6.5**	3.5*	5.5**
		24 h	2.1	4.1**	3.4**	4.9***
	DHN-MA	6 h	3.3	10.6**	6.9	10.9***
		24 h	6.6*	30.5***	4.2*	5.2***
Human hepatocytes	15*R*-PD_2	6 h	2.9	3.9	4.9***	7.7*
		24 h	3.1*	6.6	7.7***	17.4*
	Dihydro-keto PE_2	6 h	nd	nd	7.9***	12.7***
		24 h	6.1*	14.9*	24.3***	8.5***
	$iPF_{2\alpha}$-VI	6 h	4.4*	2.7**	3.9***	6.0*
		24 h	3.1*	7.9**	3.3***	7.3
	PE_2	6 h	3.6	2.9	6.3**	10.9*
		24 h	2.0	8.2**	4.5**	13.2**
	HNE-MA	6 h	nd	nd	nd	nd
		24 h	3.0*	17.0***	12.9***	18.8***
	DHN-MA	6 h	nd	nd	30.0	7.5
		24 h	5.4*	15.4***	12.0***	9.4***

Significance is indicated by *($p < 0.05$), ** ($p < 0.01$) or *** ($p < 0.001$).

viability or mitochondrial function in human hepatocyte cultures when compared to vehicle treated cells in the presence of the HRP-system (Fig. 2). A general slight increase in extracellular LDH after 24 h can be explained by the progressing culture time and involving worse cell state. However, an effect on ATP levels was not evident at that time.

3.2.2. Dose- and time-dependent increase of lipid peroxidation products as cellular response to flutamide treatment in human hepatocytes

3.2.2.1. Isoprostanes. Lipid peroxidation markers were analyzed from the same experiments that were used for cytotoxicity assessment. To determine whether cellular oxidative stress had been caused by the treatment with flutamide, a panel of isoprostane isomers was included in the analysis. Indeed, various markers showed a significant response to the applied drug in a time and dose dependent manner. Already after 6 h and upon treatment with the lower flutamide dose (50 mM) hepatocellular concentrations of different prostaglandin isomers were significantly increased. This effect was even more pronounced after 24 h of treatment. The concentration of 15*R*-prostaglandin D_2 (15*R*-PD_2) was augmented from 1437 ± 328 pg/ml in control cells to 7110 ± 870 (4.9-fold change) and 11,082 ± 3806 pg/ml (7.7-fold change) in treated cells at 50 mM and 100 mM flutamide, respectively after 6 h of treatment. This increase was even more pronounced after 24 h of treatment and resulted in an increase from 3548 ± 666 pg/ml to 27,558 ± 1091 pg/ml (7.8-fold change) and to 61,606 ± 24,274 pg/ml (17.4-fold change) at the low dose and high dose treatment. A comparable pattern was observed for the isomers 5-iso prostaglandin $F_{2\alpha}$-VI ($iPF_{2\alpha}$-VI), 13,14-dihydro-15-keto prostaglandin E_2 (dihydro-keto PE_2) and prostaglandin E_2 (PE_2) (Fig. 3).

3.2.2.2. HNE derivatives. In addition to isoprostanes, HNE conjugates are known to serve as indicators for cellular oxidative stress. The HNE mercapturic acid (HNE-MA) conjugate and its reduced form, the dihydroxynonene (DHN) mercapturic acid (DHN-MA) were analyzed with the same analytical setup. Relative quantification was conducted from the identical samples

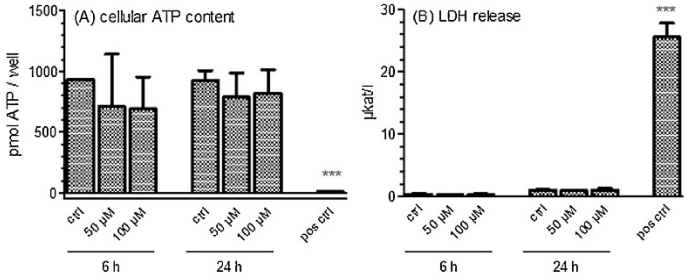

Fig. 2. Effect of flutamide on cytotoxicity markers in human hepatocytes: plated hepatocytes were incubated with 50 or 100 mM flutamide in the presence of HRP system for up to 24 h and compared to control incubations. No significant changes between control and treated cells were observed. As positive control chlorpromazine (150 mM) was used. Values are means + SD ($n = 3$).

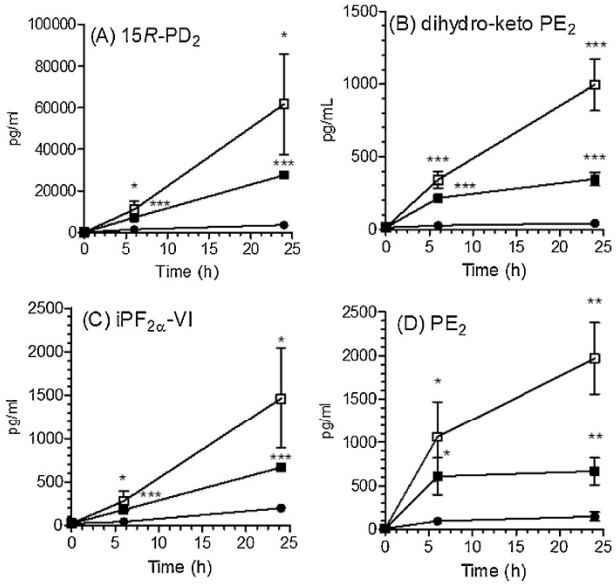

Fig. 3. Effect of flutamide on prostaglandin concentrations in human hepatocytes in the presence of HRP-system: plated hepatocytes were incubated with 50 (■) or 100 mM (□) flutamide for up to 24 h and compared to respective vehicle controls (●). Values are means + SD ($n = 3$). Significance is indicated by *($p < 0.05$), **($p < 0.01$) or *** ($p < 0.001$).

as the isoprostane biomarkers. As no authentic reference standards were available, we compared the analyte peak area relative to internal standard peak area for the relative quantification of control and treated sample. This approach was judged suitable as the focus of this work was to assess the relative response upon flutamide treatment rather than the absolute quantification. As depicted in Fig. 4, a time and concentration dependent increase of concentration was observed for both analytes upon flutamide treatment of HRP-challenged human hepatocytes. Although not statistically significant after 6 h of treatment, a trend could already be assumed that translated into a significant increase in hepatocellular HNE-MA concentration after 24 h of treatment with 50 (12.9-fold) and 100 mM (18.8-fold) flutamide. A similar observation was made for DHN-MA that showed a significant increase from controls after 24 h of flutamide treatment (9.4- to 12.0-fold). In contrast to HNE-MA, the increase of cellular concentration of DHN-MA was not found to be dose dependent in the investigated concentration range.

An overview of measured changes for all analytes included in the assay for human hepatocytes, for completeness also in the absence of HRP-system, is shown in Table 1.

4. Discussion

Oxidative stress is involved in several pathophysiological conditions such as atherosclerosis or cancer (Fam and Morrow, 2003; Choudhari et al., 2014) and acts as a risk factor for drug-induced toxicity (McGill and Jaeschke, 2013). Therefore the analysis of lipid peroxidation products as surrogate for the formation of ROS has become subject of interest.

Isoprostanes are present in various biological matrices such as urine and plasma and known to be stable products and can

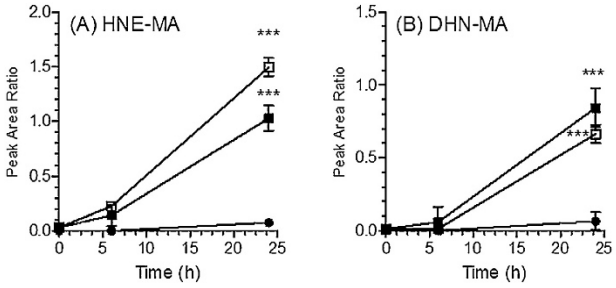

Fig. 4. Effect of flutamide on HNE-derivative concentrations in human hepatocytes in presence of HRP-system: plated hepatocytes were incubated with 50 (■) or 100 mM (□) flutamide for up to 24 h and compared to control incubations (●). Values are means ± SD ($n = 3$). Significance is indicated by ***($p < 0.001$).

therefore serve as suitable analytes (Milne et al., 2007). Especially isomers from the F-ring (dihydroxypentan) class have been investigated extensively. However, recent studies also showed that isomers from the D- and E-ring group (hydroxypentanone) can serve as biomarkers and bioactive substances (Cossette et al., 2007; Brose et al., 2011).

In contrast, hydroxynonenal (HNE), originating from peroxidation of w-6 unsaturated fatty acids (Esterbauer et al., 1991; Eckl et al., 1993), is a reactive, cytotoxic aldehyde which is difficult to determine reliably. However, as HNE is a strong electrophile, it readily reacts with nucleophiles like glutathione. HNE glutathione conjugates and their degradation products have been shown to serve as suitable biomarkers.

We chose a panel of lipid peroxidation products, comprised by different isoprostanes and HNE derivatives, as *in vitro* safety biomarkers to measure cellular oxidative stress response upon treatment with flutamide as a model compound.

Our intention was to perform experiments in a concentration and time range not exhibiting overt cellular damage and to evaluate the sensitivity of oxidative stress biomarkers therein. The chosen concentration of flutamide of 50 and 100 mM lie beneath values reported to have effects on cell viability. Different groups recently investigated cytotoxicity of flutamide in different cellular systems and found EC_{50} values of 238 mM, 294 mM (Thompson et al., 2012), 379 mM (Tolosa et al., 2013) and 143 mM (Swiss et al., 2013). In accordance with these findings, no cytotoxic effects were observed in our experiment using 50 and 100 mM flutamide. In contrast, the group of O'Brien found increased cytotoxicity in rat hepatocyte suspension treated with 75 mM flutamide, possibly due to different incubation conditions (MacAllister et al., 2013). However, in accordance to our findings, they did not detect increased toxic effects due to supplementation with H_2O_2-generating substrates. In addition, they were able to identify increased ROS formation with flutamide which was more pronounced with the HRP-system. Consistently, we emphasized this outcome by using lipid peroxidation products as biomarkers for ROS.

In the reported experiments, oxidative stress response in rat and human hepatocytes upon flutamide treatment was tested using conventional cell culture or hepatocytes cultured in the presence of a system using D-glucose, glucose oxidase and horseradish peroxidase to sensitize cells towards oxidative stress (Tafazoli et al., 2005). Under both conditions we were able to detect flutamide-induced oxidative stress. However, cellular response upon treatment was enhanced by the HRP-system (see Table 1). Thus, it was concluded, that flutamide metabolites that may undergo redox cycling or are prone to electrophilic attack (namely the nitro-reduced amine metabolite and its para-diimine counterpart, Fig. 1) are attenuated within the cells through supplementation with the H_2O_2-generating substrates. The two cytotoxicity markers, intracellular ATP content and extracellular LDH concentration, were compared with concentration changes of different prostaglandin isomers and two HNE derivatives after 6 and 24 h of treatment with 50 and 100 mM flutamide. No significant effect on cell viability could be seen in the cells co-treated with the HRP-system despite a markedly increased oxidative stress response.

A time- and dose-dependent cellular response was reflected in increased concentrations of isoprostanes upon flutamide treatment in this apparently non-toxic concentration range. Consistent with these results are recent studies investigating the effect of different substrates on isoprostane concentration. Treatment of rat hepatocytes with valproic acid, another drug induced liver injury (DILI) model compound, resulted in a time and dose-dependent increase of 8-iso prostaglandin $F_{2\alpha}$ as determined with an immunoaffinity assay (Tong et al., 2005). An increased concentration of two F_2- isoprostanes (4.1 resp. 4.7-fold as compared to control) was observed upon treatment with CCl_4 after affinity enrichment and mass spectrometric determination (Sicilia et al., 2008). In addition, concentrations of prostaglandin D_2 and PE_2 have also been shown to be affected when rat hepatocytes were exposed to CCl_4 (Johnston and Kroening, 1996). These results indicate the sensitivity of various isoprostanes upon elevated oxidative stress.

Likewise, the value of HNE derivatives as cellular markers for oxidative stress was already confirmed from previous *in vitro* rat hepatocyte experiments, indicating a time dependent response of HNE glutathione and its metabolites HNE-MA and DHN-MA upon treatment with ferric nitrilotriacetate(Volkel et al. , 2005).

Remarkably, the current study found similar concentrations of DHN-MA as response upon low and high dose flutamide treatment, potentially due to saturation effects in the reductive activity.

Putting our results in relation to other *in vitro* studies that investigated the toxic effect of flutamide treatment to cellular systems, we have identified sensitive safety biomarkers superior to conventional cytotoxicity assessment or traditional methods of oxidative stress determination. However, it has to be acknowledge that, at comparable concentration as used in our study, effects on protein synthesis in human hepatocytes were reported by Kostrubsky et al. (2007) who detected transient impairment upon treatment with 50 mM flutamide and only 20% remaining activity with 100 mM. On the other hand, the minimal effect concentration of flutamide for the production of reactive oxygen species for metabolically – competent as well as – incompetent HepG2 cells ranged at 250 mM (Tolosa et al., 2013). The reported higher concentration might be due to lower sensitivity of the applied oxidative stress detection method (fluorescence emission upon oxidation by ROS [CellROX Deep Red]).

The interspecies comparison of rat and human hepatocyte results shows that cellular generation of lipid peroxidation products after flutamide treatment proceeds simultaneously. Hence, in the case of flutamide, rodent experiments may be valid models to mimic and study effects in human systems.

In summary, we found sensitive markers for drug-induced lipid peroxidation processes as signs for cellular oxidative stress. We were able to further enhance hepatocyte response by introduction of a sensitizing HRP-system as optimized culture condition. The presented setup can support the detection of early signs of upcoming hepatotoxicity by using oxidative stress as a risk factor.

References

Alary, J., Fernandez, Y., Debrauwer, L., Perdu, E., Gueraud, F., 2003. Identification of intermediate pathways of 4-hydroxynonenal metabolism in the rat. Chem. Res. Toxicol. 16, 320–327.

Avery, S.V., 2011. Molecular targets of oxidative stress. Biochem. J. 434, 201–210.

Boess, F., Durr, E., Schaub, N., Haiker, M., Albertini, S., Suter, L., 2007. An in vitro study on 5-HT6 receptor antagonist induced hepatotoxicity based on biochemical assays and toxicogenomics. Toxicol. In Vitro 21, 1276–1286.

Boon, P.J., Marinho, H.S., Oosting, R., Mulder, G.J., 1999. Glutathione conjugation of 4-hydroxy-trans-2,3-nonenal in the rat in vivo, the isolated perfused liver and erythrocytes. Toxicol. Appl. Pharmacol. 159, 214–223.

Brose, S.A., Thuen, B.T., Golovko, M.Y., 2011. LC/MS/MS method for analysis of E(2) series prostaglandins and isoprostanes. J. Lipid Res. 52, 850–859.

Choucha Snouber, L., Bunescu, A., Naudot, M., Legallais, C., Brochot, C., Dumas, M.E., Elena-Herrmann, B., Leclerc, E., 2013. Metabolomics-on-a-chip of hepatotoxicity induced by anticancer drug flutamide and Its active metabolite hydroxyflutamide using HepG2/C3a microfluidic biochips. Toxicol Sci. 132, 8–20.

Choudhari, S.K., Chaudhary, M., Gadbail, A.R., Sharma, A., Tekade, S., 2014. Oxidative and antioxidative mechanisms in oral cancer and precancer: a review. Oral Oncol. 50, 10–18.

Cossette, C., Walsh, S.E., Kim, S., Lee, G.J., Lawson, J.A., Bellone, S., Rokach, J., Powell, W.S., 2007. Agonist and antagonist effects of 15R-prostaglandin (PG) D2 and 11-methylene-PGD2 on human eosinophils and basophils. J. Pharmacol. Exp. Ther. 320, 173–179.

Ecker, J., 2012. Profiling eicosanoids and phospholipids using LC-MS/MS: principles and recent applications. J. Sep. Sci. 35, 1227–1235.

Eckl, P.M., Ortner, A., Esterbauer, H., 1993. Genotoxic properties of 4-hydroxyalkenals and analogous aldehydes. Mutat. Res. 290, 183–192.
Esterbauer, H., Schaur, R.J., Zollner, H., 1991. Chemistry and biochemistry of 4-hydroxynonenal, malonaldehyde and related aldehydes. Free Radic. Biol. Med. 11, 81–128.
Fam, S.S., Morrow, J.D., 2003. The isoprostanes: unique products of arachidonic acid oxidation—a review. Curr. Med. Chem. 10, 1723–1740.
Higuchi, S., Kobayashi, M., Yano, A., Tsuneyama, K., Fukami, T., Nakajima, M., Yokoi, T., 2012. Involvement of Th2 cytokines in the mouse model of flutamide-induced acute liver injury. J. Appl. Toxicol. 32, 815–822.
Jenner, P., 2003. Oxidative stress in Parkinson's disease. Annals of Neurology 53 (Suppl. 3), S26–36 Discussion S36-28.
Johnston, D.E., Kroening, C., 1996. Stimulation of prostaglandin synthesis in cultured liver cells by CCl4. Hepatology (Baltimore, MD) 24, 677–684.
Kang, P., Dalvie, D., Smith, E., Zhou, S., Deese, A., Nieman, J.A., 2008. Bioactivation of flutamide metabolites by human liver microsomes. Drug Metab. Dispos. 36, 1425–1437.
Kashimshetty, R., Desai, V.G., Kale, V.M., Lee, T., Moland, C.L., Branham, W.S., New, L. S., Chan, E.C., Younis, H., Boelsterli, U.A., 2009. Underlying mitochondrial dysfunction triggers flutamide-induced oxidative liver injury in a mouse model of idiosyncratic drug toxicity. Toxicol. Appl. Pharmacol. 238, 150–159.
Kostrubsky, S.E., Strom, S.C., Ellis, E., Nelson, S.D., Mutlib, A.E., 2007. Transport, metabolism, and hepatotoxicity of flutamide, drug–drug interaction with acetaminophen involving phase I and phase II metabolites. Chem. Res. Toxicol. 20, 1503–1512.
Kraus, I., Vitezic, D., Oguic, R., 2001. Flutamide-induced acute hepatitis in advanced prostate cancer patients. Int. J. Clin. Pharmacol. Ther. 39, 395–399.
MacAllister, S.L., Maruf, A.A., Wan, L., Chung, E., O'Brien, P., 2013. Modeling xenobiotic susceptibility to hepatotoxicity using an in vitro oxidative stress inflammation model. Can. J. Physiol. Pharmacol. 91, 236–240.
McGill, M.R., Jaeschke, H., 2013. Oxidant stress, antioxidant defense, and liver injury. In Drug-Induced Liver Disease 71–84.
McGrath, L.T., McGleenon, B.M., Brennan, S., McColl, D., Mc, I.S., Passmore, A.P., 2001. Increased oxidative stress in Alzheimer's disease as assessed with 4-hydroxynonenal but not malondialdehyde. QJM 94, 485–490.
Milne, G.L., Yin, H., Brooks, J.D., Sanchez, S., Jackson Roberts Ii, L., Morrow, J.D., 2007. Quantification of F 2-Isoprostanes in biological fluids and tissues as a measure of oxidant stress. Methods Enzymol. 113–126.
Milne, G.L., Yin, H., Hardy, K.D., Davies, S.S., Roberts 2nd, L.J., 2011. Isoprostane generation and function. Chem. Rev. 111, 5973–5996.
Osculati, A., Castiglioni, C., 2006. Fatal liver complications with flutamide. Lancet 367, 1140–1141.
Sicilia, T., Mally, A., Schauer, U., Pahler, A., Volkel, W., 2008. LC–MS/MS methods for the detection of isoprostanes (iPF2alpha-III and 8,12-iso-iPF2alpha-VI) as biomarkers of CCl4-induced oxidative damage to hepatic tissue. J. Chromatogr. 861, 48–55.
Swiss, R., Niles, A., Cali, J.J., Nadanaciva, S., Will, Y., 2013. Validation of a HTS-amenable assay to detect drug-induced mitochondrial toxicity in the absence and presence of cell death. Toxicol. In Vitro 27, 1789–1797.
Tafazoli, S., Spehar, D.D., O'Brien, P.J., 2005. Oxidative stress mediated idiosyncratic drug toxicity. Drug Metab. Rev. 37, 311–325.
Thompson, R.A., Isin, E.M., Li, Y., Weidolf, L., Page, K., Wilson, I., Swallow, S., Middleton, B., Stahl, S., Foster, A.J., Dolgos, H., Weaver, R., Kenna, J.G., 2012. In vitro approach to assess the potential for risk of idiosyncratic adverse reactions caused by candidate drugs. Chem. Res. Toxicol..
Tolosa, L., Gomez-Lechon, M.J., Perez-Cataldo, G., Castell, J.V., Donato, M.T., 2013. HepG2 cells simultaneously expressing five P450 enzymes for the screening of hepatotoxicity: identification of bioactivable drugs and the potential mechanism of toxicity involved. Arch. Toxicol. 87, 1115–1127.
Tong, V., Teng, X.W., Chang, T.K.H., Abbott, F.S., 2005. Valproic acid II: effects on oxidative stress, mitochondrial membrane potential, and cytotoxicity in glutathione-depleted rat hepatocytes. Toxicol. Sci. 86, 436–443.
Volkel, W., Alvarez-Sanchez, R., Weick, I., Mally, A., Dekant, W., Pahler, A., 2005. Glutathione conjugates of 4-hydroxy-2(E)-nonenal as biomarkers of hepatic oxidative stress-induced lipid peroxidation in rats. Free Radic. Biol. Med. 38, 1526–1536.
Wen, B., Coe, K.J., Rademacher, P., Fitch, W.L., Monshouwer, M., Nelson, S.D., 2008. Comparison of in vitro bioactivation of flutamide and its cyano analogue: evidence for reductive activation by human NADPH:cytochrome P450 reductase. Chem. Res. Toxicol. 21, 2393–2406.

3.2.3 Comparison of oxidative stress markers in rodents using flutamide as a DILI model compound

Translational Biomarkers for Flutamide-Induced Oxidative Stress *In Vitro* and *In Vivo* as Early Signs of Hepatotoxicity

Marieke Teppner[1] [2], Franziska Boess[1], Beat Ernst[2] and Axel Pähler[1]

[1] DMPK, Pharmaceutical Sciences; Pharma Research and Early Development (pRED); F. Hoffmann-La Roche Ltd., Grenzacherstrasse 124; CH-4070 Basel, Switzerland

[2] Institute of Molecular Pharmacy; University of Basel, Klingenbergstrasse 50; CH-4040 Basel, Switzerland

To be published in: *Drug Metab Dispos* 44:1-10, April 2016 (proof version)

Personal contribution: Experimental design, conduction of cellular assay, LCMS analysis, PCR analysis; evaluation; manuscript preparation

1521-009X/44/4/1–10$25.00
Drug Metabolism and Disposition

http://dx.doi.org/10.1124/dmd.115.066522
Drug Metab Dispos 44:1–10, April 2016

Biomarkers of Flutamide-Bioactivation and Oxidative Stress In Vitro and In Vivo [S]

Marieke Teppner,[1] Franziska Boess, Beat Ernst,[2] and Axel Pähler

Roche Pharmaceutical Research and Early Development pRED, Pharmaceutical Sciences, Roche Innovation Center Basel, Basel, Switzerland

Received August 12, 2015; accepted January 6, 2016

ABSTRACT

The nonsteroidal androgen-receptor antagonist flutamide is associated with hepatic injury. Oxidative stress and reactive metabolite formation are considered contributing factors to liver toxicity. Here we have used flutamide as a model drug to study the generation of reactive drug metabolites that undergo redox cycling to induce oxidative stress (OS) in vitro and in vivo. Lipid peroxidation (LPO) markers, as well as genes regulated by the redox-sensitive Nrf2 pathway, have been identified as surrogates for the characterization of OS. These markers and metabolism biomarkers for drug bioactivation have been investigated to characterize drug-induced hepatic damage. Rat hepatocytes and in vivo studies showed that several LPO markers, namely the isoprostanes 15*R*-PD_2, dihydro keto PE_2, and $iPF_{2\alpha}$-VI, as well as hydroxynonenal mercapturic acid metabolites, had increased significantly by 24 hours after flutamide treatment from 4.9 to 15.3-fold in hepatocytes and from 2.6 to 31.0-fold in rat plasma. Induction of mRNA expression levels for Nrf2-regulated genes was evident as well, with heme oxygenase 1, glutathione-*S*-transferase π1 and NAD(P)H dehydrogenase showing a 3.6-, 4.1-, and 1.9-fold increase in hepatocytes and 5.6-, 7.5-, and 94.1-fold in rat liver. All effects were observed at drug concentrations that did not show overt liver toxicity. Addition of an in situ hydrogen peroxide–generating system to in vitro experiments demonstrated the formation of a reactive di-imine intermediate as the responsible metabolic pathway for the generation of OS. The dataset suggests that hepatic oxidative stress conditions can be mediated via metabolic activation and can be monitored with suitable biomarkers preceding the terminal damage.

Introduction

The nonsteroidal antiandrogen drug flutamide is used for treatment of progressed prostate carcinoma (Mutschler et al., 2001). Owing to its potential to induce liver injury, flutamide is marked with a black box warning. Case reports document elevated liver enzyme levels that were reversible in most cases but could have turned into fatal outcomes as well (Crownover et al., 1996; Cetin et al., 1999; Nakagawa et al., 1999). These effects are still considered to be under-reported (Osculati and Castiglioni, 2006), and the mechanism of toxicity so far has not been fully elucidated. However, some studies have demonstrated that bioactivation processes leading to redox cycling and GSH depletion are plausible mechanisms of flutamide toxicity (Kang et al., 2008; Wen et al., 2008).

To further evaluate the mechanism of flutamide-induced hepatotoxicity, it seemed reasonable, therefore, to further investigate metabolic liabilities involving reactive oxygen species (ROS) and oxidative stress. Oxidative stress conditions can be characterized by different parameters: The most frequently measured surrogate markers are the depletion of glutathione (GSH) or formation of peroxidation products (Muriel, 2009; Mari et al., 2013). Furthermore, analysis of prostaglandins has been established as one valid option to measure intracellular formation of radicals (Milne et al., 2011). A further group of peroxidation products are metabolites of the reactive aldehyde 4-hydroxy-2(E)-nonenal (HNE), which are known to serve as reliable in vitro and in vivo biomarkers for oxygen radicals (Volkel et al., 2005). In addition to the monitoring of byproducts, another possibility is to assess hepatic response to ROS by investigation of the Kelch-like ECH–associated protein 1 (Keap1)-Nrf2 pathway. It has been demonstrated that cytoprotection is supported by induction of detoxification enzymes via the antioxidant response element. In this case, gene transcription is stimulated via the translocation of the transcription factor nuclear factor–erythroid 2–related factor 2 (Nrf2) to the nucleus. Nrf2 activity itself is known to be regulated by Keap1, to which it is bound in cytoplasm in physiologic states [for review, see Motohashi and Yamamoto (2004) and Copple et al. (2010)] but has also been shown to be alternatively regulated, e.g., via phosphorylation states or protein/epigenetic interactions (Bryan et al., 2013). While all of the above methods are very valuable for the investigation of oxidative stress in vitro, their application in vivo is limited or not possible at all.

[1]Current affiliation: Evotec AG, Essener Bogen 7, 22419 Hamburg, Germany, marieke.teppner@evotec.com.
[2]Current affiliation: Institute of Molecular Pharmacy, University of Basel, Klingenbergstrasse 50, CH-4040 Basel, Switzerland.
dx.doi.org/10.1124/dmd.115.066522.
[S]This article has supplemental material available at dmd.aspetjournals.org.

ABBREVIATIONS: 15*R*-PD_2, 15*R* Prostaglandin D_2; ALT, alanine aminotransferase; AST, aspartate aminotransferase; CES1, carboxylesterase 1; DHN-MA, 1,4-dihydroxy-2(*E*)-nonene mercapturic acid; DILI, drug-induced liver injury; DMSO, dimethyl sulfoxide; ECH, erythroid cell–derived protein with cap and collar (CNC) homology; GCLC, glutamate-cysteine ligase, catalytic subunit; GSTα1, glutathione-*S*-transferase α1; GSTπ1, glutathione-*S*-transferase π1; HMOX1, heme oxygenase 1; HNE-MA, HNE mercapturic acid; HNE, 4-hydroxy-2(E)-nonenal; HRP, horseradish peroxidase; $iPF_{2\alpha}$-VI, 5-iso prostaglandin $F_{2\alpha}$-VI; Keap1, Kelch-like ECH-associated protein 1; LDH, lactate dehydrogenase; LC-MS/MS, liquid chromatography–tandem mass spectrometry; NQO1, NAD(P)H:quinone oxidoreductase 1; Nrf2, nuclear factor–erythroid 2–related factor 2; PD_2-d4, prostaglandin D_2-d4; ROS, reactive oxygen species; SDH, sorbitol dehydrogenase.

On the basis of this knowledge, we describe a validation study with flutamide for several noninvasive in vitro and in vivo biomarkers that composed a panel of complementary endpoints of oxidative stress, namely the integration of mRNA profiling in addition to small-molecule biomarker analysis. Isoprostanes and HNE metabolites as well as mRNA of six different Nrf2-regulated enzymes were assessed in rat hepatocytes and the corresponding rat in vivo models and then compared with established conventional parameters. The aim of these studies was to validate markers for oxidative stress that may also enable an early detection of drug-induced liver injury (DILI) and probe their clinical relevance by correlation between in vitro and in vivo results. A classification of the described markers was done by comparison with conventional cyto- and organ-toxicity markers. To increase the dynamic range of the ROS response in the in vitro system we used a horseradish peroxidase (HRP) system for the in situ generation of hydrogen peroxide. This technique was describes previously by O'Brien's group (Tafazoli et al., 2005), which showed alteration of cellular oxidative stress response for drugs that are prone to cause DILI. Particularly, drugs that carry structural moieties that may form quinone or quinone-imine metabolites are prone to undergo redox cycling. The stimulation of underlying inflammatory signals by hydrogen peroxide may lower the threshold for toxicity under these test conditions without affecting cell viability under control conditions.

Materials and Methods

Chemicals. Williams' medium E, dimethyl sulfoxide (DMSO) p.a., formic acid p.a., insulin, streptomycin, penicillin, hydrocortisone, β-D(+)-glucose, peroxidase type VI from horseradish, glucose oxidase type II from *Aspergillus* were obtained from MilliporeSigma (St. Louis, MO). Glutamine and gentamycin were purchased from Life Technologies/Invitrogen (Lucerne, Switzerland) and acetonitrile liquid chromatography–mass spectroscopy grade from Fisher Scientific (Wohlen, Switzerland). Water of chromatography grade was obtained from Merck (Darmstadt, Germany). Flutamide (CAS 13311-84-7) was synthesized in house. The prostaglandin derivatives 5-iso prostaglandin $F_{2\alpha}$-VI (iP$F_{2\alpha}$-VI, CAS 180469-63-0), prostaglandin E_2 (PE_2, CAS 363-24-6), prostaglandin D_2 (PD_2, CAS 41598-07-6), 15*R* prostaglandin D_2 (15R-PD_2, CAS 59894-05-2), 13,14-dihydro-15-keto prostaglandin E_2 (dihydro-keto PE_2, CAS 363-23-5), and deuterated prostaglandin D_2 (PD_2-d4, 9α,15*S*-dihydroxy-11-oxo-prosta-5Z,13E-dien-1-oic-3,3,4,4-d4 acid) were purchased from Cayman Chemical Company (Ann Arbor, MI).

Cell Culture Media and Test Compound. Incubation medium was prepared by supplementation of William's medium E with 4 mg/l insulin, 50,000 IU/l penicillin, 50 mg/l streptomycin, 10 mg/l gentamycin, and 2.4 mg/ml hydrocortisone.

Flutamide was dissolved in DMSO to obtain a 100 mM stock solution that was further diluted in incubation medium for use in experiments.

Hepatocyte Culture and Treatment. Rat primary cells were freshly prepared in house by a two-step liver perfusion procedure (Boess et al., 2007) and plated on collagen-coated 24-well plates at a density of 300,000 cells per well. After 2 hours' attachment time the cell-seeding medium [incubation medium (see above) supplemented with 10% fetal calf serum] was exchanged and nonadhesive cells removed. All experiments were carried out in the above described incubation medium containing 10 mM glucose, 0.05 IU/ml glucose oxidase, and 0.5 μM horseradish peroxidase as in situ hydrogen peroxide–generating system (HRP system). Incubation was performed at 37°C in a humidified atmosphere (5% CO_2/95% air) and stopped after 6 or 24 hours of incubation.

Metabolite Identification Experiments. Cryopreserved male Wistar rat hepatocytes (Celsis IVT, Brussels, Belgium) were thawed by applying the protocol of the provider and diluted in incubation medium (see above) to a final concentration of 10^6 cells/ml. Comparative experiments were carried out in medium with and without supplementation by 10 mM glucose, 0.05 IU/ml glucose oxidase, and 0.5 μM HRP system. After 15 minutes of preincubation, experiments were started by addition of 0.1% DMSO (control), 50 μM, or 100 μM flutamide. Incubation was performed at 37°C in a humidified atmosphere (5% CO_2/95% air) and stopped after 30, 60, and 180 minutes by adding 1 volume of ice-cold acetonitrile. After centrifugation of precipitated samples at 5000*g* and 8°C for 10 minutes, the supernatant was diluted 1:1 with water containing 0.1% formic acid and directly used for liquid chromatography–tandem mass spectrometry (LC-MS/MS) analysis.

The instrumental setup consisted of an Acquity UPLC (Waters, Dublin, Ireland) equipped with an Atlantis HSS C18 column (1.8 μM, 2.1 × 50 mm; Waters) at 50°C. Ten microliters of sample were injected and chromatographically separated by gradient elution with a mobile phase consisting of water containing 0.5% formic acid/acetonitrile (eluent A; 95/5, v/v), and acetonitrile containing 0.1% formic acid (eluent B). The gradient started with a total flow of 0.500 ml/min at 100% A, which was kept for 1.0 minutes. Eluent B was then increased to 16% within 2.5 minutes and further to 100% in another 2.5 minutes. The system was kept at 100% B for 0.2 minutes and then switched back to 100% A within 0.05 minutes. From 6.25 minutes until the end of the run at 10 minutes the system was re-equilibrated with 100% eluent A.

MS Detection was done with a TripleTOF 5600+ mass spectrometer (AB Sciex, Warrington, UK) using a generic data-dependent acquisition mode with positive electrospray ionization. Source parameters were set to 25 (curtain gas), 45 (gas 1), 60 (gas 2), 5500 (ionspray voltage), 500 (temperature), and 80 eV (declustering potential). For the time-of-flight mass spectrometry scan, a collision energy of 10 eV and an accumulation time of 80 milliseconds was applied for a scan range from *m/z* 130 to *m/z* 1200. Eight information-dependent MS2 scans were acquired using a collision energy of 40 ± 20 eV for the scan range from *m/z* 50 to *m/z* 1200 with an accumulation time of 50 milliseconds for ions with an intensity higher than 450 cps with a mass tolerance of 25 ppm. The resulting cycle time was 530 milliseconds.

Animal Study. Animals studies were carried out in accordance to Swiss animal welfare law and the *Guide for the Care and Use of Laboratory Animals* published by the National Institutes of Health. The animal test facility is fully accredited by the Association for Assessment and Accreditation of Laboratory Animal Care International. Twelve male Fischer 344 rats (249–269 g) were obtained from Charles River (Sulzfeld, Germany) and maintained at 23°C on a 12-hour light/12-hour dark cycle with food and water ad libitum. Two days prior to treatment animals were adjusted to metabolic cages. For the experiment, animals were divided into four groups ($n = 3$) and administered a single dose of flutamide (500 mg/kg body weight) as a microsuspension in sodium chloride/gelatin (treated group: groups 1 and 2) or vehicle alone by oral gavage (control: groups 3 and 4). Urine samples were collected on dry ice from –48 to –24 hours and –24 to 0 hours (predose) and from 0 to 24 hours (postdose) and stored at –20° C until analysis. Animals were sacrificed after 3 hours (groups 1 and 3) and 24 hours of treatment (groups 2 and 4) by CO_2 asphyxiation followed by cervical dislocation. Total blood was collected on EDTA, plasma prepared, and stored at –20°C. Livers were removed, an aliquot of approximately 300 mg transferred to a tube containing 15 ml RNAlater, which thereafter was kept at 4°C for 24 hours, and then stored at –20°C until further sample work up.

Sample Work Up. Plasma samples were precipitated with 2 volumes of ethanol containing internal standard PD_2-d4 at a concentration of 0.63 ng/ml to reach a final concentration of 0.42 ng/ml.

Urine samples were diluted with 9 volumes of acetonitrile/water cont. 0.2% formic acid [1:1] containing internal standard (PD_2-d4 at a concentration of 0.47 ng/ml to reach a final concentration of 0.42 ng/ml). To detect prostaglandin levels and 4-hydroxy-2(E)-nonenal (HNE) derivatives in hepatocyte incubations, the latter were quenched at the end of indicated treatment periods with 1 volume acetonitrile containing internal standard (PD_2-d4 at a concentration of 0.84 ng/ml to reach a final concentration of 0.42 ng/ml).

Approximately 1 g of liver tissue was homogenized with 3 volumes of water at 5500 rpm for 40 seconds using a Lysing Kit (Precellys/Bertin Technologies, Montigny, France). One milliliter of the homogenate was then precipitated with 1 volume ice-cold acetonitrile containing internal standard (PD_2-d4).

All samples were centrifuged and the supernatant was directly injected onto the LC-MS/MS system. Quantitation was achieved by calibration with dilution series of standard compounds against a deuterated internal standard in a concentration range from 20 up to a concentration of 50,000 pg/ml.

LC-MS/MS Analysis. The system consisted of a YMC-Pack ODS-AQ, 20 × 2.1 mm, 5-μm column (YMC Europe, Dislaken, Germany) as trapping column and an Atlantis T3, 100 × 2.1 mm, 3-μm column (Waters) connected to a column two-dimensional HPLC consisting of a Shimadzu LC AD vp binary pump

system and an Agilent 1100 series LC pump connected to a triple quadrupole tandem mass spectrometer (4000 QTRAP; Sciex, Warrington, UK). The analytical setup has been described for prostaglandin detection as well as for HNE analysis (Volkel et al., 2005; Sicilia et al., 2008; Ecker, 2012). Briefly, 500-μl samples were injected to the system, analytes were enriched on the trapping column, and chromatographically eluted from the analytical column. MS detection (4000 QTRAP; Sciex) operated in negative electrospray ionization mode using selected reaction monitoring (SRM) analysis. Transitions and tuning parameters were defined individually for each analyte with the help of authentic standards as follows: *m/z* 351.1 to *m/z* 271.1 for 15*R*-PD_2, *m/z* 351.1 to *m/z* 315.0 for dihydro-keto PE_2, *m/z* 353.1 to *m/z* 114.9 for $iPF_{2\alpha}$-VI, *m/z* 318.1 to *m/z* 189.0 for HNE-MA, and *m/z* 320.1 to *m/z* 191.0 for DHN-MA. Quantitation of prostaglandins was achieved by calibration with dilution series of standard compounds against deuterated internal standard. As an authentic standard was not available for DHN-MA, HNE derivatives were quantified relative to the internal standard according to published procedures (Volkel et al., 2005). For sensitivity reasons in vivo samples were measured on a TripleTOF 5600+ mass spectrometer (Sciex) by the analogous technique MRMHR.

Biochemical Analysis. Lactate dehydrogenase (LDH) in the supernatant was determined after 6 hours and 24 hours of treatment (150 μl supernatant) by a commercially available test kit (cat. no. 07502999) on an ADVIA 1650 autoanalyzer (Siemens Diagnostics, Erlangen, Germany). Intracellular ATP content was determined after 6 hours and 24 hours by means of a bioluminescence-based ATP assay kit (Roche Diagnostics, Rotkreuz, Switzerland) on a Victor plate reader (PerkinElmer, Schwerzenbach, Switzerland).

Isolation of RNA from Rat Hepatocytes. Medium was aspirated from the incubation wells and RLT buffer (Qiagen, Hombrechtikon, Switzerland) containing β-mercaptoethanol (10 μLl/ml) was added to lyse the cells. RNA was extracted from the cell matrix by means of silica-membrane purification with spin columns (Qiagen, Hombrechtikon, Switzerland). RNA yield was quantified with Nanodrop 1000 (Thermo Scientific, Wilmington, DE).

Isolation of RNA from Rat Liver Tissue. A piece of RNAlater-preserved organ tissue (~30 mg) was cut and homogenized in RLT buffer in a FastRNA tube green (cat. no. 6913-100; Qbiogene, Carlsbad, CA). After centrifugation of the lysate an aliquot of the supernatant was used for RNA extraction as described previously.

Quantitative Real-Time Polymerase Chain Reaction. A total of 500 ng of RNA was used to generate single-stranded cDNA using a commercially available cDNA synthesis kit (Transcriptor First Strand cDNA Synthesis Kit; Roche Diagnostics, Rotkreuz, Switzerland). The cDNA obtained was used as template for several PCRs along with appropriate specific primers and Taqman Hot-Start FastStart PCR Master Mix (LightCycler 480 Probes Master; Roche Diagnostics). The generation of double-stranded amplification products on a 384-multiwell plate was monitored by a LightCycler 480 instrument (Roche Diagnostics). All primer/probe mixes were from Roche Diagnostics with the assay IDs 504934 [carboxylesterase 1E (CES1)], 504937 [glutamate-cysteine ligase, catalytic subunit (GCLC)], 502674 [glutathione-*S*-transferase α1 (GSTα1)], 503103 [glutathione-*S*-transferase π1 (GSTπ1)], 502688 [heme oxygenase (decycling) 1 (HMOX1)], 502688 [NAD(P)H dehydrogenase, quinone 1 (NQO1)], 503799 [glyceraldehyde-3-phosphate dehydrogenase (GADPH)], 500152 [actin, beta (ACTB)] and 502309 [TATA box binding protein (TBP)]. Time course of the amplification cycle was as follows: An initial preincubation occurred for 10 minutes at 95°C followed by 45 amplification cycles at 95°C for 10 seconds, 60°C for 30 seconds, and 72°C for 2 seconds. In the end, cooling at 40°C was done for 60 seconds. Relative expression of genes with respect to the control cells was determined by normalization to the amount of GADPH RNA.

Determination of Liver Enzyme Levels from Plasma Samples. Levels of liver integrity markers were determined in 3- and 24-hour plasma samples with enzymatic assay kits on an ADVIA 1650 autoanalyzer (Siemens Diagnostics, Erlangen, Germany). The respective LDH, alanine transaminase (ALT), and aspartate dehydrogenase (AST) test kits were from Siemens Diagnostics; the glutamate dehydrogenase (GLDH) test kit was from Roche Diagnostics; and sorbose dehydrogenase (SDH), from Sekisui Diagnostics (Dusseldorf, Germany).

Determination of Creatinine Levels from Urine Samples. The concentration of creatinine in the collected urine samples was determined with a creatinine assay kit (Siemens Diagnostics) on an ADVIA 1650 autoanalyzer (Bayer Healthcare AG Leverkusen, Germany).

Statistical Analysis. Statistical significance defined as P value of <005 was confirmed by t test analysis using the software GraphPad Prism 5.03.

Results

Cytotoxicity Markers. Biochemical status of cells upon treatment was assessed by determination of ATP content as an indicator of mitochondrial activity and LDH release as marker for membrane integrity (Table 1). When the control cells were supplemented with the hydrogen peroxide–generating system in situ, no increase in cytotoxicity markers could be observed. This indicates that HRP supplementation does not negatively impact cell viability in absence of the drug.

In the HRP system, a transient decrease in ATP production after 6 hours of treatment with a high flutamide concentration was observed. In the HRP-free system, a similar effect was not evident after 24 hours. However, a trend for LDH was evident in the respective 24-hour incubation. On the basis of these data, an effect on cell viability with the high concentration treatment can be supposed.

Biotransformation of Flutamide in Hepatocytes with and without HRP. To evaluate the impact of the HRP system on biotransformation pathways, metabolite formation was compared from rat hepatocyte suspensions. The rate of flutamide biotransformation in general was not altered and the same metabolites were identified under both conditions. Under HRP treatment one metabolic pathway was enhanced, however. Formation of the reactive di-imine metabolite, whose structural identity was confirmed by the MS fragmentation pattern (Scheme 1, Fig. 1) and was assigned as Flu-G2, increased and led to a significantly increased concentration of its derived glutathione adduct (Fig. 2).

Lipid Peroxidation Products as Markers for Oxidative Stress. Hepatocyte oxidative stress response to flutamide treatment was further assessed by a panel of small-molecule biomarkers composed of isoprostanes, prostaglandins, and hydroxynonenal metabolites, namely mercapturic acid conjugates. Different analytes revealed a time- as well as concentration-dependent response to flutamide treatment: As depicted in Fig. 3A, a flutamide concentration of 100 μM led to an increase of prostaglandin levels for all analytes significantly different from control cells after 6 and 24 hours of treatment. For the lower concentration (50 μM flutamide treatment) only small effects were observed after 6 hours but biomarker levels were significantly increased after 24 hours. For instance, the concentration of the isoprostane isomer 15*R*-PD_2 changed from 6.29 ± 0.82 ng/ml in the 24-hour control condition by 3.1-fold to 19.3 ± 5.2 ng/ml upon 50 μM flutamide treatment and by 15.3-fold to 96.0 ± 34.8 ng/ml upon 100 μM flutamide treatment.

TABLE 1

LDH release and ATP production in rat hepatocytes upon flutamide treatment with and without HRP system

Significant changes compared with control are indicated by *($P < 0.05$), **($P < 0.01$), or *** ($P < 0.001$).

		Control	50 μM	100 μM
LDH (μkat/l) − HRP	6 h	0.85 ± 0.12	0.86 ± 0.20	0.97 ± 0.03
	24 h	1.21 ± 0.26	1.1 ± 0.1	4.26 ± 0.87
LDH (μkat/l) + HRP	6 h	0.66 ± 0.13	0.70 ± 0.17	4.18 ± 3.66
	24 h	0.57 ± 0.28	0.74 ± 0.39	6.96 ± 1.15*
ATP (pmol/well) − HRP	6 h	247 ± 61	239 ± 53	134 ± 48
	24 h	160 ± 43	198 ± 19	138 ± 52
ATP (pmol/well) + HRP	6 h	333 ± 1	456 ± 110	146 ± 2***
	24 h	230 ± 11	277 ± 7	202 ± 9

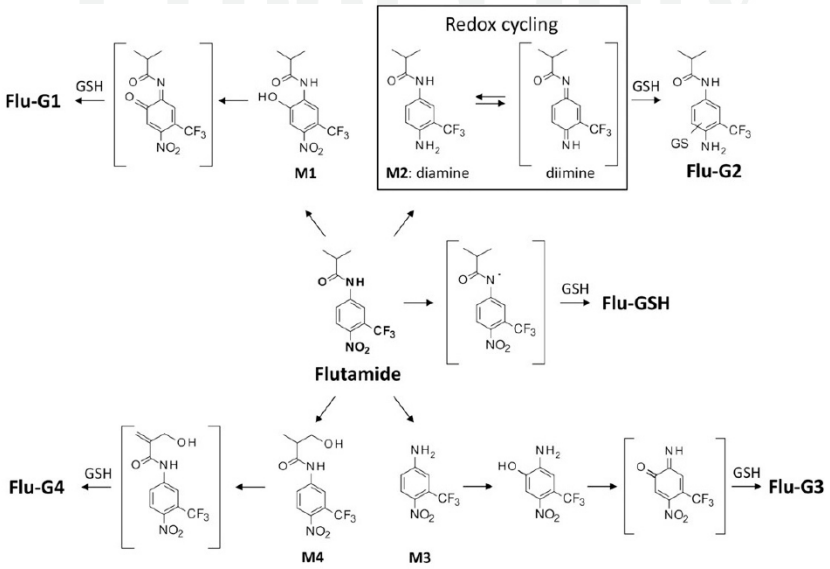

Scheme 1. Proposed mechanisms for the formation of primary metabolites of flutamide that may give rise to reactive species. Addition of H_2O_2 generating substrates leads to and increase in formation of a glutathione adduct (Flu-G2) deriving from oxidized M2.

Cellular levels of the two hydroxynonenal metabolites hydroxynonenal mercapturic acid (HNE-MA) and dihydroxynonene mercapturate (DHN-MA) were also monitored during the course of hepatocyte treatment (Fig. 3B). Both analytes were significantly increased after 24 hours upon both, 50 μM and 100 μM flutamide treatment. Even more, HNE-MA in cells treated with 100 μM flutamide changed by 5.5- and 4.8-fold compared with controls (6 and 24 hours, respectively).

mRNA Expression of Nrf2-Regulated Genes in Rat Hepatocytes. To investigate the cellular response to oxidative stress in more detail, mRNA expression levels of enzymes regulated by the Nrf2-Keap1 antioxidant response element pathway were determined: The transcript set consisted of carboxylesterase 1 (CES1), GCLC, glutathione-*S*-transferase α1 (GSTα1), glutathione-*S*-transferase π1 (GSTπ1), HMOX1, and NAD(P)H:quinone oxidoreductase 1 (NQO1).

As seen in Table 2 upregulation of the transcription was observed after 24 hours for GSTπ1, HMOX1, and NQO1 in cells treated with 100 μM of flutamide. For HMOX1, the antioxidant response was already initialized at the lower 50 μM dose. CES1, GCLC, and GSTα1 did not show significant change in mRNA expression levels at any of the investigated time points.

Response to Flutamide Administration in Fischer F344 Rats. For the in vivo biomarkers analysis, six male F344 rats were administered 500 mg/kg flutamide by gavage. A control group of six animals received 0.9% NaCl. Three hours and 24 hours postadministration three animals from each group were sacrificed. Plasma was collected on EDTA; liver was removed and placed on RNA later. Urine was collected from 2 days before treatment up to 24 hours posttreatment during three periods. Plasma levels of flutamide were determined to be 47.6 $\pm$ 11.4 μmol/l after 3 hours and 0.8 $\pm$ 0.5 μmol/l after 24 hours (Supplemental Table S1).

Liver Enzyme Levels. Several biochemical markers for hepatic damage were assessed: Levels of alanine amino transferase (ALT), aspartate amino transferase (AST), glutamate dehydrogenase, lactate dehydrogenase (LDH), and sorbitol dehydrogenase (SDH) in plasma did not show significant elevation in flutamide-treated animals compared with the control group (Table 3).

Lipid Peroxidation Products as Markers for Oxidative Stress. As for in vitro experiments, prostanoids and hydroxynonenal derivatives were determined from rat plasma. Remarkably, 15*R*-PD_2 and dihydro-keto PE_2, two prostaglandin isomers that have shown a significant increase upon flutamide treatment in vitro also showed alterations in rats in vivo (Fig. 4, top): Twenty-four hours after compound administration the concentration of 15*R*-PD_2 was increased from 80.3 $\pm$ 1.5 to 208.2 $\pm$ 1.1 pg/ml and that of dihydro-keto PD_2 from 23.2 $\pm$ 3.4 to 267.0 $\pm$ 1.3 pg/ml in response to flutamide treatment. In contrast, concentrations of $iPF_{2\alpha}$-VI were below the limit of quantification.

As with the prostaglandin response, the lipid peroxidation–derived HNE metabolites HNE-MA and DHN-MA increased as a result of drug intake, even to a higher extent than for the prostaglandins (Fig. 5A): HNE-MA levels changed by 4.1 and 18.1-fold and DHN-MA by 6.1 and 30-fold after 3 and 24 hours, respectively. These results are consistent with the in vitro effect by which both analytes revealed an increase upon flutamide treatment in a time- and concentration-dependent manner.

Prostaglandin levels from liver tissue samples showed a different time course upon treatment (Fig. 4, bottom). The two isomers 15*R*-PD_2 and dihydro-keto PE_2 demonstrated a transient concentration increase after 3 hours of treatment which was followed by a significant decrease after 24 hours.

mRNA Expression of Nrf2-Regulated Genes in Rat Liver Tissue. Flutamide-induced gene expression changes in the liver for the same proteins as in the in vitro hepatocyte study were investigated in rats: Under in vivo conditions cellular response was expressed via the matching mRNA (Table 4). GSTπ1 and HMOX1 showed 7.5- and 5.6-fold induction, respectively. NQO1 exhibited the highest upregulation

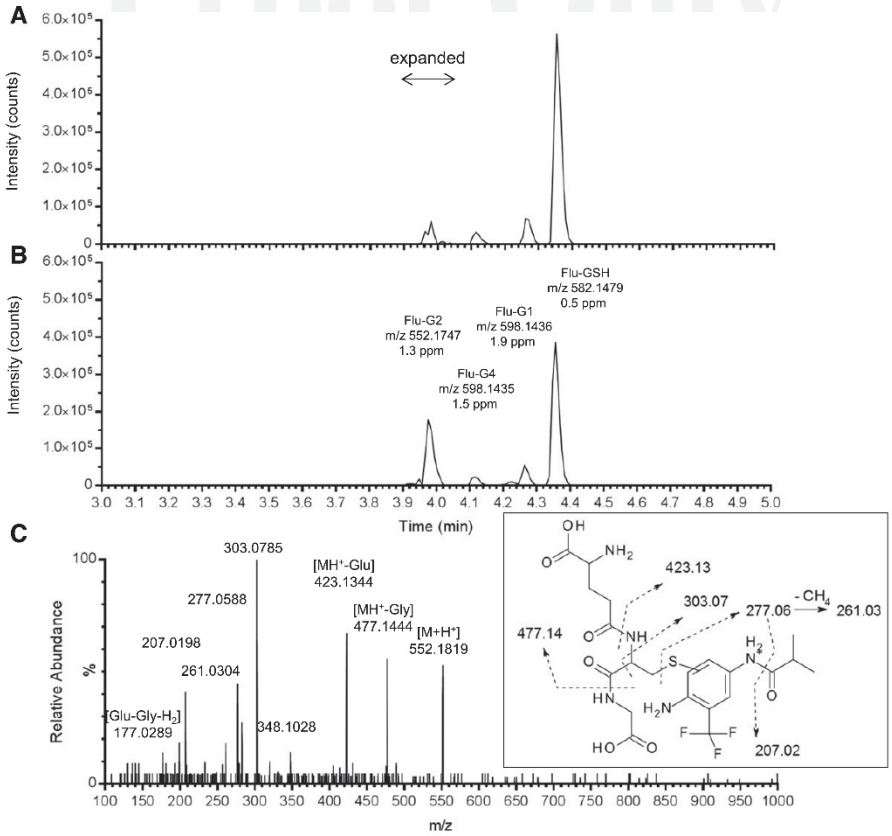

Fig. 1. LC-MS/MS analysis of G2. Top: extracted ion chromatogram of [M+H]+ at *m/z* 552.173 ± 0.01 in the positive ion mode. Bottom: MS/MS spectrum of G2 with assigned fragments.

indicated by a 7.0-fold change from control after 3 hours and even by 94-fold 24 hours after flutamide treatment.

Effects of Flutamide on Oxidative Stress Markers in Rat Urine Samples. As for rat plasma, basal levels of prostaglandin as well as hydroxynonenal metabolites were detected in rat urine samples.

For better comparability all results were normalized to urine creatinine, which revealed a slight drop (2.7-fold) in treated animals, suggesting an impact on renal function under flutamide treatment. No statistically significant change upon flutamide treatment was observed for prostaglandins (data not shown). However, a statistically significant response upon drug administration was evident for HNE-MA and DHN-MA: HNE-MA increased by 4.6-fold and DHN by 7.3-fold compared with the predose urine, and therefore both metabolites seem to be attractive accessible noninvasive biomarkers (Fig. 5B).

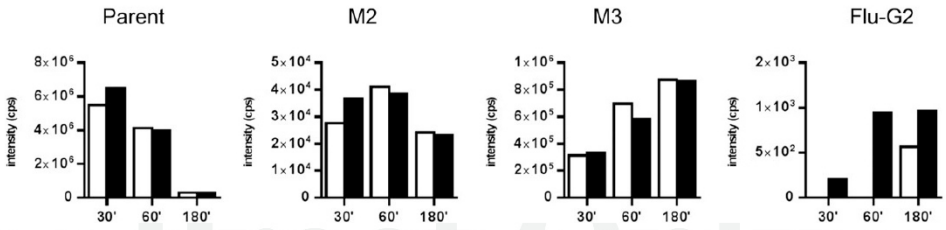

Fig. 2. Substrate depletion and metabolite formation without (□) and with the HRP (■) system indicates that HRP-derived redox-cycling of M2 results in the formation of Flu-G2.

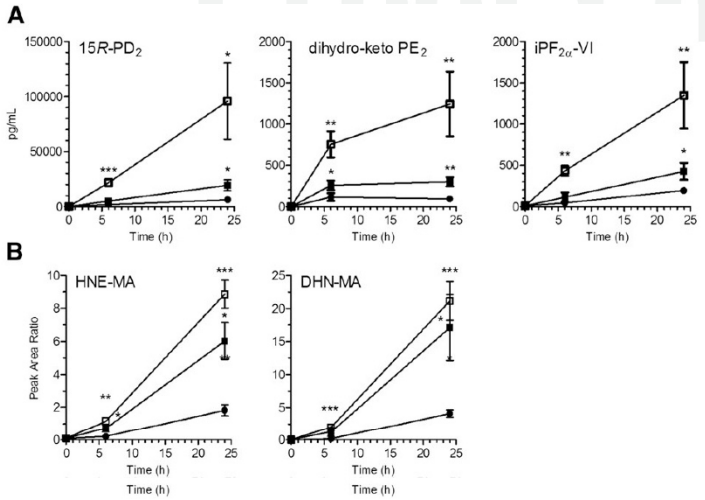

Fig. 3. Effect of flutamide on lipid peroxidation markers in rat hepatocytes: Plated hepatocytes were incubated with 50 or 100 μM flutamide for up to 24 hours and compared with control incubations. Values are means ± S.D. (n = 3). Significance is indicated by $^{*}P < 0.05$, $^{**}P < 0.01$, or $^{***}P < 0.001$.

Discussion

The purpose of this study was to elucidate the relationship between flutamide bioactivation in vitro and in vivo and the induction of hepatic oxidative stress. The temporal relationship between individual biomarker responses may suggest early noninvasive surrogates for the development of flutamide-induced liver injury. The focus of this study was the analysis of specific lipid peroxidation products and changes in gene expression as a consequence of flutamide bioactivation. These biomarkers were compared with conventional cytotoxicity markers aiming to validate biomarkers in vitro as well as in vivo experiments.

Flutamide causes DILI in rare case and is reported to induce oxidative stress as one contributing factor. Previous studies have revealed disruption of mitochondrial functions and glucose metabolism upon flutamide treatment (Kashimshetty et al., 2009; Choucha Snouber et al., 2013). Bioactivation of flutamide has been studied in the past, suggesting that the reduction of the compound's nitro residue and subsequent formation of an iminoquinone moiety leading to redox cycling may be one possible mechanism leading to toxicity. Wen and coworkers (2008) had identified the enzyme NADPH:cytochrome P450 reductase as responsible for the first reduction step. Oxidative pathways have been studied by Kang et al. (2008), who reported the formation of reactive metabolites leading to glutathione adduct formation via CYP1A2 and CYP3A4. However, a causal relation between those findings and the induction of liver toxicity was not shown.

Generally, the induction of hepatotoxicity in rodent models with flutamide is challenging (Matsuzaki et al., 2006; Kashimshetty et al., 2009); application of the relevant human dose of 250–500 mg per day does not translate into significant effects in rodents. Therefore, a relatively high dose of 500 mg/kg was administered in this study. This dose, however, does not cause overt hepatotoxicity and has been applied by other investigators (McMillian et al., 2004; Coe et al., 2006; Higuchi et al., 2012). Drug plasma concentrations 3 hours after administration in rats were between 35.2 and 57.6 μmol/l (Supplemental Table 1). Assuming that these concentrations are relatively close to the maximum plasma concentration (C_{max}), matching concentrations of 50 and 100 μM were chosen for the corresponding in vitro experiments.

Likewise, established reference markers for liver damage, ATP, LDH (cellular assays), and activities of different aminotransferases (animal study) were analyzed. In addition to terminal endpoints, we also included monitoring of key biochemical parameters such as cell signaling that can point toward the mechanism by which a chemical exerts toxicity.

Here we adopted a sensitive in vitro tool applied to primary hepatocytes via in situ hydrogen peroxide–generating system originally reported by the O'Brien group (Tafazoli et al., 2005). These conditions significantly increased the magnitude of cellular oxidative stress response as indicated by the larger dynamic range of the analyzed biomarkers. This system is particular to drugs carrying structural motifs that may form quinone, quinone-imine, or di-imine metabolites prone to redox cycling. The system was validated by comparison with an analogous HRP-free experiment to ensure the absence of intrinsic cytotoxic effects. Therefore, all subsequent in vitro experiments were conducted using the HRP system. Complementary metabolite identification (MetID) experiments revealed that formation of the reactive di-imine species increased under these test conditions as indicated by the detection of its glutathione adduct.

Flutamide did not exhibit significant effects on the biochemical markers for direct cytotoxicity at concentrations of 50 and 100 μM. A transient decrease of ATP content after 6 hours was observed and a

TABLE 2

Effect of flutamide treatment on gene expression in rat hepatocytes for glutathione-*S*-transferase π1 (GSTπ1), heme oxygenase 1 (HMOX1), and NAD(P)H:quinone oxidoreductase 1 (NQO1)

Values are means (n =3) of the fold change compared with control incubations. Significance is indicated by $^{*}P < 0.05$.

		50 μM	100 μM
GSTπ1	6 h	0.96 ± 0.05	1.3 ± 0.2
	24 h	1.7 ± 0.5	4.1 ± 1.8*
HMOX1	6 h	1.4 ± 0.2	1.8 ± 0.2
	24 h	2.7 ± 0.8*	3.6 ± 0.4*
NQO1	6 h	0.91 ± 0.04	0.82 ± 0.13
	24 h	0.87 ± 0.13	1.9 ± 0.5*

TABLE 3

Plasma of Fischer F344 rats treated with 500 mg/kg flutamide was tested for liver function by changes in the concentration of amino transferases compared with control rats

		ALT	AST	GLDH	LDH	SDH
		μkat/l	μkat/l	μkat/l	μkat/l	μkat/l
Control	3 h	0.98 ± 0.19	3.36 ± 0.55	0.28 ± 0.03	87.39 ± 26.3	0.23 ± 0.02
	24 h	1.42 ± 0.58	3.44 ± 2.01	0.15 ± 0.16	33.31 ± 35.6	0.16 ± 0.09
500 mg/kg	3 h	0.97 ± 0.09	1.47 ± 0.01	0.16 ± 0.03	7.17 ± 3.09	0.16 ± 0.07
	24 h	0.48 ± 0.33	1.19 ± 0.47	0.25 ± 0.17	9.08 ± 2.84	0.09 ± 0.01

GLDH, glutamate dehydrogenase.

slight increase of LDH levels after 24 hours, but these alterations were not considered significant for a pronounced cytotoxic effect.

A similar trend on ATP content and LDH leakage was observed with 100 μM flutamide, also in the absence of the HRP system; it was concluded that the addition of HRP to the culture system only slightly aggravates the slight intrinsic cytotoxic effect of flutamide. These results are in accordance with previous studies: Fau et al. (1994) observed significant changes for both measures only at 1 mM flutamide concentration in hepatocyte suspension. For a deficiency in oxygen consumption by 50%, more than 100 μM substrate was needed in plated HepG2 cells as investigated by Will's group (Nadanaciva et al., 2012). They investigated K562 cells also, which revealed only slight changes in ATP content and membrane integrity at 100 μM flutamide (Swiss et al., 2013). In contrast, O'Brien's group (Tafazoli et al., 2005) reported cytotoxicity in rat hepatocyte suspension when incubating with 75 μM flutamide. The different incubation conditions and higher concentrations of glucose oxidase (1 IU/ml versus 0.05 IU/ml) may explain the slightly deviating results (MacAllister et al., 2013).

Also in rats in vivo no elevations for the tested amino transferases were detected, indicating lack of overt hepatocellular damage at 1 day after administration of 500 mg/kg flutamide. The observed slight decrease for AST and LDH values upon treatment may be attributable

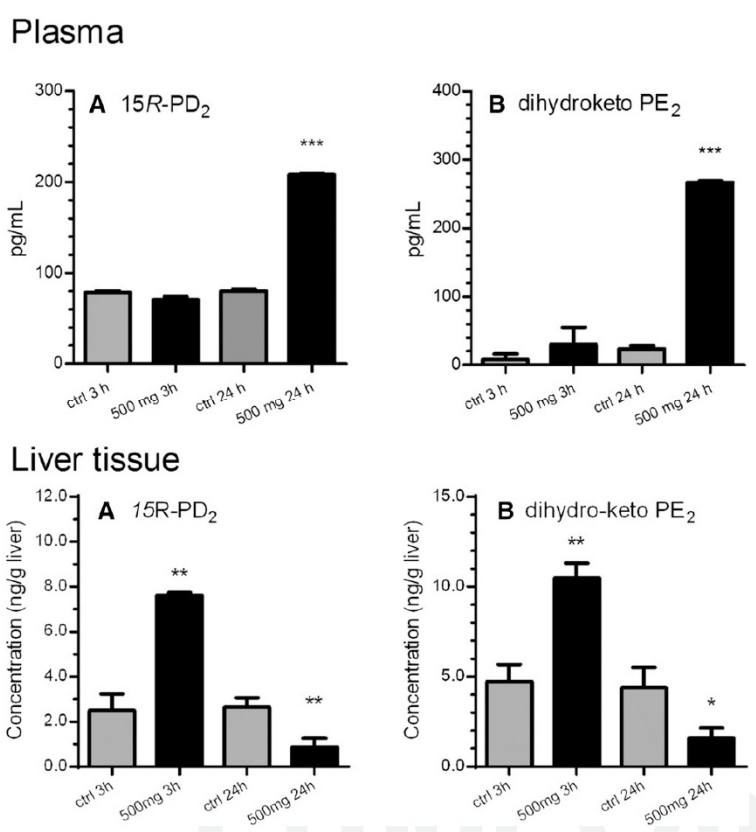

Fig. 4. Effect of flutamide (500 mg/kg) on prostaglandin concentrations in plasma and liver tissue of Fischer F344 rats: Values are means ± SD ($n = 3$). Significance is indicated by *($P < 0.05$), **($P < 0.01$) and *** ($P < 0.001$).

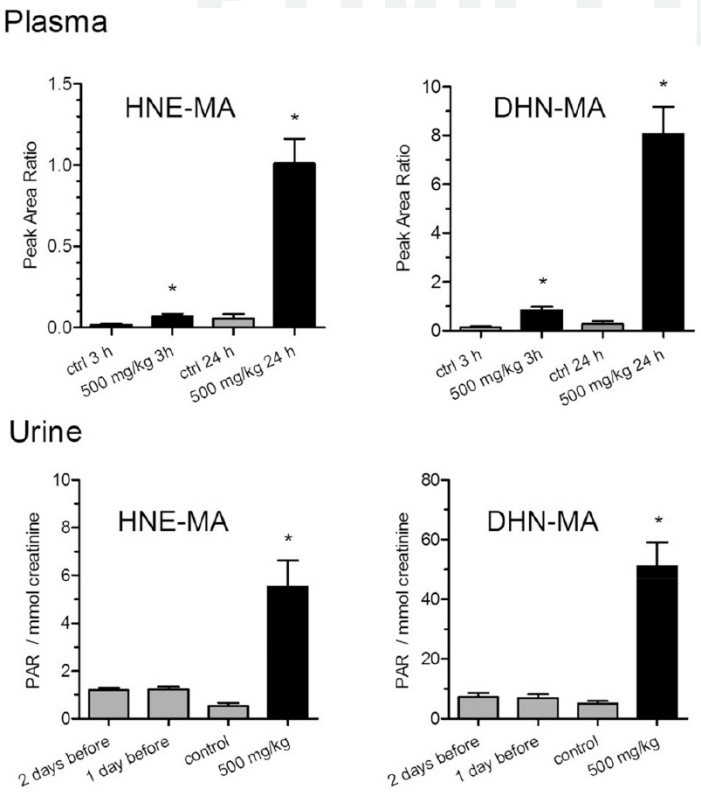

Fig. 5. Effects of flutamide treatment in vitro and in vivo on hydroxynonenal and dihydroxynonene mercapturate levels: Determination was done after 6 and 24 hour from plasma (A) after 3 and 24 hour and urine samples (B) after 24 hour. Values are means ($n = 3$) ± SD. Significant changes compared with control are indicated by *($P < 0.05$).

to intergroup differences and remained constant over the time of the experiment.

The complementary investigations of oxidative stress showed that determination of isoprostanes as well as gene expression analysis were much more sensitive: In vitro prostaglandin isomers as well as hydroxynonenal metabolites revealed a time- and dose-dependent course of an oxidative stress response, already showing significance after 6 hours of incubation and for 50 μM substrate concentration.

In accordance with our results, ROS formation upon treatment with flutamide has previously been reported after use of a hydrogen peroxide–generating substrate in rat hepatocytes (MacAllister et al., 2013). The magnitude of response as measured by the increase in a generic fluorescent marker for ROS was, however, less pronounced than the increase in individual and thus probably more sensitive and selective biomarkers in the present study.

TABLE 4

Effects of flutamide treatment on levels of gene expression of GSTπ1, HMOX1, and NQO1

Values are means (n =3) of the fold change compared with control incubations. Significance is indicated by *P < 0.05, **P < 0.01, ***P < 0.001.

		500 mg/kg
GSTπ1	3 h	1.0 ± 0.2
	24 h	7.5 ± 0.8***
HMOX1	3 h	0.9 ± 0.5
	24 h	5.6 ± 1.1**
NQO1	3 h	7.0 ± 2.8*
	24 h	94.1 ± 41.4*

In line with the in vitro studies, the in vivo results exhibited a similar pattern: The same prostaglandin isomers responded to flutamide treatment in vivo. In plasma, these markers showed significant increases compared with control animals after 24 hours. Hydroxynonenal metabolites were found to be even more markedly increased upon flutamide treatment. At 3 hours postadministration, the increase in plasma levels was already statistically significant and even further enhanced after 24 hours. Moreover, an increased renal excretion of these two markers was also evident compared with vehicle controls. These data are in line with data from previous investigation of the potential of HNE derivatives as biomarkers for oxidative stress. Most of those studies investigated HNE-derived thiol conjugates after induction of oxidative stress directly via free radicals from, e.g., carbon tetrachloride or iron nitrilo-triacetate (Kadiiska et al., 2005; Völkel et al., 2005) or under disease conditions that are associated with increase oxidative tissue injury such as Alzheimer's disease (Dalle-Donne et al., 2006; Völkel et al., 2006).

In contrast to HNE conjugates, prostaglandin levels in urine were not altered as a consequence of flutamide administration. This finding indicates that the observed changes in plasma levels originate from hepatotoxicity and probably are not caused by renal damage. Analysis

of liver tissue supports this suggestion; here, two prostaglandin isomers that were altered in plasma were increased as well. However, the transient augmentation of 15*R*-PD_2 and dihydro-keto PE_2 reverted into a significant reduction 24 hours after treatment, most likely owing to effective hepatic antioxidative regulation mechanisms.

Gene expression analysis supported these findings. Even though a change in mRNA expression was not pronounced for all examined genes regulated via Nrf2, the affected genes were consistently affected in vivo and in vitro. CES1, GCLC, and GSTα1 did not show any significant changes in expression. GSTπ1, HMOX1, and NQO1 mRNA expression was induced as a result of flutamide treatment after 24 hours. This can be a result of differences in sensitivity toward Nrf2 activation or alternative dimerization partners of Nrf2 for different target genes, as recently discussed (Goldring et al., 2004). Induction of HMOX1 and NQO1 via Nrf2 induction has been explored in the past after treatment with sulphoraphone and butylated hydroxyanisole (Nioi et al., 2003; Keum et al., 2006). Sharma et al. (2013) demonstrated induction of GSTπ1 and NQO1 by different P450-inducing xenobiotics, suggesting regulation of activating and detoxifying enzymes in rat liver. Researchers from Daiichi Sankyo investigated the effect of different drugs on Nrf2-regulated genes in human hepatocytes and found mainly effects for HMOX1, CES, NQO1, and UGT1A1 (Takakusa et al., 2008).

Park et al. (Goldring et al., 2004) had identified increased nuclear Nrf2 protein levels upon treatment of CD1-mice with the hepatotoxin acetaminophen already at nontoxic doses and could also find subsequent functional changes of mRNA levels of HMOX1, GCLC, and mEH (microsomal epoxide hydrolase). This effect is not attributable to GSH depletion alone but rather electrophilic properties of the proposed toxin are necessary to activate the Nrf2 pathway.

In good accordance with our results, a study of gene expression signature by McMillian et al. (2004) demonstrated significant induction of mRNA levels for GSTπ1, HMOX1, and NQO1 in rat liver in response to administration of 500 mg/kg flutamide to rats. These results support causality and relevance of our findings.

Conclusion

This study demonstrates the interrelation of flutamide bioactivation and its consequence on cellular oxidative stress via redox cycling after reduction of its aromatic nitro group. We were able to assemble a panel of noninvasive biomarkers and experimental conditions suitable for the characterization of drug-induced effects in vitro as well as in vivo. Previous studies showed that higher doses and repeated administration lead to liver enzyme elevations as signs of overt liver damage. Here the presented markers not only have the ability of designating oxidative stress but can serve as early signals of developing liver injury before overt toxicity manifests. In general, they support elucidation of mechanistic liabilities for DILI by monitoring mechanism-specific biomarkers and by observing relevant physiologic and drug-specific metabolism pathways. A combination of metabolism and biomarker studies may help characterize hazard potentials for drug candidates and identify imbalance between activation and detoxification pathways.

Acknowledgments

The authors thank Dr. Tobias Heckel and Corinne Nowaczyk for and introduction into mRNA isolation and PCR technology. The support from Dr. Gérald Tuffin, Christelle Rapp, Véronique Dall'Asen, and Marie Stella Gruyer for the in vivo studies is gratefully acknowledged.

Authorship Contributions

Participated in research design: Teppner, Boess, Ernst, Pahler.

Performed data analysis: Teppner, Pahler.

Wrote or contributed to the writing of the manuscript: Teppner, Boess, Ernst, Pahler.

References

Boess F, Durr E, Schaub N, Haiker M, Albertini S, and Suter L (2007) An in vitro study on 5-HT6 receptor antagonist induced hepatotoxicity based on biochemical assays and toxicogenomics. *Toxicol In Vitro* **21**:1276–1286.

Bryan HK, Olayanju A, Goldring CE, and Park BK (2013) The Nrf2 cell defence pathway: Keap1-dependent and -independent mechanisms of regulation. *Biochem Pharmacol* **85**: 705–717.

Cetin M, Demirci D, Unal A, Altinbaş M, Güven M, and Unlühizarci K (1999) Frequency of flutamide induced hepatotoxicity in patients with prostate carcinoma. *Hum Exp Toxicol* **18**: 137–140.

Choucha Snouber L, Bunescu A, Naudot M, Legallais C, Brochot C, Dumas ME, Elena-Herrmann B, and Leclerc E (2013) Metabolomics-on-a-chip of hepatotoxicity induced by anticancer drug flutamide and Its active metabolite hydroxyflutamide using HepG2/C3a microfluidic biochips. *Toxicol Sci* **132**:8–20.

Coe KJ, Nelson SD, Ulrich RG, He Y, Dai X, Cheng O, Caguyong M, Roberts CJ, and Slatter JG (2006) Profiling the hepatic effects of flutamide in rats: a microarray comparison with classical aryl hydrocarbon receptor ligands and atypical CYP1A inducers. *Drug Metab Dispos* **34**: 1266–1275.

Copple IM, Goldring CE, Kitteringham NR and Park BK (2010) The keap1-nrf2 cellular defense pathway: mechanisms of regulation and role in protection against drug-induced toxicity. *Handb Exp Pharmacol*: (196):233–266.

Crownover RL, Holland J, Chen A, Krieg R, Young BK, Roach M, and Fu KK (1996) Flutamide-induced liver toxicity including fatal hepatic necrosis. *Int J Radiat Oncol Biol Phys* **34**: 911–915.

Dalle-Donne I, Rossi R, Colombo R, Giustarini D, and Milzani A (2006) Biomarkers of oxidative damage in human disease. *Clin Chem* **52**:601–623.

Ecker J (2012) Profiling eicosanoids and phospholipids using LC-MS/MS: principles and recent applications. *J Sep Sci* **35**:1227–1235.

Fau D, Eugene D, Berson A, Letteron P, Fromenty B, Fisch C, and Pessayre D (1994) Toxicity of the antiandrogen flutamide in isolated rat hepatocytes. *J Pharmacol Exp Ther* **269**:954–962.

Goldring CE, Kitteringham NR, Elsby R, Randle LE, Clement YN, Williams DP, McMahon M, Hayes JD, Itoh K, and Yamamoto M, et al. (2004) Activation of hepatic Nrf2 in vivo by acetaminophen in CD-1 mice. *Hepatology* **39**:1267–1276.

Higuchi S, Kobayashi M, Yano A, Tsuneyama K, Fukami T, Nakajima M, and Yokoi T (2012) Involvement of Th2 cytokines in the mouse model of flutamide-induced acute liver injury. *J Appl Toxicol* **32**:815–822.

Kadiiska MB, Gladen BC, Baird DD, Germolec D, Graham LB, Parker CE, Nyska A, Wachsman JT, Ames BN, and Basu S, et al. (2005) Biomarkers of oxidative stress study II: are oxidation products of lipids, proteins, and DNA markers of CCl4 poisoning? *Free Radic Biol Med* **38**: 698–710.

Kang P, Dalvie D, Smith E, Zhou S, Deese A, and Nieman JA (2008) Bioactivation of flutamide metabolites by human liver microsomes. *Drug Metab Dispos* **36**:1425–1437.

Kashimshetty R, Desai VG, Kale VM, Lee T, Moland CL, Branham WS, New LS, Chan EC, Younis H, and Boelsterli UA (2009) Underlying mitochondrial dysfunction triggers flutamide-induced oxidative liver injury in a mouse model of idiosyncratic drug toxicity. *Toxicol Appl Pharmacol* **238**:150–159.

Keum YS, Han YH, Liew C, Kim JH, Xu C, Yuan X, Shakarjian MP, Chong S, and Kong AN (2006) Induction of heme oxygenase-1 (HO-1) and NAD[P]H: quinone oxidoreductase 1 (NQO1) by a phenolic antioxidant, butylated hydroxyanisole (BHA) and its metabolite, tert-butylhydroquinone (tBHQ) in primary-cultured human and rat hepatocytes. *Pharm Res* **23**: 2586–2594.

MacAllister SL, Maruf AA, Wan L, Chung E, and O'Brien P (2013) Modeling xenobiotic susceptibility to hepatotoxicity using an in vitro oxidative stress inflammation model. *Can J Physiol Pharmacol* **91**:236–240.

Marí M, Morales A, Colell A, García-Ruiz C, Kaplowitz N, and Fernández-Checa JC (2013) Mitochondrial glutathione: features, regulation and role in disease. *Biochim Biophys Acta* **1830**: 3317–3328.

Matsuzaki Y, Nagai D, Ichimura E, Goda R, Tomura A, Doi M, and Nishikawa K (2006) Metabolism and hepatic toxicity of flutamide in cytochrome P450 1A2 knockout SV129 mice. *J Gastroenterol* **41**:231–239.

McMillian M, Nie AY, Parker JB, Leone A, Bryant S, Kemmerer M, Herlich J, Liu Y, Yieh L, and Bittner A, et al. (2004) A gene expression signature for oxidant stress/reactive metabolites in rat liver. *Biochem Pharmacol* **68**:2249–2261.

Milne GL, Yin H, Hardy KD, Davies SS, and Roberts LJ, 2nd (2011) Isoprostane generation and function. *Chem Rev* **111**:5973–5996.

Motohashi H and Yamamoto M (2004) Nrf2-Keap1 defines a physiologically important stress response mechanism. *Trends Mol Med* **10**:549–557.

Muriel P (2009) Role of free radicals in liver diseases. *Hepatol Int* **3**:526–536.

Mutschler E, Geisslinger G, Kroemer HK and Schäfer-Korting M (2001) *Mutschler Arzneimittelwirkungen*. Wissenschaftliche Verlagsgesellschaft mbH Stuttgart.

Nadanaciva S, Rana P, Beeson GC, Chen D, Ferrick DA, Beeson CC, and Will Y (2012) Assessment of drug-induced mitochondrial dysfunction via altered cellular respiration and acidification measured in a 96-well platform. *J Bioenerg Biomembr* **44**:421–437.

Nakagawa Y, Koyama M, and Matsumoto M (1999) [Flutamide-induced hepatic disorder and serum concentrations of flutamide and its metabolites in patients with prostate cancer]. *Hinyokika Kiyo* **45**:821–826.

Nioi P, McMahon M, Itoh K, Yamamoto M, and Hayes JD (2003) Identification of a novel Nrf2-regulated antioxidant response element (ARE) in the mouse NAD(P)H:quinone oxidoreductase 1 gene: reassessment of the ARE consensus sequence. *Biochem J* **374**:337–348.

Osculati A and Castiglioni C (2006) Fatal liver complications with flutamide. *Lancet* **367**: 1140–1141.

Sharma A, Saurabh K, Yadav S, Jain SK, and Parmar D (2013) Expression profiling of selected genes of toxication and detoxication pathways in peripheral blood lymphocytes as a biomarker for predicting toxicity of environmental chemicals. *Int J Hyg Environ Health* **216**:645–651.

Sicilia T, Mally A, Schauer U, Pähler A, and Völkel W (2008) LC-MS/MS methods for the detection of isoprostanes (iPF2alpha-III and 8,12-iso-iPF2alpha-VI) as biomarkers of CCl4-induced oxidative damage to hepatic tissue. *J Chromatogr B Analyt Technol Biomed Life Sci* **861**:48–55.

Swiss R, Niles A, Cali JJ, Nadanaciva S, and Will Y (2013) Validation of a HTS-amenable assay to detect drug-induced mitochondrial toxicity in the absence and presence of cell death. *Toxicol In Vitro* **27**:1789–1797.

Tafazoli S, Spehar DD, and O'Brien PJ (2005) Oxidative stress mediated idiosyncratic drug toxicity. *Drug Metab Rev* **37**:311–325.

Takakusa H, Masumoto H, Mitsuru A, Okazaki O, and Sudo K (2008) Markers of electrophilic stress caused by chemically reactive metabolites in human hepatocytes. *Drug Metab Dispos* **36**: 816–823.

Völkel W, Alvarez-Sánchez R, Weick I, Mally A, Dekant W, and Pähler A (2005) Glutathione conjugates of 4-hydroxy-2(E)-nonenal as biomarkers of hepatic oxidative stress-induced lipid peroxidation in rats. *Free Radic Biol Med* **38**:1526–1536.

Völkel W, Sicilia T, Pähler A, Gsell W, Tatschner T, Jellinger K, Leblhuber F, Riederer P, Lutz WK, and Götz ME (2006) Increased brain levels of 4-hydroxy-2-nonenal glutathione conjugates in severe Alzheimer's disease. *Neurochem Int* **48**:679–686.

Wen B, Coe KJ, Rademacher P, Fitch WL, Monshouwer M, and Nelson SD (2008) Comparison of in vitro bioactivation of flutamide and its cyano analogue: evidence for reductive activation by human NADPH:cytochrome P450 reductase. *Chem Res Toxicol* **21**:2393–2406.

Address correspondence to: Dr. Axel Pähler, Roche Pharmaceutical Research and Early Development pRED, Pharmaceutical Sciences, Roche Innovation Center Basel, CH-4070 Basel, Switzerland. E-mail: axel.paehler@roche.com

4 SUMMARY AND OUTLOOK

The term drug-induced liver injury (DILI) describes adverse effects upon therapeutic drug treatment. They are relatively rare, affecting only 1 of 10^4 - 10^6 patients, and remain mostly unpredictable. Due to development of severe hepatotoxicity or death, drugs causing DILI display a high risk for patients and have been withdrawn from the market or severely restricted in use. For the pharmaceutical industry late stage attrition due to DILI represents a big burden stretching development time and effort and generating potential risk at high costs. A better characterization of the disease pattern and its contributing factors is needed. Currently experimental tools to build preclinical mitigation strategies are sparse, but urgently required to help establish an improved risk assessment. One possible mechanism of toxicity involves the formation of chemically reactive metabolites (RM) which interact with cellular macromolecules or signaling pathways. A direct link between RM formation and DILI remains speculative in most cases. Numerous studies of affected drugs demonstrate the plausible involvement of RM formation and subsequent covalent binding to proteins. Still, RMs are not detected for all DILI drugs and RMs do not lead to DILI in every case. Thus, a synergistic effect of multiple (unknown) mechanisms is supposed to result in DILI.

The aim of this work was to review mechanisms leading to DILI, consisting of RM formation and other potentially contributing risk factors such as oxidative stress, cyto- or mitochondrial toxicity. Results were critically evaluated in light of the predictivity for DILI and comprise a gap analysis of current approaches. Biomarkers are proposed as complementary endpoints. Development and validation of analytical methods were conducted for *in vitro* experiments followed by application of tool compounds to demonstrate the correlation to *in vivo* studies.

For the in-depth analysis of bioactivation data and its correlation to DILI, a validation set of drugs was selected. These included three groups of compounds, namely those with severe manifestation of DILI, drugs with reported DILI cases and drugs with a history of safe use. Different models were drafted to evaluate quantitative covalent binding as predictive parameter for DILI. The hypothesis was that the intrinsic property of *in vitro* covalent binding is not a descriptive parameter, as exposure of a toxic drug or metabolite in the body is determined by pharmacokinetic factors. E.g., low clearance drugs might result in experimental false negative results when they are not significantly activated *in vitro.* Thus, pharmacokinetic properties such as plasma clearance or

hepatic inlet concentration were incorporated into the correlation analysis. A quantitative description of the models was established by sensitivity, specificity, precision and negative predictive value. As previously reported, a correlation between covalent binding, the daily dose and DILI was evident. This correlation further improved when adjusted for intrinsic clearance and substituting dose with the theoretical liver inlet concentration. It is further suggested to use glutathione adduct formation as surrogate for covalent binding. This approach was able to separate safe and high risk DILI drugs when evaluated in context of dose and clearance. The correlation did not hold true for medium risk drugs where a big overlap to safe drugs was noticeable. This may be due to equivocal drug classification or the fact that additional factors contribute to the development of DILI.

One of the risk factors contributing to DILI is the excessive overproduction of reactive oxygen species (ROS), i.e. oxidative stress. Oxidative stress can be measured e.g. by cellular damage, biomarkers of lipid peroxidation or secondary signals like gene expression. Isoprostanes were chosen as biomarkers for further investigation. They derive from radical-catalyzed peroxidation of arachidonic acid. Selected isomers of this heterogeneous group were reported as biomarkers of ROS in the past. An online separation chromatography coupled mass spectrometry method was developed to simultaneously detect various isoprostanes and prostaglandins with a low limit of quantification. Analytical method validation allowed application of these biomarkers to a proof of concept study in primary rat and human hepatocytes. Results indicate a significant time and dose dependent cellular response for different isoprostane isomers by treatment with ferric nitrilotriacetic acid, a chemical known to cause oxidative stress. Furthermore, the value of isoprostanes as biomarkers of cellular oxidative stress was shown for DILI model compounds. The anticancer agent flutamide is known to cause hepatotoxicity, most likely by formation of reactive metabolites and impairment of mitochondrial function. Formation of imino-quinone intermediates may initiate redox cycling and cause excessive generation of ROS. In order to attenuate drug-induced ROS, hepatocyte cell culture was supplemented with pro-oxidant substrates for the *in situ* generation of hydrogen peroxide. Treatment of rat and human hepatocytes with flutamide induced oxidative stress as indicated by a time and dose dependent increase of isoprostane concentration. Other lipid peroxidation products, namely the hydroxynonenal (HNE) derived conjugates, HNE mercapturic acid (MA) and its reduced form dihydroxynonene MA, were found to be

augmented upon treatment with flutamide as well. These were included into the biomarker panel. Under the test conditions no cytotoxicity was present, emphasizing the potential of lipid peroxidation products to early detect upcoming liver damage in *in vitro* systems. The described biomarkers could be translated between species from rat to human in hepatocytes. Further, results in Fischer F344 rats revealed their applicability to *in vivo* and enabled their classification relative to other cellular oxidative stress markers. In rats, the antioxidant response pathway was investigated via quantitative determination of mRNA for cytoprotective enzymes. In rat hepatocytes and rat liver increased RNA expression levels for glutathione-S-transferase, heme oxygenase, and NADPH:quinone oxidoreductase were detected. This suggests adaptation of cell homeostasis upon oxidative stress induced damage prior to overt cellular or organ damage. It can be assumed that pro-oxidant processes result in pathophysiological changes contributing to manifestation of DILI. Thus, the characterization of bioactivation potentials and oxidative stress conditions as contributing factor to DILI may be appropriate to characterize DILI risk. The development of new analytical tools using state of the art mass spectrometry enabled quantitative biomarker analysis and glutathione adduct screening from the same sample.

In conclusion, this work describes the advances and limitations of RM characterization as risk for DILI. It highlights the value of characterizing danger signals, e.g. induced by oxidative stress. Specifically, biomarkers derived from lipid peroxidation and cell signal analysis may support preclinical risk assessment. It further stresses the importance of integrated risk mitigation strategies that are able to capture a variety of relevant drug properties and the mechanism by which they modulate toxicity. It must be also taken into account that patient related risk factors are likely to play a major role in development of DILI. Therefore, it is necessary to judge elucidated pathways on their potential to cause inter-individual differences. To minimize the general risk of adverse effects including DILI, the predominant goal in drug discovery must be the optimization of pharmacokinetic drug properties to yield low dose and selective drugs.

5 ZUSAMMENFASSUNG UND AUSBLICK

Der Begriff arzneimittelinduzierter Leberschaden (engl.: drug-induced liver injury [DILI]) beschreibt adverse Effekte, die durch Arzneimittelanwendung in therapeutischen Dosen ausgelöst werden. Diese treten relativ selten, bei nur 1 von 10^4 - 10^6 Patienten, auf und sind mehrheitlich unvorhersehbar. Aufgrund der Entwicklung schwerwiegender Hepatotoxizität und Letalität stellen DILI-auslösende Arzneimittel ein hohes Risiko für Patienten dar und müssen vom Markt genommen oder gravierend anwendungsbeschränkt werden. Ein Entwicklungsstopp in späten Phasen der klinischen Arzneimittelprüfung aufgrund von DILI bedeutet für die pharmazeutische Industrie eine große Belastung, die die Zeit und den Aufwand der Entwicklung vergrößert und potenzielles Risiko verbunden mit hohen Kosten generiert. Aus diesen Gründen ist eine bessere Charakterisierung des Krankheits-bildes und seiner Einflussfaktoren notwendig. Aktuell sind experimentelle Hilfsmittel zum Aufbau präklinischer Strategien zur Risikominimierung rar, jedoch zur Etablierung einer besseren Risikoabschätzung dringend erforderlich. Ein möglicher Mechanismus ist die Bildung von chemisch reaktiven Metaboliten (RM), die mit zellulären Makromolekülen oder Signalwegen interagieren können. Allerdings ist ein direkter Zusammenhang zwischen RM Bildung und DILI in den meisten Fällen bisher spekulativ. Zahlreiche Studien mit betroffenen Arzneistoffen zeigen die mögliche Beteiligung von RM und der daraus resultierenden kovalenten Bindung an Proteine. Dennoch sind RM nicht für alle DILI-Fälle nachgewiesen und es gibt Arzneistoffe, in denen RM nicht zu DILI führen. Daher wird ein synergistischer Effekt aus vielen (unbekannten) Mechanismen als Auslöser für DILI vermutet.

Ziel dieser Arbeit war es, Mechanismen, die zu DILI führen, zu überprüfen; hierzu gehörten sowohl die Bildung von RM als auch andere potenzielle Risikofaktoren wie oxidativer Stress, zelluläre oder mitochondriale Toxizität. Ergebnisse wurden in Hinblick auf Prädiktivität für DILI bewertet und stellen eine sog. GAP-Analyse (engl. gap = Lücke) der bestehenden Ansätze dar. Hierfür werden Biomarker als komplementäre Endpunkte vorgeschlagen. Für diese wurden analytischen Methoden für *in vitro* Experimente entwickelt und validiert, die daraufhin für Modellsubstanzen angewendet und zu *in vivo* Studien korreliert wurden.

Für die detaillierte Analyse von Bioaktivierungsdaten und ihrer Korrelation zu DILI wurde ein Validierungssatz von Substanzen ausgewählt. Dieser beinhaltete drei

Gruppen: Substanzen mit schwerwiegender DILI-Form, Substanzen, für mit DILI-Fallberichte existieren und solche, die in Bezug auf DILI sicher angewendet werden können. Um kovalente Binding quantitativ als prädiktiven Parameter für DILI zu beurteilen, wurden verschiedene Modelle entworfen. Diese basierten auf der Hypothese, dass die intrinsische Fähigkeit zu kovalenter Bindung *in vitro* als deskriptiver Parameter nicht ausreicht, da die Exposition einer toxischen Substanz oder ihres Metaboliten im Körper durch ihre Pharmakokinetik bestimmt wird. Zum Beispiel können Substanzen mit niedriger Stoffwechselrate zu einem falsch negativen Ergebnis führen, wenn sie *in vitro* nicht aktiviert werden. Daher wurden pharmakokinetische Eigenschaften wie Plasmaelimination oder hepatische Einströmungskonzentration für die Korrelationsanalyse einbezogen. Quantitativ wurden die Modelle durch Sensitivität, Spezifität, Präzision und negativen Vorhersagewert beschrieben. Wie im Vorfeld berichtet, war ein Zusammenhang zwischen kovalenter Bindung, der Dosis und DILI vorhanden. Die Korrelation wurde besser, wenn kovalente Bindung gegenüber der intrinsischen Clearance normalisiert oder die Dosis durch eine theoretische Portalvenenkonzentration ersetzt wurde. Weiterhin kann die Bildung von Glutathionaddukten als Surrogat für kovalente Bindung vorgeschlagen werden. Mit diesem Ansatz war es möglich, sichere Arzneistoffe von solchen der Hochrisikiogruppe zu trennen, wenn er im Kontext von Dosis und Clearance betrachtet wurde. Für die Substanzen der mittleren Risikokategorie galt dieser Zusammenhang nicht; hier war eine große Überschneidung zu den sicheren Substanzen vorhanden. Die Ursache hierfür könnte einerseits die Unsicherheit in der Klassenzuordnung sein oder die Tatsache, dass zusätzliche Faktoren bei der Entwicklung von DILI mitwirken.

Einer der Risikofaktoren, die zu DILI beitragen, ist die exzessive Überproduktion von reaktiven Sauerstoffspezies (engl. reactive oxygen species [ROS]), also oxidativer Stress. Oxidativer Stress kann z.B. durch Zellschäden, Lipidperoxidation oder sekundäre Signale wie Genexpression gemessen werden. Für weitere Untersuchungen wurden Isoprostane als Biomarker ausgewählt. Diese stammen aus der radikalkatalysierten Peroxidation von Arachidonsäure. Einzelne Isomere dieser heterogenen Gruppe wurden schon in der Vergangenheit als Biomarker für ROS beschrieben. Es wurde eine kombinierte Methode für Festphasenextraktion und chromatographische Trennung mit massenspektrometrischer Detektion entwickelt, die die gleichzeitige Analyse von diversen Isoprostanen und Prostaglandinen bei

niedrigem Quantifizierungslimit erlaubte. Die Validierung der Analytik ermöglichte in der Folge die Anwendung der Biomarker in einer Machbarkeitsstudie mit primären humanen - und Rattenhepatozyten. Die Ergebnisse mehrerer Isoprostanisomere zeigen eine signifikante zeit- und dosisabhängige zelluläre Reaktion auf Behandlung mit Eisennitrilotriazetat, einer Chemikalie, die oxidativen Stress auslöst. Weiterhin wurde auch für DILI Modellsubstanzen die Bedeutung von Isoprostanen als Biomarker für zellulären oxidativen Stress gezeigt. Das Krebstherapeutikum Flutamid ist dafür bekannt, Hepatotoxizität auszulösen, wahrscheinlich durch die Bildung von RM und Schädigung der mitochondrialen Funktion. Die Bildung von Iminochinonzwischenstufen könnte Redox-Cycling initiieren und dadurch exzessive Generierung von ROS triggern. Um die Hepatozyten auf den Effekt arzneistoffinduzierter ROS zu sensibilisieren, wurde die Zellkultur mit pro-oxidativen Substraten für die *in situ* Bildung von Wasserstoffperoxid ergänzt. Durch die Flutamidbehandlung von Ratten- und humanen Hepatozyten wurde oxidativer Stress ausgelöst, erkennbar durch einen zeit- und dosisabhängigen Anstieg der Isoprostankonzentrationen. Andere Lipidperoxidationsprodukte, namentlich die Hydroxynonenalderivate (HNE) HNE-Merkaptursäure (MA) und ihr reduziertes Analogon Dihydroxynonen-MA, zeigten ebenfalls eine Konzentrationserhöhung durch Flutamidbehandlung. Daher wurden sie zum Biomarkerset hinzugefügt. Unter den Testbedingungen konnte keine Zytotoxizität festgestellt werden, eine Tatsache, die das Potential der Lipidperoxidationsprodukte, entstehende Leberschäden in *in vitro* Systemen früh zu erkennen, hervorhebt. Die beschriebenen Biomarker zeigten Übertragbarkeit zwischen den Spezies Ratte und Human in Hepatozyten. Des Weiteren bezeugten Ergebnisse in Fischer F344 Ratten deren Anwendbarkeit *in vivo* und ermöglichten eine Einordnung relativ zu anderen zellulären Markern für oxidativen Stress. In Ratten wurde die antioxidative Reaktion durch quantitative Bestimmung von mRNA Expressionsleveln für zytoprotektive Enzyme untersucht. Hepatozyten und Leberproben von Ratten zeigten eine erhöhte Expression der RNA für Glutathion-S-Transferasen, Hämoxygenasen und NADPH:Chinon Oxido-reduktasen. Dieses deutet auf eine Adaption der Zellhomöostase an Schäden induziert durch oxidativen Stress hin, die sich bemerkbar macht, bevor ein offensichtlicher Zell- oder Organschaden auftritt. Daraus kann geschlossen werden, dass prooxidative Prozesse zu pathophysiologischen Veränderungen führen, welche zur Manifestierung von DILI beitragen. Deswegen ist die Charakterisierung von Bioaktivierungspotential und

oxidativem Stress als Beitrag zu DILI für eine Risikobewertung sinnvoll. Die Entwicklung von neuen analytischen Verfahren mit Massenspektrometern aktueller Technik ermöglicht zum Beispiel quantitative Biomarkeranalyse und Messung von Glutathionaddukten aus derselben Probe.

Zusammengefasst beschreibt diese Arbeit die Fortschritte und Limitationen der Charakterisierung von RM als Risikofaktor für DILI. Sie stellt den Wert der Analyse von Warnsignalen, die z.B. durch oxidativen Stress ausgelöst werden können, heraus. Besonders Biomarker, die aus der Peroxidation von Lipiden hervorgehen, und die Analyse von Zellsignalwegen können die präklinische Risikobewertung unterstützen. Die Arbeit betont weiterhin die Bedeutung von integrativen Strategien zur Risikominimierung, die in der Lage sind, viele relevante Substanzeigenschaften zu erfassen und damit auch die Mechanismen, durch die sie Toxizität modulieren. Es muss jedoch auch berücksichtigt werden, dass wahrscheinlich patientenabhängige Risikofaktoren eine bedeutende Rolle in der Entwicklung von DILI spielen. Daher ist es notwendig, beteiligte Mechanismen in Hinblick auf ihr Potential, interindividuelle Unterschiede zu verursachen, zu bewerten. Um das generelle Risiko für adverse Effekte (einschließlich DILI) zu reduzieren, muss es das erste Ziel der Arzneistoffentwicklung sein, niedrig dosierte und selektive Substanzen durch die Optimierung pharmakokinetischer Eigenschaften zu erlangen.